APPLICATION OF 2D MATHEMATICAL MODEL FOR VERIFICATION OF WATER VELOCITY AT COASTAL AREA OF BANGLADESH

MD. DELWAR HOSSAIN

DEPARTMENT OF WATER RESOURCES ENGINEERING

BANGLADESH UNIVERSITY OF ENGINEERING AND TECHNOLOGY, DHAKA-1000

JANUARY 2012

APPLICATION OF 2D MATHEMATICAL MODEL FOR VERIFICATION OF WATER VELOCITY AT COASTAL AREA OF BANGLADESH

By

Md. Delwar Hossain

(Roll No. 100716021P)

MASTER OF SCIENCE IN WATER RESOURCES ENGINEERING

DEPARTMENT OF WATER RESOURCES ENGINEERING

BANGLADESH UNIVERSITY OF ENGINEERING AND TECHNOLOGY, DHAKA-1000

JANUARY 2012

CERTIFICATE OF APPROVAL

The thesis titled **"Application of 2D Mathematical Model for Verification of Water Velocity at Coastal Area of Bangladesh"** submitted by Md. Delwar Hossain, Roll No. 100716021(P), Session: October 2007, has been accepted as fulfilling this part of the requirement for the degree of Master of Science in Water Resources Engineering on January 2012.

_____

Dr. Umme Kulsum Navera
Professor and Head
Department of Water Resources Engineering
BUET, Dhaka

Chairman of the Committee
(Supervisor)

_____

Dr. Md. Mirjahan
Professor
Department of Water Resources Engineering
BUET, Dhaka

Member

_____

Dr. Md. Sabbir Mostafa Khan
Professor
Department of Water Resources Engineering
BUET, Dhaka

Member

_____

Professor Dr. M.R. Kabir
Pro Vice-chancelor
The University of Asia Pacific
Block-A, House No. 49/C, Road No. 4/A
Dhanmandi R/A, Dhaka

Member
(External)

DECLARATION

It is hereby declared that this thesis work **"Application of 2D Mathematical Model for Verification of Water Velocity at Coastal Area of Bangladesh"** has been done by me. Neither of the thesis nor any part of it has been submitted elsewhere for the award of any degree or diploma.

Signature of the candidate

Md. Delwar Hossain

ABSTRACT

The coastal areas of Bangladesh are different from the rest of the country due to its unique geo-physical characteristics and vulnerability to several natural disasters like cyclones with associated storm surges, erosion and accretion. Natural hazards are increasing with high frequency and intensity along the coast of Bangladesh with the changes of global climate. These extreme natural events are termed disasters when they adversely affect the whole environment including the human beings, their shelters or the resources essential for their livelihoods. Water movement in the coastal zone of Bangladesh is determined by the influences of fresh water flow from the rivers, tide coming from the Bay of Bengal, and meteorological conditions (low pressure systems, wind, storms and cyclones).

A mathematical model study has been carried out to simulate the tidal flow velocity in the near shore coastline of Bangladesh. In this study a two dimensional hydrodynamic model DIVAST (Depth Integrated Velocity and Solute Transport) has been used considering the different parameters like co-efficient of eddy viscosity, Manning roughness, advective and diffusion co-efficient etc. of the Bay of Bengal. The DIVAST model is based on FORTRAN PROGRAMING and it has a number of modules for different purposes with different sets of equations. In this study hydrodynamic module has been used.

The hydrodynamics of the selected area of the Bay of Bengal has been simulated by solving two-dimensional depth integrated momentum and continuity equations numerically with finite difference method. Consequently the water elevation η with respect to mean sea level and the respective velocity components U, V in the x and y directions are calculated across the selected coastal domain for a prescribed set of initial and boundary conditions. Simulated velocity has been verified at selected locations of coastal area with the measured field data and compared with the other study carried out in the coastal region of Bangladesh. Viewing over the DIVAST simulated results very good agreement is found between the measured data as well as to the other study. This encouraging good result justifies that the DIVAST model works reasonably well for the selected domain of the Bay of Bengal.

ACKNOWLEDGEMENT

I would like to express my deepest gratitude and sincere appreciation to my supervisor Dr. Umme Kulsum Navera, Professor and Head, Department of Water Resources Engineering (WRE), Bangladesh University of Engineering and Technology (BUET), Dhaka for providing her continuous supervision, cordial co-operation, valuable suggestions, support, guidance and encouragement during the thesis work. Her constructive comments, keen interest, and expertise helped me to better understand and enrich my knowledge to accomplish my thesis work seamlessly.

My sincere thanks are also to the members of the Examination Committee Dr. M. Mirjahan, Professor, Department of Water Resources Engineering, BUET, Dhaka, Dr. Md. Sabbir Mostafa Khan, Professor, Department of Water Resources Engineering, BUET, Dhaka and Professor Dr. M. R. Kabir, ProVice-Chancellor, The University of Asia Pacific for their valuable comments and constructive suggestions regarding this study.

I would like to thank Mr. Zahirul Haque Khan, Head, Coast Port and Estuary Management Division, and Mr. Rubayet Alam of IWM for providing related necessary bathymetry and velocity data to run the hydrodynamic model of Bay of Bengal. I also express my deep gratitude to Survey of Bangladesh (SOB) and Bangladesh Water Development Board (BWDB) for providing related tidal water level data at different locations of coastal areas. I convey my gratitude to the persons and professionals helping me regarding this thesis work.

I also convey my deep appreciation to all of my family members, specially my mother Zahura Khatun, my wife Shahnaz Hossain, my son Rizwan Rafid and my daughter Fariha Tabassum for their great sacrifice, also my friends and all well-wishers for their co-operation and for supporting me to complete the M.Sc. Engg. Degree.

Above all, I am grateful to Almighty Allah, Who has given me the strength and opportunity to do this research work.

TABLE OF CONTENTS

CHAPTER 3

THEORY AND METHODOLOGY

CHAPTER 4

RESULTS AND DISCUSSIONS

CHAPTER 5

COMPARISON OF TIDAL VELOCITY WITH OTHER STUDY

LIST OF FIGURES

LIST OF TABLES

LIST OF NOTATIONS

η	Sea surface elevation (m)
U	Depth-averaged velocity in x direction
V	Depth-averaged velocity in y direction
H	Total depth of flow
β	Momentum correction factor for non-uniform vertical velocity profile
f	Coriolis parameter
g	Gravitational acceleration
P_a	Atmospheric pressure
τ_{xw}	Surface wind shear stress component in x direction
τ_{yw}	Surface wind shear stress component in y direction
τ_{xb}	Bed shear stress component in x direction
τ_{yb}	Bed shear stress component in y direction
$\bar{\varepsilon}$	Depth-averaged eddy viscosity
k	Von Karman's constant
C	Chezy's roughness coefficient
C_s	Air-water resistance coefficient
P_a	Air density
W_s	Wind speed
W_x	Wind velocity component in x direction
W_y	Wind velocity component in y direction

V_s	Depth-averaged fluid speed
f	Darcy–Weisbach resistance coefficient
k_s	Nikuradse equivalent sand-grain roughness
R_e	Renolds number
υ	Kinematic viscosity
U_*	Shear velocity

LIST OF ABBREVIATIONS

AR4	Fourth Assessment Report
BIWTA	Bangladesh Inland Water Transport Authority
BMD	Bangladesh Metrological Department
BoBM	Bay of Bengal Model
BTM	Bangladesh Transverse Mercator
BUET	Bangladesh University of Engineering and Technology
BWDB	Bangladesh Water Development Board
CCC	Climate Change Cell
CDMP	Comprehensive Disaster Management Program
CEGIS	Centre for Environmental and Geographic Information Services
CERP	Coastal Embankment Rehabilitation Project
CPP	Cyclone Protection Project
CSPS	Cyclone Shelter Preparatory Study
CZPo	Coastal Zone Policy
DEM	Digital Elevation Model
DHI	Danish Hydraulic Institute
DIVAST	Depth Integrated Velocity and Solute Transport
DoE	Department of Environment
FF&WC	Flood Forecasting and Warning Centre
FTCS	Forward Time Central Space
GBM	Ganges-Brahmaputra-Meghna
GoB	Government of Bangladesh

HRA	High Risk Area
IPCC	Intergovernmental Panel on Climate Change
IWM	Institute of Water Modelling
JTWC	Joint Typhoon Warning Centre
LMR	Lower Meghna River
LME	Lower Meghna Estuary
LRP	Land Reclamation Project
MCSP	Multi Purpose Cyclone Shelter Programme
MES	Meghna Estuary Study
MSL	Mean Sea Level
NAPA	National Adaptation Programme of Action
NOAA	National Oceanic and Atmospheric Administration
PWD	Public Works Datum
SAARC	South Asian Associations for Regional Cooperation
SLR	Sea level rise
SMRC	SAARC Meteorological Research Centre
SOB	Survey of Bangladesh
SPM	Shore Protection Manual
UNDP	United Nations Development Programs
UTM	Universal Transverse Mercator

CHAPTER 1
INTRODUCTION

1.1 General

The coastal zone is essentially a multi resource system which provides space, living and non- living resources for human activities and it has a regulatory function for the natural and manmade environment. Private and public bodies use the resources for subsistence (water and food), economic activities (space, living and non-living resources, energy) and recreation. The coastal zone has a great economical and ecological value as it supports extensive agricultural activities, large forestry and a plentiful marine life. Industrialization, commercial development and steadily growing population pressure in many places resulted in an increase of loss of wetlands, pollution, flooding, erosion, over population of land and water resources in the coastal zone. Coastal areas are increasingly threatened by natural processes like storm surges that cause severe coastal erosion (SPM, 1984). The most significant natural erosive forces along the open shorelines are wind driven wave action, tidal current with water level changes which results from tide, wind set-up, sea level rise and storm surges.

Meghna Estuary, the central and important part of coastal zone of Bangladesh, is one of the largest estuaries on the earth in terms of sediment-water discharge. It is formed by the combined flows from three mighty rivers in the south-east Asia, the Ganges, the Brahmaputra and the Meghna. The tidal behavior, upland discharges and wind field varies distinctly from season to season. These factors induce noticeable variation of hydrodynamics in the estuary and adjacent bay region (Azam et al., 2000). Such variations keep modifying the tidal as well as the hydrodynamic characteristics over the year. The tidal current has a typical speed of 1-2 m/s (Kabir et al., 1999). Such tide can create a nearly constant very high production of turbulent kinetic energy close to the seabed. The area is also characterized by high level of hydrodynamic activities. Continuous morphological changes are threatening physical safety and social security of inhabitants and infrastructure in the coastal region.

1.2 Zoning of Coastal Region of Bangladesh

Bangladesh is a flood plain delta, sloping gently from the north to the south and meets the Bay of Bengal at the southern end. The coastline of Bangladesh is 710 kilometres long and runs parallel to the Bay of Bengal (CZPo, 2005). According to the coastal zone policy (CZPo, 2005) of the Government of Bangladesh, 19 districts out of 64 are in the coastal zone covering a total of 147 upazillas of the country (Figure 1.2.1). Out of these 19 districts, only 12 districts meet the sea or lower estuary directly.

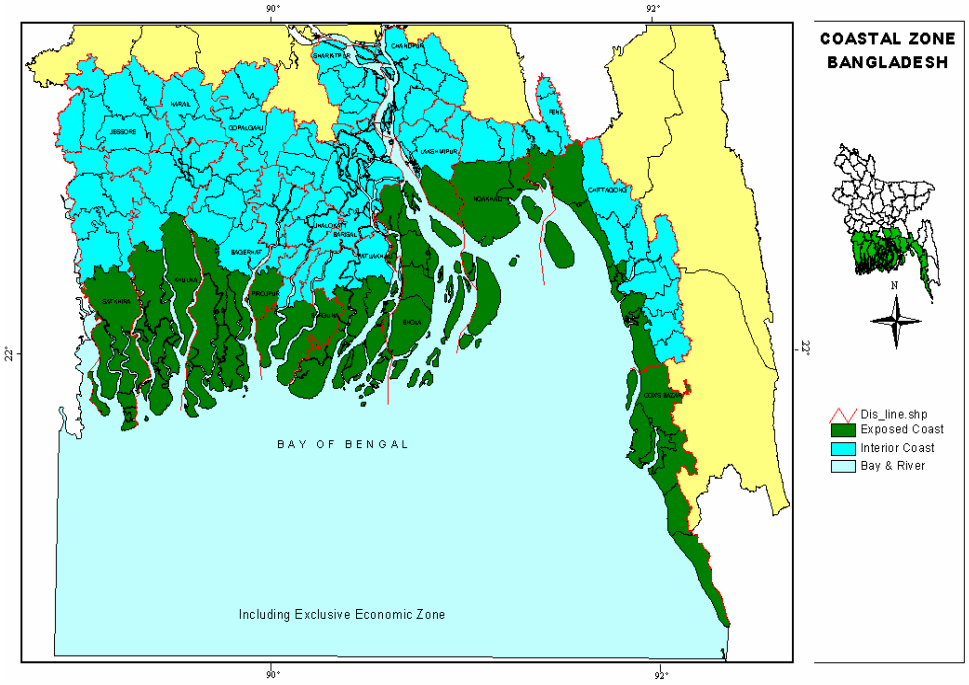

Figure 1.2.1: Coastal Zone of Bangladesh (Source: Islam, 2004)

The zone is divided into exposed and interior coast according to the position of land. The upazillas that face the coast or river estuary are treated as exposed coastal zone. Total number of upazillas that fall on exposed coastal zone is 48 in 12 districts. A total of 99 upazillas that are located behind the exposed coast are treated as interior coast. The exposed coast embraces the sea directly and is affected by different coastal hazards like cyclone, storm surge, salinity intrusion, tidal level variation, erosion, accretion, sea level rise due to tidal wave and current etc.

The southern part of Bangladesh falls under coastal zone that receives discharge of numerous rivers, including Ganges-Brahmputra-Meghna (GBM) river system, creating one of the most productive ecosystems of the world. Except Chittagong-Cox's Bazar, other parts of the coastal zone are plain land with extensive river networks and accreted land, which is known as char land in Bangladesh. India is at the west of the zone whereas Myanmar is at the east of the coast. The coastal zone of Bangladesh has been divided into three regions namely western, central and eastern coastal region. However, the shape of the coastal zone is quite unstable and that is changing with course of time due to erosion and accretion (Islam, 2001).

Western coastal zone

The western coastal zone is covered with Sundarbans mangrove forest, covering greater Khulna and part of Patuakhali district. Because of presence of mangrove forest, the zone is relatively stable in terms of soil erosion. Mangrove swamps, tidal flats, natural levees and tidal creeks are characteristics of the zone. Mangroves of the area support feeding and breeding grounds for fish and shrimps species, enriching the area in fisheries bio-diversity. The area lies at 0.9 to 2.1 metre above mean sea level (Iftekhar and Islam, 2004). Soil characteristics of the western coastal zone are silty loams or alluvium. Mangrove dominated coastal areas have developed on soil formations of recent origin consisting of alluvium washed down from the Himalayas. The zone also has tourist attraction in the Sundarbans (Islam, 2003)

Central coastal zone

Central coastal zone extends from Feni river estuary to the eastern corner of the Sundarbans, covering Noakhali, Barisal, Bhola and Patuakhali districts. The zone receives a large volume of discharge from the Ganges-Bhrahmputra-Meghna river system, forming high volume of silty deposition. More than 70% of the sediment load of the region is silt; with an additional 10% sand (Allison et al., 2003). Because of the sediment discharge and strong current, the morphology of the zone is very dynamic and thus erosion and accretion rates in the area are very high. Numerous islands are located in the area including the country's only island district Bhola. Many islands have been formed in last few years in the area by the process of land

accretion. At the same time many have been eroded or disappeared (Rahman et al., 2001). Kuakata, an attractive sandy beach is located at the zone under Khepupara upazilla of Patuakhali district.

Eastern coastal zone

The eastern coastal zone starts from the Feni river estuary to Bodormokam, the southern tip of mainland. This zone is very narrow. A series of small hills are run parallel to this zone. Karnafuly, Sangu and Matamuhury rivers fall into the Bay of Bengal in this area. The Naf river falls to the Bay of Bengal dividing Bangladesh from Myanmar. Soil characteristics of the eastern coastal zone are dominated by submerged sands and mudflats (Islam, 2001). The submerged sand of the zone has formed a long sandy beach of 145 km from Cox's Bazar towards Teknaf. Two of the country's most important sandy beaches from tourists' perspective, namely Patenga and Cox's Bazar are located in this coastal zone. Fish farming, fishing in the bay, salt production and tourism are main economic activities of the zone.

Islands

About 60 islands are identified in the coastal zone to date (Islam, 2004). Most of the islands are located in the central coastal zone, because of the dynamic river flow of the Ganges- Brahmputra-Meghna river system. Hatia, Sandwip and Maishkhali, are three upazilas and Bhola, an administrative district are four bigger islands in the zone. Saint Martin is the only coral island of the country located in Bay of Bengal, about 9.8 km to the southeastern side of mainland (Hossain, 2001). The island has an area of 7.5 sq km and situated under Teknaf thana of Cox's Bazar district. A total number of 177 char lands are also identified in the coastal zone (Islam, 2004)

1.3 Background of the Study

There has been a growing public concern with an increased awareness of different impacts on coastal zone. Numerous number of mathematical models have been developed to study different coastal processes of different coast throughout the world like: Flow and water quality modeling in coastal and inland water (Falconer, 1992)**;** Modeling of morphological changes due to coastal structures (Leonet'yev, 1999);

Nonlinear propagation of unidirectional wave field over varying topography (Girard et al., 1999); Estimation of 3-D current fields near the Rhine outflow from HF radar surface current data (Valk, 19999); Some observations of wave current interaction(Wolf, 1999); Wave deformation and vortex generation in water wave propagating over a submerge dyke(Huang, 1999); Initial motion of sediment under wave and wave-current combined motions(Tanaka, 1995); Sediment transport near the break point associated with cross-shore gradients in vertical eddy diffusivity (Black et al., 1995); etc. Numerical models for simulating tidal level, flow and pollutant transport has become increasingly important in hydraulic and environmental engineering.

A number of modeling studies of the Bay of Bengal have also been carried out to assess various impacts like: Sensitivity of the tidal signal around the Meghna Estuary to the changes in river discharge: a model study (Azam et al., 2000); Application of the two dimensional computer model for impact assessment of the interventions for the purpose of land reclamation in the Meghna Estuary (Kabir et al., 2000); Sediment Dynamics in the Meghna Estuary, Bangladesh: A Model Study (Ali et al., 2007); Impact assessment of climate change on the coastal zone of Bangladesh (IWM, 2005); Investigating the impact of relative sea-level rise on coastal communities and their Livelihoods in Bangladesh (IWM and CEGIS, 2007); Salinity intrusion, coastal and fluvial flood modeling (Khan et al., 2006); Impacts of climate change and sea-level rise on cyclonic storm surge floods in Bangladesh (Karim and Mimura, 2008); Residual flow in the Meghna Estuary on the coastline of Bangladesh (Jacobsen et al., 2002); etc.

Institute of Water Modelling (IWM) is maintaining the two-dimensional Bay of Bengal Model for various impact assessments in the coastal areas of Bangladesh since 1991. The software used for the development of the mathematical model of the Bay of Bengal is MIKE21 FM module of Danish Hydraulic Institute (DHI) Water and Environment. The first version of the model was applied in Cyclone Protection Project (CPP, 1991) and was further developed as a part of the Cyclone Shelter Preparatory Study (CSPS, 1998). The model was further updated as a part of second Coastal Embankment Rehabilitation Project (CERP, 2000). The storm surge

modelling study has been done based on the two-dimensional Bay of Bengal Model of Second CERP.

The numerical model DIVAST (Depth-Integrated Velocities and Solute Transport) is a robust and reliable numerical model for solving the two-dimensional depth-integrated equations by using a uniform rectangular mesh grid (Falconer, 1992). Two-dimensional depth-integrated numerical models are more widely used at present time because three-dimensional hydrodynamic numerical models are sensitive and not always successful which implies a relatively large cost-benefit ratio (Kevin and Daniel, 2004). Two-dimensional depth integrated hydrodynamic equations are commonly used in numerical models to determine the tidal level and the tide-induced current structure (Falconer et al, 1991). The numerical DIVAST model simulates two dimensional distributions of currents, water surface elevations and various water quality parameters within a modeling domain as functions of time, taking into account the hydraulic characteristics governed by the bed topography and the boundary conditions.

In this study, for the first time DIVAST model is used in Bay of Bengal. The bathymetry of Bay of Bengal has been set up based on data of Meghna Estuary Study (MES) phase I and phase II. The bathymetry data has been collected from Institute of Water Modelling (IWM) in Bangladesh Transverse Mercator (BTM) co-ordinate system. The data has been transformed to Universal Transverse Mercator (UTM) co-ordinate system and finally to corresponding latitude-longitude for setting up the bathymetry of Bay of Bengal. The study describes the calibration and verification of DIVAST model simulated tidal velocity against the measured tidal velocity at some prime locations in the Bay of Bengal. In view of that, six locations in the Bay of Bengal have been chosen such as Noakhali-Urirchar Channel, Sandwip-Zahajerchar Channel, Hatia-Noakhali Channel, Sandwip-Sitakundu Channel, Sandwip-Urirchar Channel and Shahbazpur-Monpura Channel. Available measured tidal velocity has been compared with the simulated velocity of DIVAST model in these locations during the respective time periods. The simulated tidal velocity of DIVAST model has also been compared with MIKE 21 simulated tidal velocity of other studies at Charchenga, Feni River Mouth and Patenga during different time periods.

1.4 Aim of the Study

The velocity data is very important to analyze the effects of tide, turbulent diffusion, dispersion, wind induced diffusion, the variation of individual water quality solutes and over all hydrodynamics of the coastal zone. Model simulations are generally undertaken for several tides. Using high resolution numerical models covering a part of Bay of Bengal is a rather new scientific approach for this area. A number of modeling studies have been carried out for coastal zone of Bangladesh with varying degree of success and limitations during last several decades.

In this thesis work, a mathematical model study has been carried out in the coastal zone of Bangladesh using DIVAST model. Aim of this study is to set up the model and to verify the tidal velocity in coastal arena of Bay of Bengal. It is important to mention that monitoring and forecasting of tidal currents are necessary for assessing morphological behavior, erosion, accretion, water level fluctuation with tidal cycle, activities such as ship navigation, routine operation of ports and offshore platform and construction of coastal structures. Dispersion studies for tracking sediment movement, oil slicks and other pollutants require detailed descriptions of currents for model validation and for data assimilation in real-time forecasting. Statistics derived from long-term current measurements are often used to calculate probabilities including extreme conditions likely to be encountered at specific locations. Thus such monitoring and forecasting of velocities, identifying low and high velocity field and directional movement of flows are very much important and essential for designing and planning purposes, e.g. construction of coastal structures such as embankments, barrages, erosion protection works, tidal sluices, regulators, cross dams, closures to connect coastal islands, jetties, sea ports, offshore platforms, enhancement of land reclamation, oil rigs, sea bed conditions for placement of pipelines, etc.

1.5 Objectives of the Study

Following objectives have been set up for the present study:

1. To set up the model with the bathymetry of Bay of Bengal to simulate tidal velocity.

2. To verify the simulated velocity with existing measured data at different coastal locations of Bangladesh.
3. To compare simulated velocity with other study

1.6 Organization of the Contents

This thesis paper has six chapters in it. The contents of each chapter have been summarized briefly as follows:

Chapter-1 of the study gives a brief description of the coastal zone of Bangladesh, background of the study and aim of the study. It also includes the main objectives of the study and the organization of the contents.

Chapter-2 gives a short accounts of the previous studies and literature review available for the study regarding the Bay of Bengal as well as some other Bays in the world. It also gives brief ideas about some prominent mathematical models in the world related with the processes of coasts, estuaries and rivers.

Chapter-3 explains the concept of tide and tide theory. Brief discussion about the different methods of solving partial differential equations (analytical and numerical) and forms of approximation and corresponding truncation errors in the solutions are illustrated thereof.

This chapter also deals with the alternating direction implicit (ADI) method and shows the gradual steps of solving the governing hydrodynamic equations such as continuity equation and momentum equations in x and y directions and its solution techniques. It also describes the DIVAST model, Bathymetry setup and development of Bay of Bengal model.

Chapter-4 describes the results and discussions with interpretation, calibration and validation of model with the tidal velocity of six prime locations throughout the coast of Bangladesh showing the matching of measured velocity with simulated velocity.

Chapter-5 incorporates the comparison of simulated velocity of this study with the other study. The Study comes to an end in chapter-6 by drawing conclusions and recommendations for further study.

CHAPTER 2

LITERATURE REVIEW

2.1 General

The coastal region of Bangladesh is marked by morphologically dynamic river network, sandy beaches and estuarine system. Meghna Estuary is one of the largest estuaries on the earth in terms of sediment-water discharge which is located at the central part of the coastal zone of Bangladesh. The coast comprises a number of deltaic islands that are morphologically highly dynamic. Erosion and accretion take place continuously in this area. The tidal behavior, upland discharges and wind fields vary distinctly from season to season. Many coastal processes modeling studies have been carried out worldwide and also in Bangladesh to assess the impacts of different coastal processes, natural hazards etc. Several different coastal processes studies regarding coastal zone of Bangladesh as well as of the world are reviewed in this chapter.

2.2 Preview of the Earlier Studies

Many numerical modeling studies have been carried out on the coastal area of Bangladesh as well as different coastal areas in the World to understand the impact of various events like: climate change induced SLR, storm surge, tide-surge interaction etc. Some of them are cited in the following sections.

2.2.1 Studies on the Bay of Bengal

Alam (2003) studied that tides in Bangladesh coast originate in the Indian Ocean. It enters the Bay of Bengal through two submarine canyons named ‘Swatch of No Ground’ and ‘Burma Trench’ and arrives very near to the 10 fathom contour line at Hiron Point and Cox’s Bazar respectively at about the same time. The most dominant principle constituents are M2 and S2 whose natural periods of oscillations are 12 hours 25 minutes and 12 hours respectively. Extensive shallowness of the north-eastern bay gives rise to partial reflections and thereby increases the tidal range and friction distortions concurrently. Moreover Large seasonal effects of meteorological origin coupled with the complexity of the non-linear shallow water interaction give

rise to considerable number of higher harmonics. All such higher harmonic terms are needed in predicting tide to make it as nearly representative as possible. Besides numerous inlets, there are six major entrances through which tidal waves penetrate into the waterways system in Bangladesh. The major entrances are: Pussur entrance; Harin Ghata entrance; Tetulia entrance; Shahbazpur entrance; Hatia channel entrance and Sandwip channel entrance. Strong tide is caused at the north of Sandwip by the shallowness and funnel effect in the Hatia river. The spring range noticed here is more than 4 meter during vernal equinoxes and at upstream of Sandwip the tidal wave entering the channel sometimes deforms into a bore.

Ahmed (1998) studied tidal and sediment volume computed from hourly measurements and their residual direction in the estuary of the lower Meghna river. This study was based upon an analysis of tidal velocity and sediment concentration. He conducted this during full tidal cycles mostly at the time of premonsoon and post-monsoon for the period of 1986-1994 during the influence period of spring and neap tide. Study revealed that residual volume and direction give the overall circulation pattern of water and sediment caused by asymmetry of tidal wave. Tidal environment along the Bangladesh coastline mostly mesotidal and the tidal range decreases gradually from east to west in the estuary. The overall trend of land cover changes between 1973 to 1994 shows a consistent increase in mudflat area and there is a net gain of land 37,770 ha, much of which is attributed to latest morphological changes. Suspended sediment concentration is higher during spring tides and at the locations where tidal ranges are higher. Study shows that morphologically active areas have the highest concentration of sediment. During both spring and neap tides, some channels are inflow dominated and some are outflow dominated.

Allision (1998) studied that the Ganges and the Brahmaputra deliver approximately 1.6 billion tons of sediment annually to the face of Bangladesh. These sediments compensate for the natural compaction and subsidence of the delta and keep its size relatively stable. Sediment replenishment is considered to balance the subsidence of the delta that results in a net sea level rise. A study by the SAARC Meteorology Research Centre (SMRC) found that tidal level at Hiron Point, Char Changa and Cox's Bazar rose by 4.0 mm/year, 6.0 mm/year and 7.8 mm/year respectively based

on the tidal gauge record of the period 1977-1998. The rate of the tidal trend on the eastern coast is almost double that of the western coast. This difference could be due to subsidence and uplifting of land. The Bangladesh Inland Water and Transport Authority (BIWTA) recorded 4.27 m neap tides and 6.10 m spring tides in the coastal area of Sandwip Island, Chittagong. However, the tidal range is reduced toward the south along the south-eastern coast of Bangladesh.

Ali et al. (1997) studied that one of the important reasons for disastrous floods in Bangladesh was the back water effect from the Bay of Bengal on the flood water outflow. A two-dimensional vertically integrated hydrodynamic model of the northern Bay of Bengal was used to study the back water effect due to storm surges and astronomical tides in the Meghna estuarine region of Bangladesh. The model also investigated the impact of flood water discharge on tides and storm surges. It has been found that a significant amount of water was held up inside the country by back water effect. Not only that, a huge amount of water penetrates inside Bangladesh particularly due to storm surge and astronomical tides.

As-Salek and Yasuda (2001) studied a numerical model of $(1/120)^0$ resolution. The study found that in general the tide-surge interaction in the Meghna estuary shows a progressive wave nature of the local tide. If the peak of the maximum surge coincides with the tidal peak near the landfall, the surge propagates toward the north faster than when the surge peak coincides with the tidal trough. Cyclones that make landfall before the arrival of the tidal peak produce higher but shorter duration surges than those that make landfall after the arrival of the tidal peak. If the landfall time of the cyclone is kept fixed, the surge peaks are found to arrive earlier with the increase in the propagation speed of the cyclone and with the decrease of the radius of the maximum cyclonic wind. The arrival time of maximum peak surge in the northernmost estuary may be delayed by about 3-4 hours from the arrival time in the southern landform point.

As-Salek (1997) in his study has shown that negative surges destroy coastal aquaculture installations and hinder rescue-evacuation operations during cyclones and storm surges in the Meghna estuary of Bangladesh. The influence of the characteristics of the cyclones striking the Noakhali-Chittagong-Cox's Bazar coast

on the negative surges in the Meghna estuary is examined. The negative surges of the Meghna estuary are found to have a duration of 4-6 hours, occurring before the main surge. The negative surges in the region show remarkable sensitivity to the astronomical tides and to the propagation path of a cyclone. The mechanism of the negative surges in the Meghna estuary is also discussed.

Azam et al. (2000) observed that the Meghna estuary can be described as the zone of transformation of the Meghna River into a wide, shallow shelf followed by a deeper basin. A number of large deltaic islands like Bhola, Hatia, and Sandwip are located around the river mouth. The Meghna River falls into the Bay of Bengal through a number of channels namely Tetulia River, Shahbazpur channel and Hatia channel. The Shahbazpur channel carries the major portion of the flow. Due to the variation in precipitation between the two main seasons which are hydrologically known as the dry and monsoon seasons, the rivers and estuaries in Bangladesh experience wide variation of hydrological conditions and consequent physical processes. The geomorphology of the Lower Meghna estuary is influenced by a complex interaction between river and tide. The tidal currents in these areas play a dominant role in determining the fate of the river-borne sediments. The major obstacle for understanding the morphological processes within this estuary is the scarcity of knowledge of sediment dynamics in this region, which is subject to strong seasonal variation of river flow and tidal action.

Flather (1994) used a numerical model for simulating and predicting tides and storm surges in regions that include areas of open sea combined with estuarine channels and intertidal banks. The model was applied to the northern shelf of the Bay of Bengal and the Ganges Delta, including the coast of Bangladesh devastated by a cyclone surge in April 1991. Hindcast and "forecast" simulations of this event, using forcing derived from a semi-analytical cyclone model with data supplied by the Joint Typhoon Warning Centre were described. It was shown that the timing of cyclone landfall and its coincidence with high tide determine the area worst affected by flooding. The "forecast" was based on a standard JTWC warning issued 12-18 hours ahead of the event. The predicted landfall was located accurately but its timing was about 5 hours late. As a result, the area of highest water levels shifted north.

Improvements in the model and procedures required to produce useful warnings are discussed. Finally, results for the April 1991 storm are compared with those from a simulation of the great cyclone in November 1970. Peak surges and water levels were similar in magnitude in the two events, but differences in track and tidal conditions are again shown to be important, producing flooding in a large area of the southern delta in 1970 but along the mainland coast south of Chittagong in 1991.

Flather (1994) studied that coastal floods produced by cyclone generated storm surges are a major cause of life in the coastal areas surrounding the Bay of Bengal. Bangladesh is vulnerable for a number of reasons. First, it lies in the path of tropical cyclones; second it has a wide and shallow continental shelf; third the coastal areas in Bangladesh comprises of low-lying and poorly protected land, much of it being the delta of the Ganges and Brahmaputra rivers. Coastal defenses typically taking the form of earth banks, are designed primarily to prevent flooding by the normal tides and are overtopped and seriously damaged by a cyclone surge. Fourth, the coastal regions support a large population, many of them in poorest people forced to live in vulnerable areas in order to feed themselves by farming and fishing.

Flierl and Robinson (1992) observed in their study that the coastal areas and off-shore islands of Bangladesh are low lying and very flat. The height above mean sea level of the coastal zone is less than 3m. The range of astronomical tide along the coast of Bangladesh is so large that the storm induced sea level is apt to become very high. The normal tidal range is about 3m near the Indian border in the west and becomes higher to the east (central coastal part) to about 5m near Sandwip island at the mouth of the Meghna estuary. The tidal range in the southeastern part is about 3.5 to 4 m. The situation becomes disastrous if storm surges are superimposed on high tides. A funneling coast line reduces the width of storm induced waves and increases the height. Also the fact that the coasts are situated at right angles in the northern corner of the Bay of Bengal causes higher storm induced waves compared to a straight coast line.

Hossain (2001) observed that the tides in the coastal and estuarine areas are semi-diurnal with two high and two low periods per day and have maximum amplitude of 3-4 m at spring tide. The tidal activity is an important mechanism for the movement

of water and nutrients especially in the estuarine areas and this is probably a reason for the wide range of biodiversity in the estuarine water. The tidal range and river discharge are responsible for the extension of estuarine environment in the sea. The variation of tide level in the coastal areas may be attributed to the depth of the bay and varying topography of coastal water. The tide penetrates up to 170 km in the south-west and 0-50 km in the south-east area of Bangladesh during lean period (April-May) depending on the topography and channels in the area.

Jakobsen et al. (2002) studied the hydrodynamics of the Bay of Bengal in detail using a calibrated and validated two dimensional numerical hydrodynamic model. The Flood Forecasting and Warning Center (FF&WC) of Bangladesh supported by the Institute of Water Modeling (IWM) in Dhaka and DHI have developed an operational salinity intrusion forecast model enabling both short-term and long-term forecasting of salinity conditions in the delta. The Bay of Bengal model was transferred to the FF&WC during a DANIDA supported project from 2000 to 2006 in order to test the feasibility of carrying out operational cyclone forecasting. Later on the Bay of Bengal model was transferred into a flexible mesh model technology based on the finite element method. This has allowed for a more detailed resolution in the deltaic region and up into the river systems and thereby enhancing the accuracy of modeling of saline intrusion. Salinity intrusion forecasting requires the use of a well calibrated hydrodynamic model that describes the river discharges, water levels and currents correctly from the upstream river systems through the deltaic, coastal regions and out into the Bay of Bengal. An advection-dispersion model is coupled to the hydrodynamic model describing the transport and mixing of the fresh water outflows from the river with the saline Bay of Bengal waters. The combined hydrodynamic and advection-dispersion model is referred as the Bay of Bengal model. The Bay of Bengal model was originally developed by IWM and used in a number of projects where it has been updated, re-calibrated and verified.

MES (2001) studied that the lower Meghna River is highly influenced by tidal interactions and consequential backwater effect. Riverine processes dominate the Lower Meghna and Tetulia River as well as Shahbazpur channel and yet, there could be distinct ebb and flood channels in some reaches because of tidal influence. It has

been observed that the tidal range is one of the most important variables that control coastal geomorphology. The tide is semi-diurnal that is two highs and two lows during a period of 24 hours and 50 minutes. The tidal waves approaching the coastal areas of Bangladesh are affected at least by Coriolis acceleration, the width of the transitional continental shelf, the coastal geometry and frictional effects due to fresh water flow. The tide approaching the estuary from southwesterly direction penetrates strongly into the lower Meghna except for periods with very high upland discharges. The vertical tide moves up to Chandpur in the monsoon season and upto Sylhet in dry season. Though the tide is strong in the Shahbazpur River, it is relatively weak at the Tetulia River because of shallowness of the outlet of the river into the Bay of Bengal. Again the tide is pre-dominant in the Pussur-Shibsa river system and a very strong saline intrusion occurs there. Tidal forces are very much pre-dominant in the Hatia channel; in the area between Hatia and Sandwip and the Sandwip channel. The maximum tidal range in the Meghna estuary may vary from 3.5 m at southern end of Hatia and Sandwip to 7.5 m in the extreme northeastern end near the Feni closure dam. The area around Sandwip Island is a macro-tidal area with tidal variation in a range of about 3 to 6 m. The area between Bhola and Hatia (Shabhazpur Channel) falls in the meso-tidal class with a tidal range of 2 to 4 m. Tides in the Tetulia River and the upper reach of lower Meghna upstream of the Char Gazariaare micro-tidal class with a tidal range less than 0.2 m.

IWM (2009) stated that during pre-monsoon (April to May) and post monsoon (October to December) disastrous tropical cyclones form in the Bay of Bengal. Most of the cyclones hit the coasts of Bangladesh with north-eastward approaching angle. Over the last 47 years (1960-2007) about 18 cyclones hit the coast of Bangladesh. Hindcasting (Modeling of past) of the storm surge has been made using available storm surge model available in IWM to assess the storm surge height and risk of inundation of the coastal area. An inundation risk map has been prepared based on the maximum inundation depths of past 18 cyclones. The inundation risk map shows that the highest inundation depth having range between 5 m and 7 m lies in the Noakhali coast, Bhola, Urir Char, Sandwip and small islands in the Meghna Estuary. The eastern coast experiences maximum inundation between 4 m and 6 m and western coast experiences inundation within the range of 3 to 5 m.

CERP (2000) carried out the storm surge modeling study based on the two-dimensional Bay of Bengal Model. Since 1995, IWM is maintaining the two-dimensional Bay of Bengal Model. The first version of the model was applied in Cyclone Protection Project (CPP, 1991) and was further developed as a part of the Cyclone Shelter Preparatory Study (CSPS, 1998). The model was further updated as a part of Second Coastal Embankment Rehabilitation Project (2nd CERP, 2000). In this study the model has been updated with existing data and upgraded in 200 m grid resolution incorporating Sundarban area and it has been extended to the sea up to 16º latitude. The storm surge model is the combination of Cyclone and Hydrodynamic models. For simulating the storm surge and associated flooding, Bay of Bengal model based on MIKE21 hydrodynamic modeling system has been adopted. In the hydrodynamic model simulations meteorological forcing like cyclone is given by wind and pressure field derived from the analytical cyclone model. The MIKE 21 modeling system includes dynamical simulation of flooding and drying processes, which is very important for a realistic simulation of flooding in the coastal area and inundation.

2.2.2 Related Studies on other Bays in the World

Dabrowski et al. (2003) applied two and three dimensional models to simulate hydrodynamic circulation patterns in the Irish Sea. There are two main features in the region: a relatively deep and narrow north channel, and a wider shallower St. George' channel. The main force governing circulation in the region is the semi diurnal tide; summer solar heating is also important. The model domain was divided into 65000 squares each having 2km sides to perform hydrodynamic calculation in three dimensions; a 1km rectangular grid was also used for hydrodynamic calculation in two dimensions. Extensive simulations for calibration of the hydrodynamic model were carried out for different types of boundary conditions and diversities of roughness coefficient. Models were calibrated accordingly to available data which include current velocities at 14 locations and tidal elevation at 15 locations along the Irish and British Coasts. Comparison between individual models runs were made and results were related to the field data indicating that models represent circulation pattern reasonably well.

Falconer (1991) developed the flow and water quality modeling in coastal and inland water. The study highlights the increasing international public concern relating to hydro-environmental issues and cites examples of some of the water quality problems now being considered by hydraulic engineers on a regular basis. General details are given of numerical models used for flow velocity and water quality concentration predictions in coastal and inland hydraulic basins and two example research projects are described. In the first of these studies comparisons are made between dynamically and non-dynamically linked nested models, with the results indicating that in some circumstances non-dynamically linked models can give inaccurate velocity field predictions. In the second example higher order accurate schemes are compared for modeling the advection of abrupt concentration gradients, with computational efficiency and simplicity often being important in hydraulic engineering studies where complex boundaries, often including flooding and drying, can cause added difficulties. Finally, the importance of basic original research is also highlighted, particularly as national and international research funding agencies place increasing emphasis on applied research.

Falconer and Alstead (1990), has undertaken a recent research programme to develop, refine and apply two different types of combined coarse and fine grid numerical models with such numerical models being increasingly used to obtain higher resolution of flow and water quality parameter distributions in regions of particular interest. For example, a fine grid model may be used to obtain a detailed prediction of the velocity and solute distributions within a harbour, whereas a course grid model can be used outside the harbor where a lower level of accuracy may be tolerable. Furthermore, nested models are increasingly being used for numerical hydraulic model studies where open boundary conditions in regions of interest. The two main models considered in the current study involved a nested (or non-dynamically linked) and a patched (or dynamically linked) model, with there being advantages and disadvantages of both schemes. In particular, emphasis was also focused on fully including the advcetive accelerations at the interface between the fine and coarse grid boundaries in the patched model, thereby allowing eddies and fine grid flow features to be advected out of the fine grid domain as accurately as possible.

Lin and Wilde (1996) studied in detail the development and application of a 2D depth-integrated finite method of numerical conformal mapping, based upon a boundary integral equation formulation, has been used to generate the mesh. The method is able to map a general polygonal region with curved sides onto a regular region with the same number of sides: thus it is able to generate curvilinear meshes directly on general curved polygonal regions. If more control over the distribution of the grid mesh lines is necessary, a stretching transformation is then employed. The mesh thus generated is still orthogonal but no longer conformal. Three test cases were used to test the model performance, namely (i) tidal propagation in the Bristol Channel, U.K., (ii) tidal propagation and solute transport in the Humber Estuary, U.K. and (iii) flow and solute transport in a laboratory meandering channel.

Radjawane and Riandini (2009) applied a 3-dimensional numerical model to simulate the tidal current circulation and cohesive sediment transport in the Jakarta Bay, Indonesia. Sediment load comes from three river mouths i.e. Angke River, Karan River and Ancol River. The model was simulated to analyze the effects of tidal current and river discharge. A constantly westrnly and eastrnly was used as input of the model to see the influence of the monsoonal season. The numerical result showed that the tidal current flows from east to western part of the Bay during ebb tide and vice versa during flood tide. The surface current circulation was dominantly influenced by the tidal current compared with the wind and the river discharge effects. High turbidity level was found near the river mouth with the range of 50 to 100 mg/l. This high sediment concentration was caused by the effect of sediment load from the river upstream. In the offshore area of the Bay the sediment concentration decreases up to 10 mg/l. The movement of sediment followed the current circulations. During the flood tide, the sediment concentration from the mouth of Angke River moved to the western part of the bay. Model simulated for increasing the river discharge into two times showed that sediment distributed to the offshore direction two times longer compared with the normal debit. Transport of sediment from the Angke and Karang Rivers to the offshore area reached > 6 km, while it just reached $\pm$ 2.5 km from the Ancol River.

Sankarnarayan et al. (2003) applied a three-dimensional (3D) hydrodynamic model to the Bay of Fundy using a boundary-fitted coordinate hydrodynamic model. The Saint John River and Harbour area were of interest for their study. They used a very fine grid with a resolution range of 50–100 m in the Saint John Harbour region and a grid resolution of about 2 to 3 km was used in the Bay of Fundy. The model forcing functions consisted of tidal elevations along the open boundary and fresh water flows from the Saint John River. The model predicted surface elevation compared well with the observed surface elevation at Saint John and the root mean square error in the model predicted surface elevation for a 60-day period was found to be 4%. The amplitudes and phases of the major tidal constituents at 24 tidal stations, obtained from a harmonic analysis of a 60-day simulation were very close with the observed data obtained from Canadian Hydrographic Survey. The predicted harmonic amplitudes and phases of the M_2 tidal constituent were respectively within 20 cm and 7° of the observed data. The counterclockwise gyre observed in the body of Bay of Fundy was reproduced in the model.

2.3 Numerical Models Research Studies

2.3.1 Numerical Model – DIVAST

DIVAST (**D**epth **I**ntegrated **V**elocity **A**nd **S**olute **T**ransport) is a two dimensional depth integrated, hydrodynamic and solute transport, time variant model, which has been developed for estuarine and coastal modelling. It is suitable for water bodies that are dominated by horizontal, unsteady flow and do not display significant vertical stratification. The model simulates two dimensional distribution of currents, water surface elevations and various water quality parameters within a modelling domain as functions of time, taking into account the hydraulic characteristics governed by the bed topography and the boundary conditions. DIVAST was developed using the FORTRAN 77 programming language by Prof. R.A. Falconer, Halcrow Professor of Environmental Water Management, and Dr. B. Lin, both of the Cardiff School of Engineering, Cardiff University, UK. DIVAST is continually updated and improved by both Prof. Falconers team in Cardiff University and the MarCon staff.

The hydrodynamic module is based on the solution of the depth integrated Navier-Stokes equations and includes the effects of local and advective accelerations, the earths rotation, barotropic and free surface pressure gradients, wind action, bed resistance and a simple mixing length turbulence model. The differential equations are written in their pure differential form, thereby allowing momentum conservation in the finite difference sense. Particular emphasis has been focussed in the development of the model on the treatment of advective accelerations, a surface wind stress and the complex hydrodynamic phenomena of flooding and drying.

For the water quality and sediment transport module, the advective-diffusion equation is solved for a range of water quality indicators. The general depth integrated equations include; local and advective effects, turbulent dispersion and diffusion- including wind effects where appropriate, source and sink inputs, and decay and kinetic transformation processes. For the sediment transport module, the equilibrium suspended flux is included in the model using the van Rijn formulation. However, other formulations are available.

The governing differential equations are solved using the finite difference technique and using a scheme based on the alternating direction implicit formulation. The advective accelerations are written in a time centered form for stability, with these terms and the turbulent diffusion terms being centered by iteration. Whilst the model has no stability constraints, there is a Courant number restriction for accuracy in the hydrodynamic module. The finite difference equations are formulated on a space staggered grid scheme, with the water surface elevations and the x-direction velocity components being initially solved for during the first half time step by using Gaussian elimination and back substitution. The water quality indicators and sediment flux distributions are then evaluated, before proceeding to the second half time step and repeating the process for the implicit description of the y-direction derivatives and velocity components. In the water quality and sediment transport modules the advective terms are treated using a higher order accurate ULTIMATE QUICKEST formulation.

The model has been extensively calibrated and verified against laboratory and field data with details of model refinements and verification tests being reported in over 100 publications by the original author. The original model has been used to date on over 200 projects in Ireland and the UK and is considered an industry standard for all aspects of water quality management.

2.3.2 Numerical Model – FASTER

FASTER (**F**low **A**nd **S**olute **T**ransport Model for **E**stuaries and **R**ivers) is a numerical hydrodynamic, solute and sediment transport model for unsteady and subcritical gradually varied flow in a one-dimensional well-mixed river or estuarine system. The unsteady gradually varied flow is solved through an implicit finite difference scheme with varying grid size over a space staggered grid. The solute and sediment transport part of the model is solved by a new implicit scheme, which is a combination between finite volume central scheme and the highly accurate ULTIMATE QUICKEST scheme. The model accommodates variable channel geometry and any number of interacting channel segments or reaches. There is complete flexibility in the specification of open boundary conditions, also the junction solutions are established by an influence line technique.

The fundamental notions and hypotheses used in the mathematical modelling of rivers are formalised in the equations of unsteady open channel flow. It is assumed that all the St. Venant hypotheses are valid. The basic assumptions are that the flow is in one-dimension, the water is homogeneous and that hydrostatic pressure distributions and Coriolis accelerations may be neglected.

In the model, the cross sectional areas of the flow at the nodes are calculated by means of a divided channel method. According to this method the model divides each cross section into several subsections and it has been assumed that the whole discharge passing through the section is the summation of the discharges passing through all the subsections. Since the model is able to specify the dry and wet parts in the cross section, the cross sectional area, wetted perimeter, top width of flow and the other hydraulic parameters related to the cross sections can be calculated accurately. (Kashefipour and Falconer,1999)

2.3.3 Numerical Model - POM

POM (**P**rinceton **O**cean **M**odel) is a three dimensional, sigma coordinate, hydrodynamic and thermodynamic model. POM was originally develop by Alan Blumberg and George Mellor in 1977 and applied to oceanographic problems in the Atmospheric and Oceanic Sciences Program of Princeton University and the Geophysical Fluid Dynamics Laboratory of NOAA. Published papers that describe the numerical model or applications of the numerical model may be found at the model website here.

The principle attributes of the POM model are:

- It contains an imbedded second moment turbulence closure sub-model to provide vertical mixing coefficients.
- It is a sigma coordinate model, in that the vertical coordinate is scaled over the water column depth.
- The horizontal grid uses curvilinear orthogonal coordinates or rectilinear coordinates and an 'Arakawa-C' differencing scheme.
- The horizontal time differencing is explicit whereas the vertical differencing is implicit.
- The model has a free surface and a split time step:
    - The external mode portion of the model is two dimensional and uses a short time step based on the Courant-Friedrichs-Levy (CFL) condition and the external wave speed.
    - The internal mode portion of the model is three dimensional and uses a long time step based on the CFL condition and the internal wave speed.
- Complete thermodynamics have been included.

The equations governing the dynamics of coastal circulation contain fast moving external gravity waves and slow moving internal gravity waves. It is desirable in terms of computer economy to seperate the vertically integrated equations (external mode) from the vertical structure equations (internal mode). This technique, known as mode splitting permits the calculation of the free surface elevation with little

sacrifice in computational time by solving the velocity transport separately from the three dimensional calculation of the velocity and thermodynamic properties. The velocity transport, external mode equations are obtained by integrating the internal mode equations over the depth, thereby eliminating all vertical structure. The external mode calculations results in updates for surface elevation and vertically averaged velocities. The internal mode calculations result in updates for the sigma layer velocities, thermodynamics and turbulence quantities.

The Courant-Friedrichs-Levy, (CFL), computational stability condition on the vertically integrated, external mode, transport equations limits the time step according to a relationship based on water depth and maximum current velocity. There are other restrictions but the CFL is the most stringent. The model time step is usually ~90% of the CFL limit. The internal mode has a much less stringent time step constraint since the fast moving external mode effects have been eliminated. The computational stability criteria for the internal model limits the timestep according to a relationship based on the maximum internal gravity wave speed and the maximum advective speed. For typical coastal ocean conditions the ratio of the time steps INT/EXT is often a factor of 50 - 80 or greater.

There is an extensive online POM users community, of which the MarCon staff are members, involved in the application, extension and modification of the POM source code and the discussion or various aspects of coastal and ocean modelling.

2.3.4 Numerical Model – RCPWAVE

RCPWAVE (**R**egional **C**oastal **P**rocesses **WAVE** propagation model) is a two-dimensional, steady-state short-waved numerical model used to predict linear, plane wave propagation over an region of arbitrary bathymetry. RCPWAVE uses linear wave theory because it has been shown to yield accurate first-order solutions to wave propagation problems at a relatively low cost. Refractive and bottom-induced diffractive effects are included in the model. The model results can be used as a forcing function to drive models that calculate long-shore and cross-shore sediment transport.

The governing equations solved in the model are the 'mild slope' equation for linear, monochromatic waves, and the equation specifying irrotationality of the wave phase function gradient. Finite-difference approximations of these equations are solved to predict wave propagation outside the surf zone. These equations account for shoaling, refraction and bottom-induced diffraction within a study area. Included in the model is an algorithm for treating wave breaking. Results include wave height, wave angle, and wave number at each grid location. (Ebersole el al.,1986)

2.4 Summary

A brief description of various earlier studies in the Bay of Bengal and some other bays in the world has been presented in this chapter. In addition few numerical model research studies have also been mentioned here. It was found that several studies had been carried out on the coastal area of Bangladesh to understand the impact of climate change, modeling of storm surge, tide-surge interaction at the Meghna estuary. As coastal area of Bangladesh is low lying and exposed to the sea, they are more vulnerable to tidal level induced velocity action that causes more erosion and accretion than that of other land areas. That is why the main focus of the study is to simulate the tidal water velocity using DIVAST numerical model and to verify the simulated tidal water velocity with measured tidal water velocity data of several locations in the coastal zone of Bangladesh. In addition to these the simulated tidal water velocity has been compared with that of other study in this coastal zone.

CHAPTER 3

THEORY AND METHODOLOGY

3.1 General

The prediction technique of flow velocity and water level through numerical simulation is illustrated in this chapter. A 2-dimensional numerical hydrodynamic (Depth Integrated Velocity and Solute Transport) DIVAST model has been set up using the bathymetry of Bay of Bengal. This model has been developed based on the FORTRAN program. DIVAST model has a number of modules for different purposes and each module deals with different sets of equations. In this study hydrodynamic module of the DIVAST model has been used to simulate tidal velocity at several prime locations in the Bay of Bengal. Concept of tide and tide theory, different methods of solving partial differential equations (analytical and numerical), approximation and corresponding truncation errors in the solutions are illustrated thereof. The gradual steps of solving the governing hydrodynamic equations and its solution techniques through ADI (alternating direction implicit) method have been discussed here. A short description of DIVAST model, Bathymetry generation, development of Bay of Bengal model with the governing equations of hydrodynamic module of DIVAST and key stages of model development have been illustrated in the following sections.

3.2 Theory of Tide

3.2.1 Introduction

Tides are the rise and fall of sea levels caused by the combined effects of the gravitational forces exerted by the Moon and the Sun and the rotation of the Earth. The pull of gravity is what keeps the earth and moon revolving round one another, and what keeps this pair revolving round the sun. Gravity is stronger, the closer one get to the object causing it. With the moon, which is quite close to us, this is significant; at the side of the earth which is closest to the moon its gravitational pull is stronger, and at the opposite side of the earth the moon’s gravitational pull is correspondingly weaker.

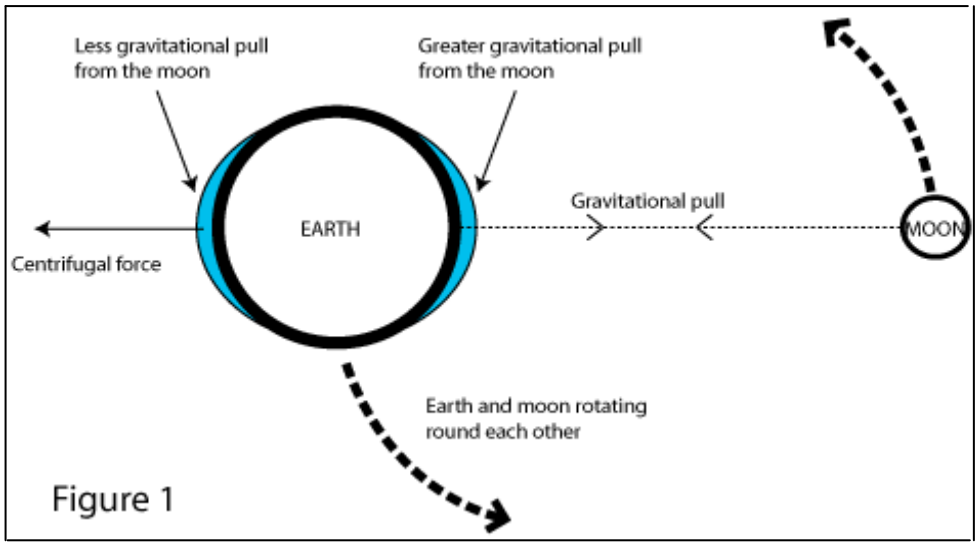

Figure 3.2.1 Rotation of Earth and Moon producing Tide

(Source: NOAA)

On land, nothing can really move in response to this difference is gravitational force, but water can move. What it actually does is form two bulges in the oceans: one on the side facing the moon and the other on the opposite side as shown in figure 3.2.1 (one looking down on the earth from above the north pole). The one on the side closest to the moon is caused because the stronger gravitational pull attracts the water. The one on the furthest side from the moon side is caused because the centrifugal force (which here is stronger than the gravitational force) throws the water outwards as the earth rotates around the Sun.

The earth also spins on its axis. It takes 24 hours for each point on the earth to get from one noon (i.e. facing towards the sun) to the next noon. It takes slightly longer (about 24 hours 50 minutes) between successive lunar noons, because the moon moves with respect to the sun - it rises a little later each day. (Wood, 2001)

In this 24 hour 50 minute period each place will experience the forces that cause the two tidal “bulges” mentioned above, i.e. in general, two high tides and two low tides. The typical pattern is shown in figure 3.2.2, where once again one is looking down on the earth from above the north pole. Here two high tides and two low tides in the 24 hour period are shown (to make the numbers simpler, shown a 24 hour cycle).

This tidal pattern is called **semi-diurnal,** meaning "every half day". High tides are about 12 hours apart.

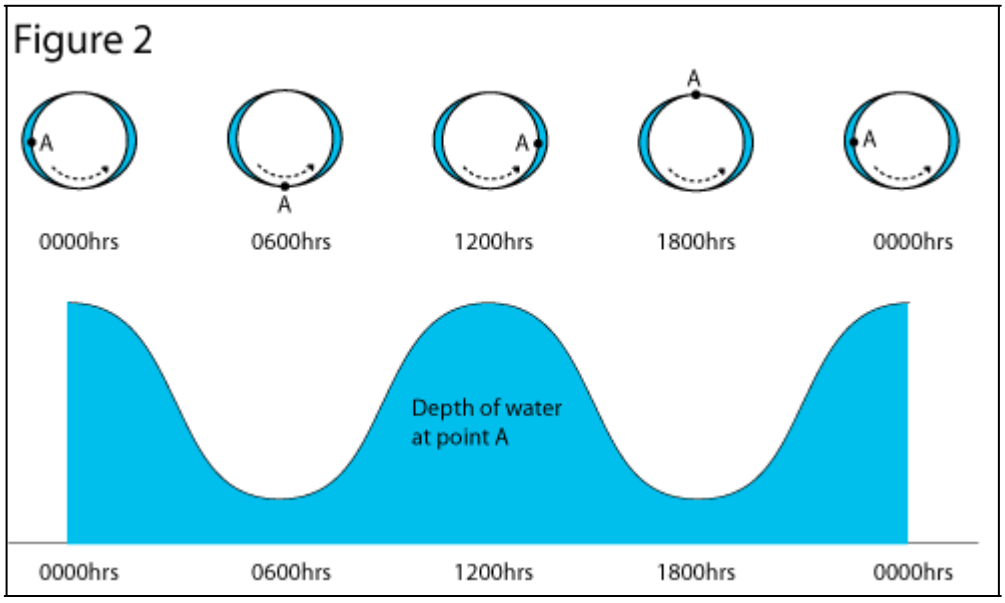

Figure 3.2.2: A place on the Earth experiences two high tides and two low tides (Source: NOAA)

Another way of looking at it is as a "system" undergoing a regular cycle of forces. Any point on the earth's surface experiences the full cycle tidal forces from the moon in each 24 hour 50 minute period. This regularly changing set of tidal forces causes the water to oscillate. This is like any object or structure - solid or fluid - which is made to oscillate by a force which has a steady frequency. If for example, one fill a basin with water and then move his hand back and forth in it to a regular rhythms, quite an impressive oscillation can build up. Such a system will oscillate at the same frequency as the forces applied to it. In figure 3.2.2 it is also seen that the water level changes smoothly in response to the forces. This is typical of oscillations and waves of various kinds. There are no sudden jerky movements (it is called harmonic motion).

3.2.2 Complex Tidal Patterns

Life would be very simple if the earth was covered with a single ocean of even depth. Then the tide everywhere would be like figure 3.2.2. But the earth is irregular, oceans vary in depth and each ocean basin has its own natural frequency for oscillations, and also water has to flow in and out of narrow gaps between land masses in order to get to where the high tide is. So the pattern of the tidal oscillation is quite complicated and differs depending on the position on the earth.

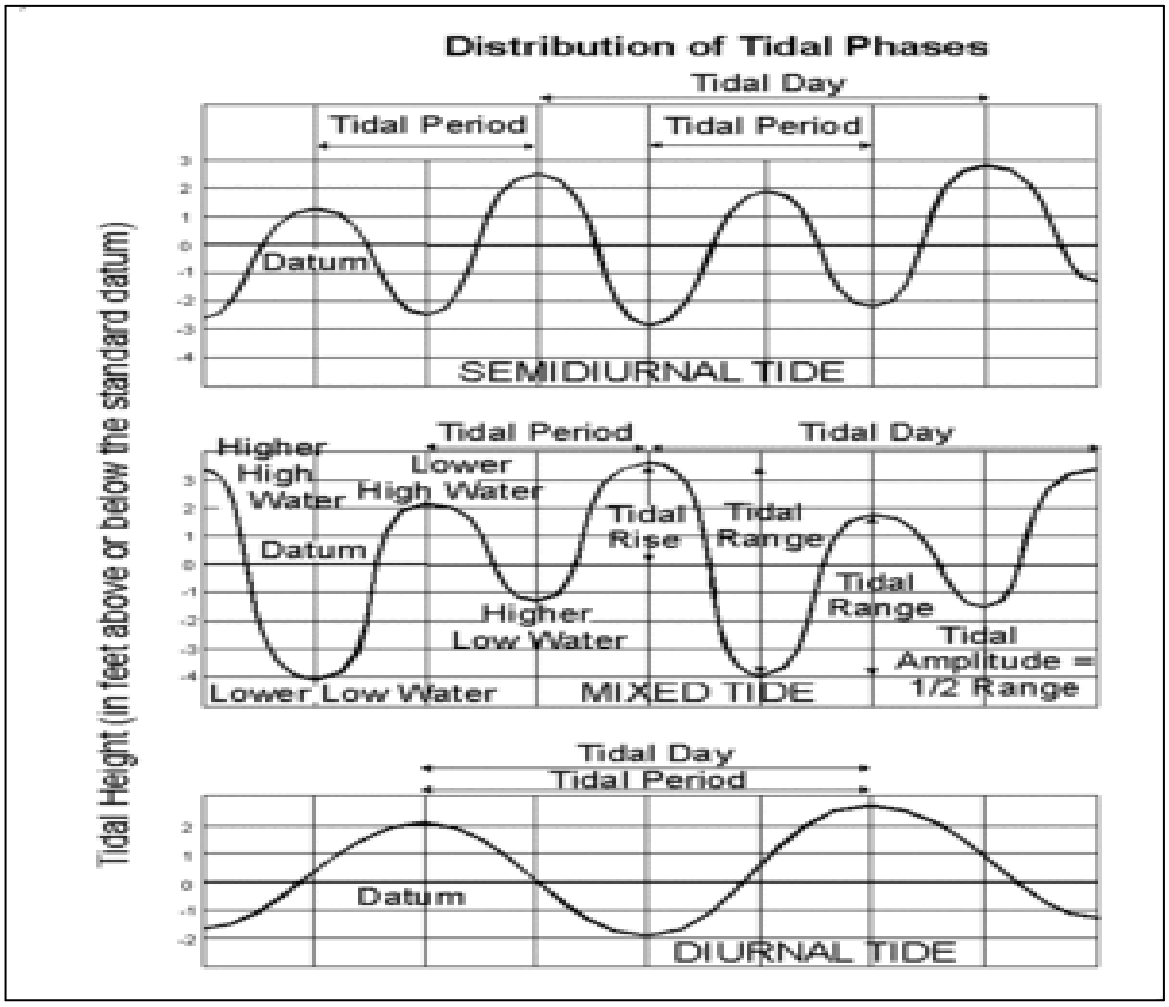

Figure 3.2.3: Types of Tides (Source: Sumich, 1996)

Most places in the ocean usually experience two high tides and two low tides each day (semidiurnal tide), but some locations experience only one high and one low tide each day (diurnal tide). The times and amplitude of the tides at the coast are

influenced by the alignment of the Sun and Moon, by the pattern of tides in the deep ocean and by the shape of the coastline and near-shore bathymetry.

Tides vary on timescales ranging from hours to years due to numerous influences. To make accurate records, tide gauges at fixed stations measure the water level over time. Gauges ignore variations caused by waves with periods shorter than minutes. These data are compared to the reference (or datum) level usually called mean sea level. While tides are usually the largest source of short-term sea-level fluctuations, sea levels are also subject to forces such as wind and barometric pressure changes, resulting in storm surges, especially in shallow seas and near coasts. Tidal phenomena are not limited to the oceans, but can occur in other systems whenever a gravitational field that varies in time and space is present. For example, the solid part of the Earth is affected by tides, though this is not as easily seen as the water tidal movements.

In most European coastal areas the tide is semi-diurnal, but some parts of the English south coast have a tidal pattern which is very different from the simple harmonic pattern in figure 3.2.2. This is usually because of the way the water flows round headlands and in and out of complex waterways. One can get double high tides or prolonged **stands** - periods when the tide does not rise or fall.

Despite that, the system behaves in a predictable way. Wherever one is, the pattern of tides - however complex - will repeat itself in time with the forces that are causing it. One could imagine holding a tray of water with a scale model of the Bay of Bengal on it. One tips it slowly one way and the other with a regular rhythm. The water in different places won't all move at exactly the same time; there will be a delay as the water pushes up the bay and swirls round the corners. But the motion, however complicated, will repeat itself exactly in time with the tipping of the tray (Sumich, 1996).

3.2.3 Diurnal Tides

The origin of semi-diurnal tide has already been explained, but what about diurnal tides? It is known that even semi-diurnal tides are often of unequal amplitude and in

some places the tides are entirely diurnal. Thus we get diurnal inequalities. Diurnal tides are affected by the changes in solar and lunar declination. Fig 3.2.4 shows, in an exaggerated form, how the declination produces an asymmetry between the two high and two low water levels observed at the mid-latitude point **P** as it rotates under the two bulges. Both water levels are equal at the equator, but in high latitudes one high water disappears altogether.

The maximum lunar monthly declination north and south of the equator varies from 18.3° to 28.6° over the 18.6 year nodal period. The solar declination varies seasonally from 23.5° in June to –23.5° in Dec. Thus the combined effect of the sun and the moon will increase the diurnal effect on the tides when their combined declinations are both large, either in the same or opposite sense. Thus the greatest diurnal effects occur when the moon is full, at solstices, ie in June and December in the Southern Hemisphere (Moyer, 1996).

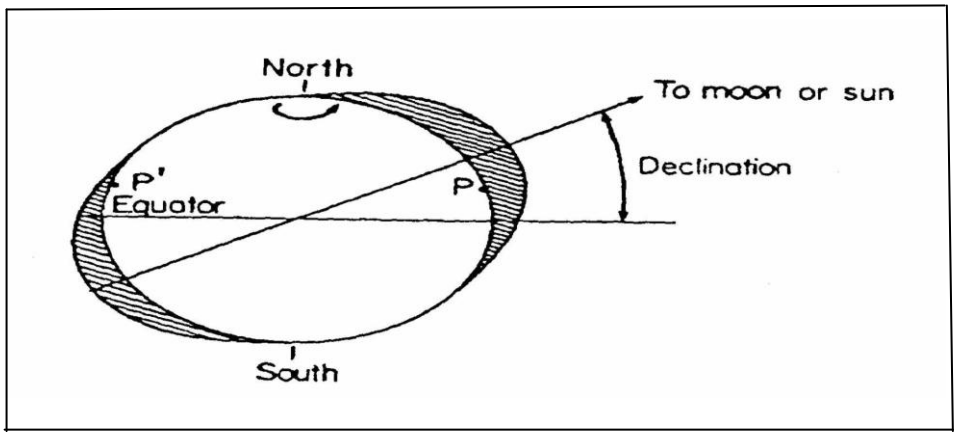

Figure 3.2.4 Effects of declination, diurnal tide generation (Source: Moyer, 1996)

3.2.4 Tidal Characteristics

Tide changes proceed via the following stages:

- Sea level rises over several hours, covering the intertidal zone; flood tide.
- The water rises to its highest level, reaching high tide.
- Sea level falls over several hours, revealing the intertidal zone; ebb tide.
- The water stops falling, reaching low tide.

Tides produce oscillating currents known as tidal streams. The moment that the tidal current ceases is called slack water or slack tide. The tide then reverses direction and is said to be turning. Slack water usually occurs near high water and low water. But there are locations where the moments of slack tide differ significantly from those of high and low water.

Tides are most commonly semidiurnal (two high waters and two low waters each day), or diurnal (one tidal cycle per day). The two high waters on a given day are typically not the same height (the daily inequality); these are the higher high water and the lower high water in tide tables. Similarly, the two low waters each day are the higher low water and the lower low water. The daily inequality is not consistent and is generally small when the Moon is over the equator. Semidiurnal range differences occur when there are two high tides each day with different heights (and two low tides also of different heights), the pattern is called a mixed semidiurnal tide. (Moller, 1996)

3.2.5 Tidal Constituents

Tidal changes are the net result of multiple influences that act over varying periods. These influences are called tidal constituents. The primary constituents are the Earth's rotation, the positions of Moon and the Sun relative to Earth, the Moon's altitude (elevation) above the Earth's equator, and bathymetry. Variations with periods of less than half a day are called harmonic constituents. Conversely, cycles of days, months, or years are referred to as long period constituents. The tidal forces affect the entire earth, but the movement of the solid Earth is only centimetres. The atmosphere is much more fluid and compressible so its surface moves kilometres, in the sense of the contour level of a particular low pressure in the outer atmosphere.

3.2.6 Principal Lunar Semidiurnal Constituent

In most locations, the largest constituent is the "principal lunar semidiurnal". Its period is about 12 hours and 25.2 minutes, exactly half a tidal lunar day, which is the average time separating one lunar zenith from the next, and thus is the time required for the Earth to rotate once relative to the Moon. Simple tide clocks track this

constituent. The lunar day is longer than the Earth day because the Moon orbits in the same direction the Earth spins.

The Moon orbits the Earth in the same direction as the Earth rotates on its axis, so it takes slightly more than a day—about 24 hours and 50 minutes—for the Moon to return to the same location in the sky. During this time, it has passed overhead (culmination) once and underfoot once (at an hour angle of 00:00 and 12:00 respectively), so in many places the period of strongest tidal forcing is the above mentioned, about 12 hours and 25 minutes. The moment of highest tide is not necessarily when the Moon is nearest to zenith or nadir, but the period of the forcing still determines the time between high tides.

Because the gravitational field created by the Moon weakens with distance from the moon, it exerts a slightly stronger tidal force on the side of the Earth facing the Moon than on the opposite side. The Moon thus tends to "stretch" the Earth slightly along the line connecting the two bodies. The solid Earth deforms a bit, but ocean water, being fluid, is free to move much more in response to the tidal force, particularly horizontally. As the Earth rotates, the magnitude and direction of the tidal force at any particular point on the Earth's surface change constantly; although the ocean never reaches equilibrium there is never time for the fluid to "catch up" to the state it would eventually reach if the tidal force were constant—the changing tidal force nonetheless causes rhythmic changes in sea surface height (David, 1999).

3.2.7 Mathematical Treatment of Tidal Force

Revolution of the earth/moon system introduces a centripetal force. The horizontal component of the difference between the gravitational and centripetal force is what ‘drives’ the tides. These horizontal tidal tractive forces are very small and are inversely proportional to the cube of the distance between the earth and the moon but because they are not balanced forces they cause water movement. Their distribution on the earth’s surface is shown in Fig 3.2.5. The pattern created by these tide producing forces produce bulges of water over the areas on the near and far sides to the moon where the forces are directed outward from the earth’s surface. Depressions are noted between these areas where the forces are directed inwards. Figure 3.2.5

shows an imaginary earth covered with water, having no land masses, and the effect of the tide producing forces.

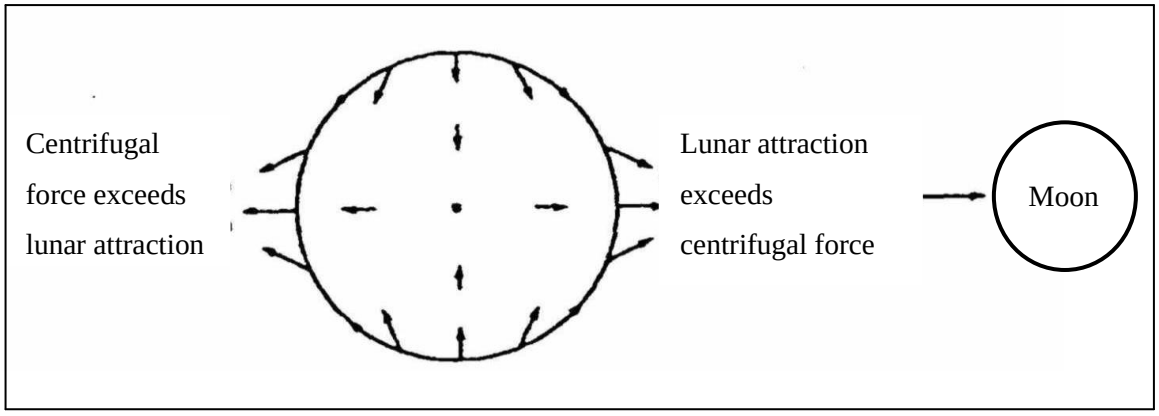

Figure 3.2.5: Distribution of the horizontal tidal tractive forces on the earth's surface (Source: Moyer, 1996)

By Newton's law of universal gravitation and laws of motion, a body of mass m distance R from the center of a sphere of mass M feels a force $\vec{F}$ equivalent to an acceleration $\vec{a}$, where:

$$\vec{F} = -\vec{r}G\frac{Mm}{R^2} \quad \text{.....(3.2.1)}$$

$$\vec{a} = -\vec{r}G\frac{M}{R^2} \quad \text{.....(3.2.2)}$$

Where $\vec{r}$ is a unit vector pointing from the body M to the body m (here, acceleration from m towards M has negative sign). Considering now the acceleration due to the sphere of mass M experienced by a particle in the vicinity of the body of mass m. With R as the distance from the center of M to the center of m, let Δr be the (relatively small) distance of this other particle from the center of the body of mass m. For simplicity, distances are first considered only in the direction pointing towards or away from the sphere of mass M. If the body of mass m is itself a sphere of radius Δr, then the new particle considered may be located on its surface, at a distance (R ± Δr) from the centre of the sphere of mass M, and Δr may be taken as positive where the particle's distance from M is greater than R. Leaving aside whatever gravitational acceleration may be experienced by the particle towards m on

account of m's own mass, we have the acceleration on the particle due to gravitational force towards M as:

$$\vec{a} = -\vec{r}G\frac{M}{(R\pm\Delta r)^2} \quad \text{(3.2.3)}$$

Pulling out the R^2 term from the denominator gives:

$$\vec{a} = -\vec{r}G\frac{M}{R^2}\frac{1}{(1\pm\Delta r/R)^2} \quad \text{(3.2.4)}$$

The Maclaurin series of $1/(1 + x)^2$ is $1 – 2x + 3x^2 – ...$, which gives a series expansion of:

$$\vec{a} = -\vec{r}G\frac{M}{R^2} \pm \vec{r}G\frac{2M}{R^2}\frac{\Delta r}{R}\text{-} \quad \text{(3.3.5)}$$

The first term is the gravitational acceleration due to M at the center of the reference body m, i.e. at the point where Δr is zero. This term does not affect the observed acceleration of particles on the surface of m because with respect to M, m (and everything on its surface) is in free fall. Effectively, this first term cancels. The remaining (residual) terms represent the difference mentioned above and are tidal force (acceleration) terms. Where Δr, is small compared to R, the first of the tidal acceleration terms is usually much more significant than the others, giving for the tidal acceleration $\vec{a}_t$(axial) for the distances Δr considered, along the axis joining the centers of m and M:

$$\vec{a}_{t(axial)} \approx \pm\vec{r}2\Delta rG\frac{M}{R^3} \quad \text{(3.2.6)}$$

When calculated in this way for the case where Δr is a distance along the axis joining the centers of m and M, $\vec{a}_t$ is directed outwards, relative to the center of m where Δr is zero. Tidal accelerations can also be calculated away from the axis connecting the bodies m and M, requiring a vector calculation. In the plane perpendicular to that axis, the tidal acceleration is directed inwards (towards the center where Δr is zero), and its magnitude is $|\vec{a}_t(axial)|$ / 2 in linear approximation as in Figure 3.2.5.

The tidal accelerations at the surface of planets in the Solar System are generally very small. For example, the lunar tidal acceleration at the Earth's surface along the

Moon-Earth axis is about 1.1×10^{-7} g, while the solar tidal acceleration at the Earth's surface along the Sun-Earth axis is about 0.52×10^{-7} g, where g is the gravitational acceleration at the Earth's surface. Modern estimates put the size of the tide-raising force (acceleration) due to the Sun at about 45% of that due to Moon (Bretana, 1987).

3.2.8 Spring Tides and Neap Tides: Range variation

Both the moon and the sun cause a tidal effect. The moon's is 2.5 times greater than the sun because the moon is closer. The semidiurnal range (the difference in height between high and low waters over about a half day) varies in a two-week cycle. Approximately twice a month, around new moon and full moon when the Sun, Moon and Earth form a line the tidal force due to the Sun reinforces that due to the Moon, the tidal effect is stronger because the sun and moon's tidal forces are combined; the sun and the moon's "double bulge" effect reinforce each other, and this causes bigger tides known as **Spring Tide or** just springs. It is not named after the season but, like that word, derives from an earlier meaning of "jump, burst forth, rise" as in a natural spring. This happens when the moon is full (opposite side of the earth to the sun) or new (same side as the sun), as shown in figure 3.2.6. It takes a couple of days for this to produce the largest tides, so they occur a couple of days after the new and full moons.

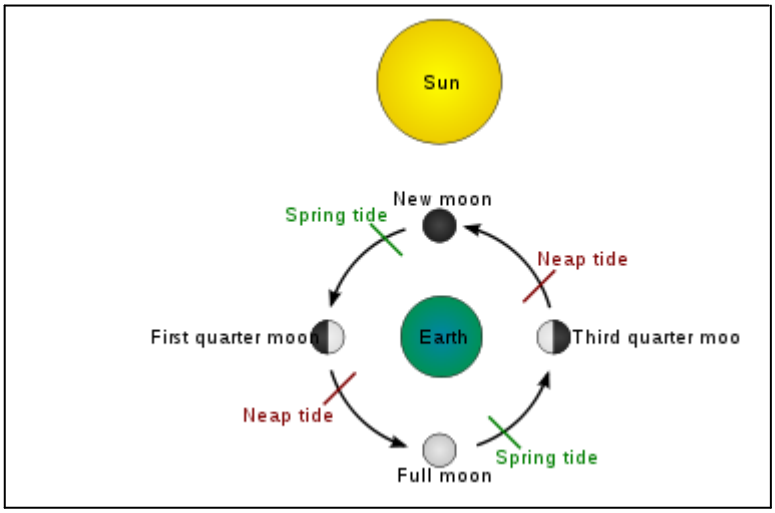

Figure 3.2.6: Two spring and two neap tides in a lunar month (Source: Sumich, 1996)

When the Moon is at first quarter or third quarter, the Sun and Moon are separated by 90° when viewed from the Earth, and the solar tidal force partially cancels the Moon's. At these points in the lunar cycle, the tide's range is at its minimum: this is called the neap tide, or neaps (a word of uncertain origin). Spring tides result in high waters that are higher than average, low waters that are lower than average, 'slack water' time that is shorter than average and stronger tidal currents than average. Neaps result in less extreme tidal conditions. There is about a seven-day interval between springs and neaps. (Swerdlow, 1984)

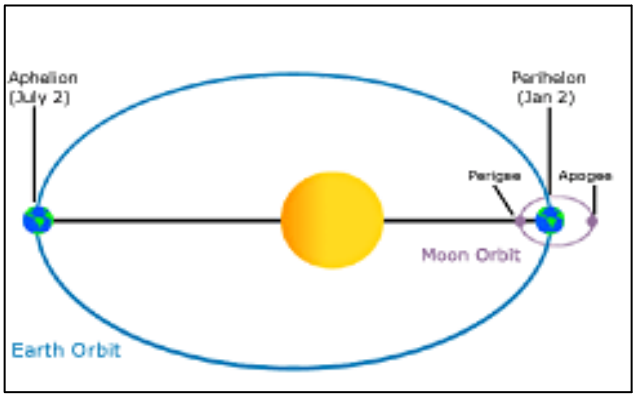

Figure 3.2.7: Elliptical orbits of the Moon around the Earth and the Earth around the Sun: effects on the earth's tide (Source: NOAA).

3.2.9 Lunar Altitude

The changing distance separating the Moon and Earth also affects tide heights. When the Moon is at perigee, the range increases, and when it is at apogee, the range shrinks. Just as the angles of the sun, moon and Earth affect tidal heights over the course of a lunar month, so do their distances to one another. Because the moon follows an elliptical path around the Earth, the distance between them varies by about 31,000 miles over the course of a month. Once a month, when the moon is closest to the Earth (at perigee), tide-generating forces are higher than usual, producing above-average ranges in the tides. Every 7½ lunations (the full cycles from full moon to new to full), perigee coincides with either a new or full moon causing perigean spring tides with the largest tidal range. If a storm happens to be moving onshore at this

time, the consequences (property damage, etc.) can be severe. About two weeks later, when the moon is farthest from the Earth (at apogee), the lunar tide-raising force is smaller, and the tidal ranges are less than average. A similar situation occurs between the Earth and the sun. When the Earth is closest to the sun (perihelion), which occurs about January 2 of each calendar year, the tidal ranges are enhanced. When the Earth is furthest from the sun (aphelion), around July 2, the tidal ranges are reduced (Sumich, J.L., 1996; Thurman, H.V., 1994).

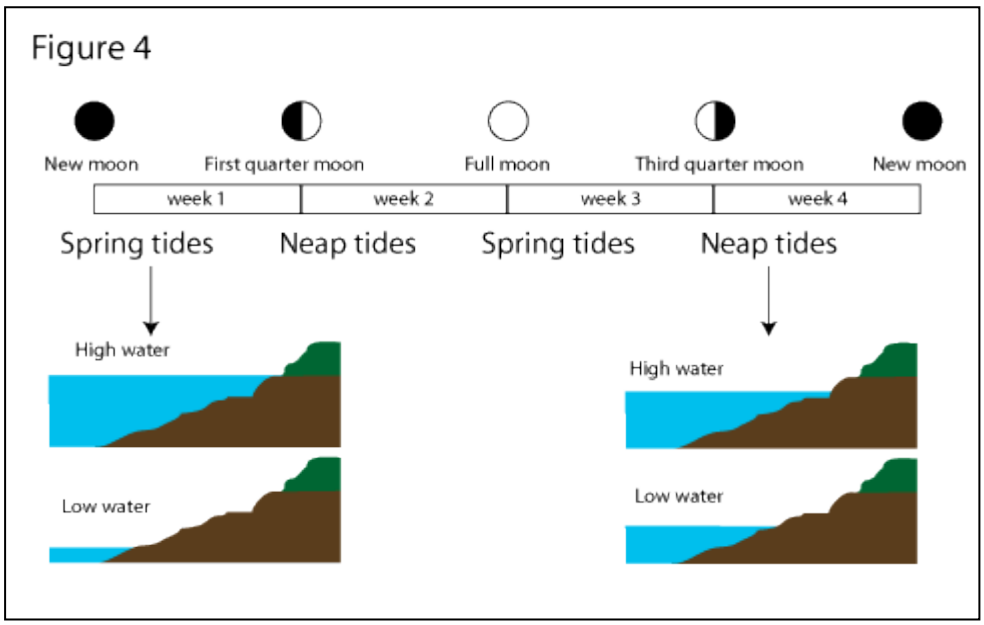

Figure 3.2.8: Sequence of spring and neap tides. (Source: Sumich, 1996)

3.2.10 Bathymetry

The shape of the shoreline and the ocean floor changes the way that tides propagate. So there is no simple, general rule that predicts the time of high water from the Moon's position in the sky. Coastal characteristics such as underwater bathymetry and coastline shape mean that individual location characteristics affect tide forecasting; actual high water time and height may differ from model predictions due to the coastal morphology's effects on tidal flow. However, for a given location the relationship between lunar altitude and the time of high or low tide (the lunitidal interval) is relatively constant and predictable, as is the time of high or low tide relative to other points on the same coast. For example, the high tide at Norfolk,

Virginia, predictably occurs approximately two and a half hours before the Moon passes directly overhead.

Land masses and ocean basins act as barriers against water moving freely around the globe, and their varied shapes and sizes affect the size of tidal frequencies. As a result, tidal patterns vary. For example, in the U.S., the East coast has predominantly semi-diurnal tides, as do Europe's Atlantic coasts, while the West coast predominantly has mixed tides (Thurman, 1994).

3.2.11 Current

The tides' influence on current flow is much more difficult to analyse, and data is much more difficult to collect. A tidal height is a simple number which applies to a wide region simultaneously. A flow has both a magnitude and a direction, both of which can vary substantially with depth and over short distances due to local bathymetry. Also, although a water channel's center is the most useful measuring site, mariners object when current-measuring equipment obstructs waterways. A flow proceeding up a curved channel is the same flow, even though its direction varies continuously along the channel. Surprisingly, flood and ebb flows are often not in opposite directions. Flow direction is determined by the upstream channel's shape, not the downstream channel's shape. Nevertheless, current analysis is similar to tidal analysis: in the simple case, at a given location the flood flow is in mostly one direction, and the ebb flow in another direction. Flood velocities are given positive sign, and ebb velocities negative sign. Analysis proceeds as though these are tide heights.

In more complex situations, the main ebb and flood flows do not dominate. Instead, the flow direction and magnitude trace an ellipse over a tidal cycle (on a polar plot) instead of along the ebb and flood lines. In this case, analysis might proceed along pairs of directions, with the primary and secondary directions at right angles. An alternative is to treat the tidal flows as complex numbers, as each value has both a magnitude and a direction.

Tide flow information is most commonly seen on nautical charts, presented as a table of flow speeds and bearings at hourly intervals, with separate tables for spring and neap tides. The timing is relative to high water at some harbour where the tidal behaviour is similar in pattern, though it may be far away.

3.3 Theory of Mathematical Modeling

A natural phenomenon can be represented through mathematical formulation (development of differential equations) considering all parameters involved with that particular phenomenon. When the partial differential equations for a certain problem are defined properly, together with required initial and boundary conditions, solution can be sought. There are two types of methods for solving partial differential equations such as: analytical methods and numerical methods.

3.3.1 Analytical Method

The solution of partial differential equations for certain boundary conditions can sometimes be obtained analytically. This method is not as powerful as solving partial differential equations numerically. However, analytical method must not be neglected. In general, they give more insight into the characteristics of the solutions than the numerical methods. In this respect, analytical and numerical methods are complementary.

For linear and quasi-linear equations and domain of regular geometry, it is possible to obtain an exact solution by analytical methods. This is often obtained by separation of variables or by applying a transformation that makes the separation of variables possible. Occasionally, the complex variable technique, the Greens function approach, the Laplace or Fourier transformation of the partial differential equation leads to an exact solution (Fletcher, 1991). However, problems involving non-linear equations and regions of irregular geometry (an open channel) are generally intractable analytically. In general, the partial differential equations in water resources engineering cannot be solved analytically.

3.3.2 Numerical Methods

Most differential equations in Water Resources Engineering cannot be solved analytically without simplification. Analytical treatment of the differential equations often with certain simplification is mainly meant to obtain qualitative insight into the characteristics of the solutions. For quantitative information, numerically solving the differential equations, with the modern digital computer is a powerful method. The exact or analytical solutions of the differential equations are usually continuous functions in the time-space domain. When the differential equations are solved numerically, the solutions are obtained at a finite number of grid points or nodes in the time-space domain (Halim and Faisal, 1995). This is done by replacing the differential equations by the difference equations (e.g. $\partial U/\partial t \rightarrow \Delta U/\Delta t$).

Computer-based numerical methods are now-a-days practically the major tools for solving surface and subsurface flow and contaminant transport forecasting problems as encountered in practice. In recent years, parallel to the advance in computer technology, much effort has been devoted to the development of the methodology and technique for numerical simulation of partial differential equations, which govern the flow of water in the open channel of various types. There are several numerical methods available for the solution of differential equations. The methods can be classified in to the following three categories.

1. Finite difference method
2. Finite element method
3. Method of characteristics

In this study finite difference method has been used to solve the hydrodynamic equations of DIVAST model. Different aspects of this method have been illustrated in the following sections.

3.3.3 Finite Difference Method

The finite difference method is a numerical technique of solving the differential equations in which the derivatives are replaced by finite difference quotients so that the governing differential equations are converted into a set of algebraic finite

difference equations. These later equations are solved numerically, usually on a digital computer.

Differential equation: Numerical Scheme: Finite difference equation:

$\frac{\partial f}{\partial t} + \frac{\partial f}{\partial x} = 0$

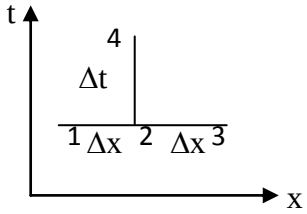

$\frac{f4-f2}{\Delta t} + \frac{f3-f1}{2\Delta x} = 0$

derivatives discretization with nodal points finite difference quotients

Fig.3.3.1 Relation between partial differential equation, numerical scheme and finite difference equation

The governing equations are solved at a finite number of grid points within the considered domain. Suppose, the differential equations to be solved involved two independent variables x and t, then an (x, t) diagram (Figure.3.3.2) constitutes the solution domain and the dependent variables can be defined at any point on the (x, t) plane within the end boundaries. As it is impossible to obtain solutions for the dependent variables at all points on the (x, t) diagram, the numerical solutions are obtained only at some fixed grid points, the choice of which depends on the features of the problem and the finite difference scheme to be used.

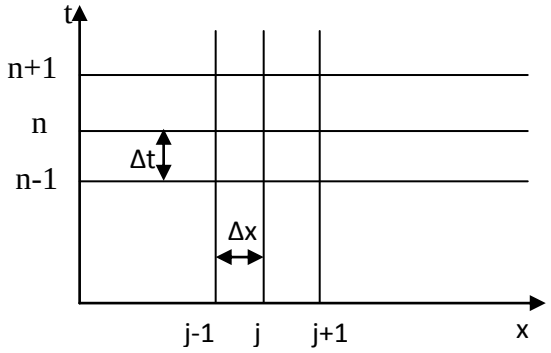

Figure.3.3.2 Finite difference computational grid in (x,t) plane

The computational grid may be uniform in space (along the x-axis) in which case there are (J-1) equal space intervals Δx. If the grid in not uniform, space intervals Δx are of variable length. In general the discretization along x-axis may be described as a set of points $x_j = j\Delta x, j = 1, 2, 3, \ldots., J$; $\Delta x_j = x_{j+1} - x_j$. In the same way the

discretization in time is defined by a set of points $t_n = n\Delta t, n = 1, 2, 3 \ldots\ldots, N$; $\Delta t_n = t_{n+1} - t_n$. The computational grid in the (x, t) plane is then defined by the set $\{(x_j\ ,\ t_n); j = 1, 2, 3, \ldots., J; n = 1, 2, 3, \ldots\ldots, N\}$. A non uniform computational grid is convenient when one wishes to refine the representation of the phenomena of interest in certain parts of the domain where the flow parameters and/or channel geometry vary more widely.

Concept of Explicit and Implicit schemes:

In a fixed grid finite difference method the Δx and Δt values are fixed to have a rectangular grid in the (x, t) plane as shown in Fugre.3.3.2. There are two basic types of fixed grid finite difference schemes-explicit schemes and implicit schemes. Explicit schemes are those in which the value of a variable at any point at the advance time level (n+1) is computed explicitly from known values at a few adjacent points at the time level n and independently of the other points at the times level n+1. Thus, the equations are arranged to solve for one point at a time and the unknown value is expressed direct in terms of known values.

For stability, the step sizes Δx and Δt of an explicit scheme must be so chosen that the Courant-Friedrichs-Lewy condition (shortly Courant number) is satisfied throughout the computation space which in turn puts a limit on the size of the time step Δt. The FTCS (forward time central space) scheme, the modified Lax scheme and the leap-frog scheme are three examples of the explicit finite difference schemes.

An implicit scheme, on the other hand, solves for a group of points at the advance time level (n+1) which include the unknown values at the time level (n+1) and the known values at the time level n. Thus, in this scheme the unknown values at the unknown time level occurs implicitly in the finite difference form. The method most commonly employed is to solve for entire row, i.e. for all the grid points at the time level (n+1) through the use of simultaneous equations containing the unknowns. This entails a more complicated computer program than the explicit method, but it allows one to use a longer time step than the explicit method without any stability problem. The Crank-Nicholson scheme and the Preissmann scheme are two examples of the implicit finite difference schemes.

Explicit scheme: $\frac{\partial f}{\partial x} = \frac{f_{j+1}^{n} - f_{j-1}^{n}}{2\Delta x}$,……(3.3.1)

$$\frac{\partial f}{\partial t} = \frac{f_{j}^{n+1} - \frac{1}{2}(f_{j+1}^{n} + f_{j-1}^{n})}{\Delta t} \quad \ldots\ldots\ldots\ldots\ldots\ldots\ldots\ldots\ldots\ldots(3.3.2)$$

Implicit scheme: $\frac{\partial f}{\partial x} = \frac{1}{2\Delta x}(f_{j+1}^{n} - f_{j}^{n} + f_{j+1}^{n+1} - f_{j}^{n+1})$……...(3.3.3)

$$\frac{\partial f}{\partial t} = \frac{1}{2\Delta t}(f_{j}^{n+1} - f_{j}^{n} + f_{j+1}^{n+1} - f_{j+1}^{n}) \ldots\ldots\ldots\ldots(3.3.4)$$

In general, the implicit method is more difficult to handle and it requires more computational efforts especially when a system of equations is solved or nonlinear equations are solved. However, it is sometimes more practical to choose an implicit method, especially when different time scales are present in a system of equations. Usually the largest time scale determines the behavior of the system whereas the smallest time scale determines the time-step restriction due to stability condition.

Finite Difference Forms

Another important difference between the finite difference schemes is the way they translate the derivatives into the finite difference quotients. The well-known finite difference forms are

i) Forward difference
ii) Backward difference, and
iii) Central difference

The difference between the difference equation and the original differential equation is called the truncation error or order of approximation. The truncation error, which depends on the form of the finite difference scheme applied, can be determined from an expansion of the Taylor series with respect to a well-chosen reference point, i.e.

$$f(x+\Delta x)=f(x) + \Delta x \frac{\partial f(x)}{\partial x} + \frac{\Delta x^2}{2!}\frac{\partial^2 f(x)}{\partial x^2} + \quad \ldots\ldots\ldots\ldots\ldots\ldots\ldots\ldots\ldots\ldots(3.3.5)$$

$$f(x-\Delta x)=f(x) - \Delta x \frac{\partial f(x)}{\partial x} + \frac{\Delta x^2}{2!}\frac{\partial^2 f(x)}{\partial x^2} - \quad \ldots\ldots\ldots\ldots\ldots\ldots\ldots\ldots\ldots\ldots..(3.3.6)$$

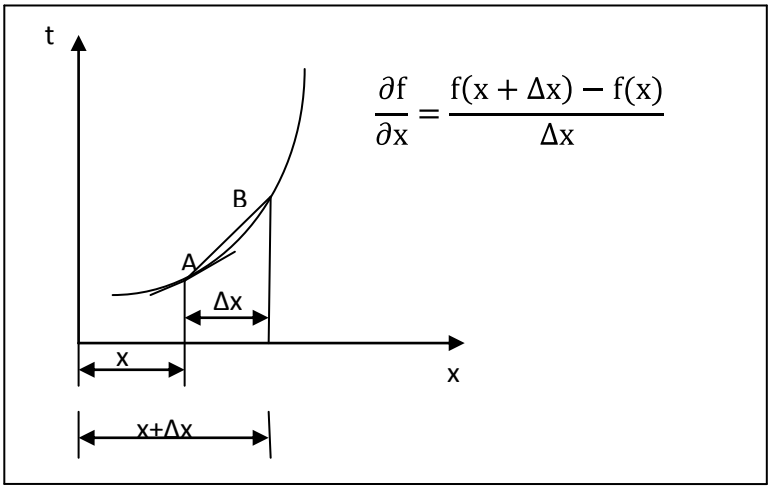

Figure 3.3.3: Forward finite difference form with respect to point A

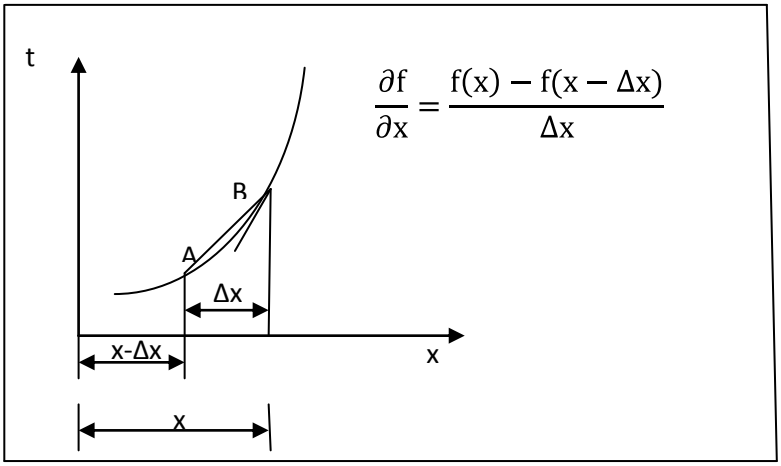

Figure 3.3.4: Backward finite difference form with respect to point B

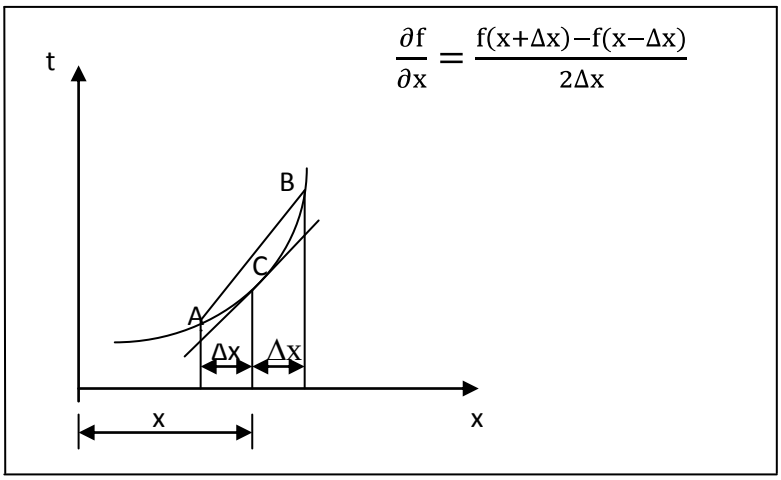

Figure 3.3.5: Central finite difference form with respect to point C

Truncation error or order of approximation

Following truncation errors for the forward, backward and central difference forms are obtained by rearranging equation (2.3.5) and (2.3.6).

$$\frac{\partial f}{\partial x} = \frac{f(x+\Delta x)-f(x)}{\Delta x} - \underbrace{\frac{\Delta x}{2!}\frac{\partial^2 f(x)}{\partial x^2} - \frac{\Delta x^2}{3!}\frac{\partial^3 f(x)}{\partial x^3} - \ldots\ldots\ldots\ldots\ldots\ldots\ldots}_{\text{Forward difference truncation error}} \quad (3.3.7)$$

$$\frac{\partial f}{\partial x} = \frac{f(x)-f(x-\Delta x)}{\Delta x} - \underbrace{\frac{\Delta x}{2!}\frac{\partial^2 f(x)}{\partial x^2} + \frac{\Delta x^2}{3!}\frac{\partial^3 f(x)}{\partial x^3} - \ldots\ldots\ldots\ldots\ldots\ldots\ldots}_{\text{Backward difference truncation error}} \quad (3.3.8)$$

$$\frac{\partial f}{\partial x} = \frac{f(x+\Delta x)-f(x-\Delta x)}{2\Delta x} - \underbrace{\frac{\Delta x^2}{3!}\frac{\partial^3 f(x)}{\partial x^3} - \ldots\ldots\ldots\ldots\ldots\ldots\ldots\ldots\ldots}_{\text{Central difference truncation error}} \quad (3.3.9)$$

Both forward and backward finite difference approximation are first-order accurate. Central finite difference approximation is referred to as second order accurate. It is clear from the above curves and equations that central finite difference form is more accurate than the forward or backward finite difference forms.

Characteristics of finite difference schemes:

Some characteristics are important in solving the finite difference equations such as consistency, stability, convergency and accuracy. A finite difference scheme is said to be consistent or compatible when the truncation error tends to vanish and the solutions to the finite difference equations approach the solution to the differential equations as the computational mesh is refined (i.e. $\Delta x \rightarrow 0$ and $\Delta t \rightarrow 0$). Otherwise, it is inconsistent or incompatible.

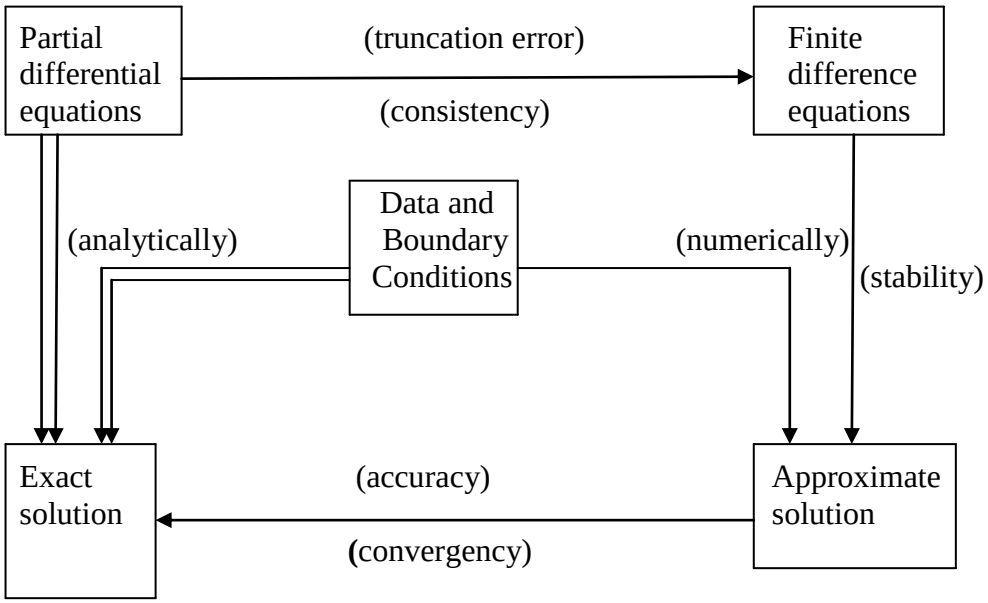

Fig. 3.3.6: Conceptual relationship between consistency, stability and convergency

Stability:

The stability of a finite difference method concerns the amplification errors. These errors may be introduced by inaccurate initial and/or boundary conditions or due to rounding up errors. Stability is tested by asking if a particular part of the solution is likely to amplify without limit until it destroys the calculation.

There is a stability criterion named Courant-Friedrichs-Lewy (CFL) criterion simply called Courant number to check stability of a finite difference scheme.

The conditions for stability of a finite difference scheme may be defined as

$$\Delta t \leq \frac{\Delta x}{\sqrt{gh}} \quad \text{.....(3.3.10)}$$

Or

$$|\sigma| = |\sqrt{gh}|\frac{\Delta t}{\Delta x} \leq 1 \quad \text{.....(3.3.11)}$$

Where, h is the depth of flow and σ is the Courant number.

Convergency:

If the discrete (i.e. numerical) solutions to the governing differential equations approach the exact (i.e. analytical) solutions to the same equations as the computational mesh is refined, i.e. as $\Delta x \rightarrow 0$ and $\Delta t \rightarrow 0$, for a consistent finite difference scheme, then it is said to be a convergent scheme.

Accuracy:

Accuracy is tested by the ability of the finite difference method to reproduce the terms of the differential equation without introducing extraneous terms which are large enough to affect the solutions. A stable finite difference method is not necessarily an accurate one. There are three ways of investigating the accuracy of numerical methods:

i) By determining the truncation error.
ii) By analyzing the wave propagation and comparing the analytical and the numerical solutions.
iii) By doing experiments with different numerical parameters (Δx, Δt etc.).

3.4 DIVAST Model

The numerical model DIVAST (Depth-Integrated Velocities and solute Transport), is a robust and reliable numerical model for solving 2D depth-integrated shallow water equations using a uniform rectangular mesh grid. It has been widely used by many U.K. and overseas consultants, universities and research organizations for both industrial and research projects. DIVAST model was developed using the FORTRAN 77 programming language by Prof. Roger Falconer, Halcrow Professor of Environmental Water Management and Dr. Binliang Lin, both of them from Cardiff School of Engineering, Cardiff University, UK. DIVAST is continually updated and improved by both Prof. Falconer's team in Cardiff University and the MarCon staff.

DIVAST is a two dimensional, depth integrated, hydrodynamic and solute transport, time variant model which has been developed for estuarine and coastal modeling. It

is suitable for water bodies that are dominated by horizontal, unsteady flow and do not display significant vertical stratification. The model simulates two dimensional distributions of currents, water surface elevations and various water quality parameters within a modeling domain as functions of time, taking into account the hydraulic characteristics governed by the bed topography and the boundary conditions.

The DIVAST model is based on the solution of the depth-integrated Navier–Stokes equations and includes the effects of local and advective accelerations, the earth's rotation, free surface pressure gradients, wind action, bed resistance and a simple mixing length turbulence model. The differential equations are written in their pure differential form, thereby allowing momentum conservation in the finite-difference sense. Particular emphasis has been focused in the development of the model on the treatment of the advective accelerations, a surface wind stress and the complex hydrodynamic phenomenon of flooding and drying.

The governing differential equations are solved using the finite difference technique and using a scheme based on the alternating direction implicit (ADI) formulation. The advective accelerations are written in a time centered form for stability, with these terms and the turbulent diffusion terms being centered by iteration. Whilst the model has no stability constraints, there is a Courant number restriction for accuracy in the hydrodynamic module. The finite difference equations are formulated on a space staggered grid scheme, with the water surface elevations and the x-direction velocity components being initially solved for during the first half time step by using Gaussian elimination and back substitution (Falconer, 1992)

3.5 Governing Equations of Model

The DIVAST model has a number of modules for different purposes with different sets of equations. In this study hydrodynamic module has been used. The numerical model used here is based on the solution of the depth-integrated Reynolds averaged Navier–Stokes equations. Full details of the derivation of these depth-integrated

equations are given in Falconer and Chen (1996) but the final representations of the governing equations are cited herein for convenience with the conservations of mass and momentum in the x and y directions.

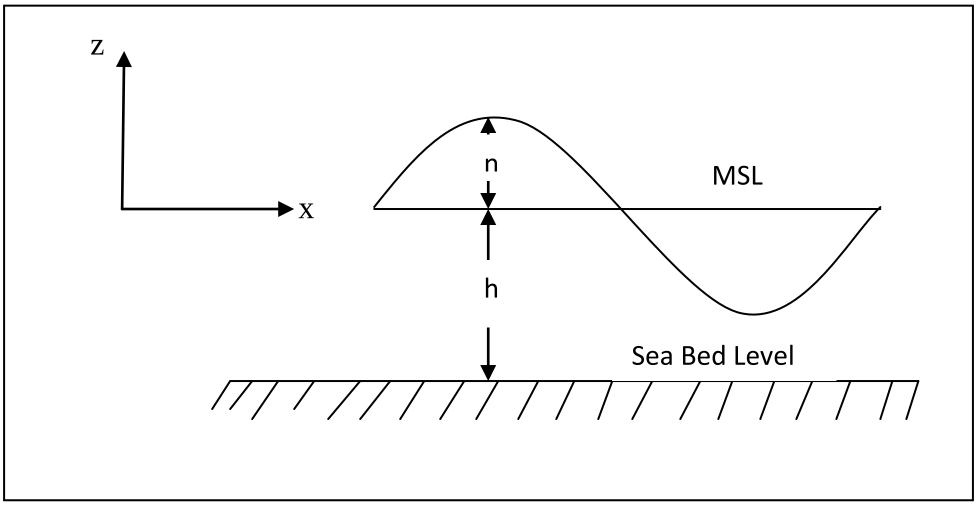

Figure 3.5.1: Definition sketch with notations and co-ordinates

The depth integrated continuity equation:

$$\frac{\partial \eta}{\partial t} + \frac{\partial UH}{\partial x} + \frac{\partial VH}{\partial y} = 0 \quad \ldots\ldots(3.5.1)$$

Where U, V are the depth-average velocity components in the x, y directions, η is water surface elevation due to tide from still water level, H is the total depth of flow (=h + η).

The depth integrated momentum equation:

For x direction:

$$\underbrace{\frac{\partial UH}{\partial t}}_{(1)} + \underbrace{\beta\left[\frac{\partial U^2H}{\partial x} + \frac{\partial UVH}{\partial y}\right]}_{(2)} = \underbrace{fVH}_{(3)} - \underbrace{gH\frac{\partial \eta}{\partial x}}_{(4)} - \underbrace{\frac{H}{\rho}\frac{\partial P_a}{\partial x}}_{(5)} + \underbrace{\frac{\tau_{xw}}{\rho}}_{(6)} - \underbrace{\frac{\tau_{xb}}{\rho}}_{(7)} +$$

$$\underbrace{2\frac{\partial}{\partial x}\left[\bar{\varepsilon}\frac{\partial UH}{\partial x}\right] + \frac{\partial}{\partial y}\left[\bar{\varepsilon}\frac{\partial UH}{\partial y} + \bar{\varepsilon}\frac{\partial VH}{\partial x}\right]}_{(8)} \quad \ldots\ldots(3.5.2)$$

For y direction:

$$\underbrace{\frac{\partial VH}{\partial t}}_{(1)} + \underbrace{\beta\left[\frac{\partial UVH}{\partial x} + \frac{\partial V^2H}{\partial y}\right]}_{(2)} = \underbrace{-fUH}_{(3)} - \underbrace{gH\frac{\partial \eta}{\partial y}}_{(4)} - \underbrace{\frac{H}{\rho}\frac{\partial P_a}{\partial y}}_{(5)} + \underbrace{\frac{\tau_{yw}}{\rho}}_{(6)} - \underbrace{\frac{\tau_{yb}}{\rho}}_{(7)} +$$

$$\underbrace{2\frac{\partial}{\partial y}\left[\bar{\varepsilon}\frac{\partial VH}{\partial y}\right] + \frac{\partial}{\partial x}\left[\bar{\varepsilon}\frac{\partial UH}{\partial y} + \bar{\varepsilon}\frac{\partial VH}{\partial x}\right]}_{(8)} \quad \ldots\ldots\ldots\ldots\ldots\ldots\ldots\ldots\ldots\ldots\ldots\ldots\ldots\ldots(3.5.3).$$

Where, t is the time, x and y the horizontal coordinates toward east and north, U, V are the depth-averaged velocities in x, y direction, H is the total depth of flow (=h+η), η, the water surface elevation due to the tide from the still water level, β is the momentum correction factor for non-uniform vertical velocity profile, P_a is the atmospheric pressure on the sea surface, ρ (=1.03×10^3 kg/m^3) is the seawater density, g is the gravitational acceleration and f is the Coriolis parameter (=2ω sinψ, where ω=7.29×10^{-5} rad/s is the angular speed of the rotation of the earth and ψ is the latitude of grid point). Here, τ_{xw}, τ_{yw}= surface wind shear stress components in x, y direction, τ_{xb}, τ_{yb}= bed shear stress component in x, y direction and $\bar{\varepsilon}$= depth-averaged eddy viscosity.

The individual terms in momentum equations (3.5.2 & 3.5.3) refers to: The local acceleration (term 1); the advective acceleration (term 2); the coriolis acceleration arising as a result of earth's rotation (term 3); the pressure gradient or surface slope (term 4); the barometric pressure gradient (term 5); the surface wind stress (term 6); the bed roughness resistance (term 7) and the turbulent diffusion of momentum (term 8). Similar equation can be obtained in y direction also.

In practical model studies of flow on tidal floodplains and in the absence of extensive field data on the vertical velocity profiles, the momentum correction factor is either set to unity or a vertical velocity profile is assumed. For an assumed logarithmic vertical velocity profile as derived from Prandtl's mixing length hypothesis (Goldstein, 1938), it can readily be shown that the value of β is given by:

$$\beta=\left[1 + \frac{g}{C^2k^2}\right] \quad \ldots\ldots\ldots\ldots\ldots\ldots\ldots\ldots\ldots\ldots\ldots\ldots\ldots\ldots\ldots\ldots\ldots\ldots(3.5.4)$$

where k is the Von Karman's constant (=0.4) and C is Chezy's roughness coefficient.

Alternatively, the term involving u^2dz in the momentum equation may be integrated from bed level to the free surface provided a velocity distribution is specified. Assuming a seventh power low

$$u = u_* \frac{(h+z)^{1/7}}{(h+\eta)^{1/7}} = \frac{8}{7} U \frac{(h+z)^{1/7}}{(h+\eta)^{1/7}} \quad \text{.....(3.5.5)}$$

$$\int_{-h}^{\eta} u^2 dz = \left(\frac{8}{7}U\right)^2 \int_{-h}^{\eta} \frac{(h+z)^{2/7}}{(h+\eta)^{2/7}} dz = \frac{8}{7} X \frac{8}{7} X U^2 \frac{1}{(h+\eta)^{2/7}} \left[\frac{7}{9} X (h+z)^{9/7}\right]$$

$$= 1.016(h + \eta)U^2 \quad \text{.....(3.5.6)}$$

$$\text{So, } \frac{\delta}{\delta x}\int_{-h}^{\eta} u^2 dz = 1.016 \frac{\delta U^2 (h+\eta)}{\delta x} = \beta \frac{\delta U^2 (h+\eta)}{\delta x} \quad \text{.....(3.5.7)}$$

leads to a constant value for β of 1.016.

For the surface wind shear stress components a quadratic friction law is assumed based on a balance of the horizontal forces for a steady uniform flow, giving:

$$\left.\begin{aligned} \tau_{xw} &= C_s \rho_a W_x W_s \\ \tau_{yw} &= C_s \rho_a W_y W_s \end{aligned}\right\} \quad \text{.....(3.5.8)}$$

Where C_s= air-water resistance coefficient, ρ_a= air density, W_x, W_y = wind velocity components in x, y directions and W_s= wind speed ($= \sqrt{W_x^2 + W_y^2}$). Various constant values and formulae have been proposed for the resistance coefficient C_s with one of the most widely used representations being the piecewise formulation (Wu, 1969), giving:

$$\left.\begin{aligned} C_s &= 1.25 \times 10^{-3} W_S^{-0.2} && \text{for } W_s \leq 1 \text{ ms}^{-1} \\ C_s &= 0.5 \times 10^{-3} W_S^{-0.5} && \text{for } 1 < W_s \leq 15 \text{ ms}^{-1} \\ C_s &= 2.6 \times 10^{-3} && \text{for } W_s > 15\, ms^{-1} \end{aligned}\right\} \quad \text{.....(3.5.9)}$$

For most tidal floodplain studies the bed stress is also represented in the form of a quadratic friction law as given by:

$$\left.\begin{aligned}\tau_{xb} &= \rho g U V_s C^{-2} \\ \tau_{yb} &= \rho g V V_s C^{-2}\end{aligned}\right\} \quad \text{.....(3.5.10)}$$

Where V_s= depth-averaged fluid speed (= $\sqrt{U^2 + V^2}$). The Chezy value is determined from the Colebrook–White equation can be used (Henderson, 1966) giving:

$$C = \sqrt{\frac{8g}{f}} = -\sqrt{32g}\ \log_{10}\left[\frac{k_s}{14.84H} + \frac{1.255C}{Re\sqrt{2g}}\right] \quad \text{.....(3.5.11)}$$

Where f = Darcy–Weisbach resistance coefficient, k_s= Nikuradse equivalent sand-grain roughness and R_e= Reynolds number for open channel flows, namely 4 * V_s * H/υ (with υ being the kinematic viscosity of the fluid).

For the depth average eddy viscosity coefficient, the simplest relationship is based on Prandtl's mixing length theory giving

$$\bar{\varepsilon} = C_c U_* H \quad \text{..... (3.5.12)}$$

Where C_c is the constant and U_* is the shear velocity.

3.6 Methodology

Setting up DIVAST Model for Bay of Bengal using Bathymetry data of Bay of Bengal has been summarized in the following sections:

3.6.1 Bathymetry generation for Bay of Bengal Model

The bathymetry data has been collected through field survey campaigns undertaken by the Meghna Estuary Study (MES) Phase I and Phase II. During year 1997 Phase I surveys were carried out. But some shallow areas were not covered during this survey. The shallow areas were surveyed in Phase II during the dry period of 1998 - 1999. The coastline has been formed from the LANDSAT imagery from 1998. To

cover areas outside of the Meghna estuary and topography the following earlier data was included:

- British Admiralty Chart Nos. 814, 829 and 859.
- BIWTA depth charts along the coastline of Chittagong and along the northwestern part of the study Area, datum CD.
- BWDB, Padma River, Upper and Lower Meghna Rivers, datum PWD.
- CSPS design polder levels, datum mPWD.
- Land levels of Bangladesh, Digital Elevation Model, FAP 19, datum PWD.
- Land levels of Khulna-Jessore area, KJDRP, 1997, datum PWD.
- Land levels of Bangladesh, new Digital Elevation Model based on FINNMAP data, datum PWD.
- Coast lines of Bangladesh from LANDSAT imagery from February 1996.

The bathymetry data has been collected from Institute of Water Modelling (IWM) in BTM (Bangladesh Transverse Mercator) co-ordinate system. Then these data has been converted from BTM co-ordinate system to UTM (Universal Transverse Mercator) co-ordinate system and finally it has been converted into corresponding latitude-longitude for setting up the bathymetry of the Bay of Bengal model. As the DIVAST model does not have the option of varying scales of grid squares and has the option to select square grid of constant spacing, grid spacing of 5680 meters has been selected within the model area. The DIVAST model generated Bathymetry of Bay of Bengal model area is shown in Figure3.6.1.

Figure 3.6.1 presents the simplified bathymetric contour map of the model area consists of a two-way nested using a mesh of 181 × 91 grid squares with a constant grid spacing of 5680 m. The model has two open boundaries: the northern boundary is in the Lower Meghna River near Chandpur and the southern boundary is in the open sea located along the line extending from Vishakhapatnam of India to Gwa Bay of Myanmar.

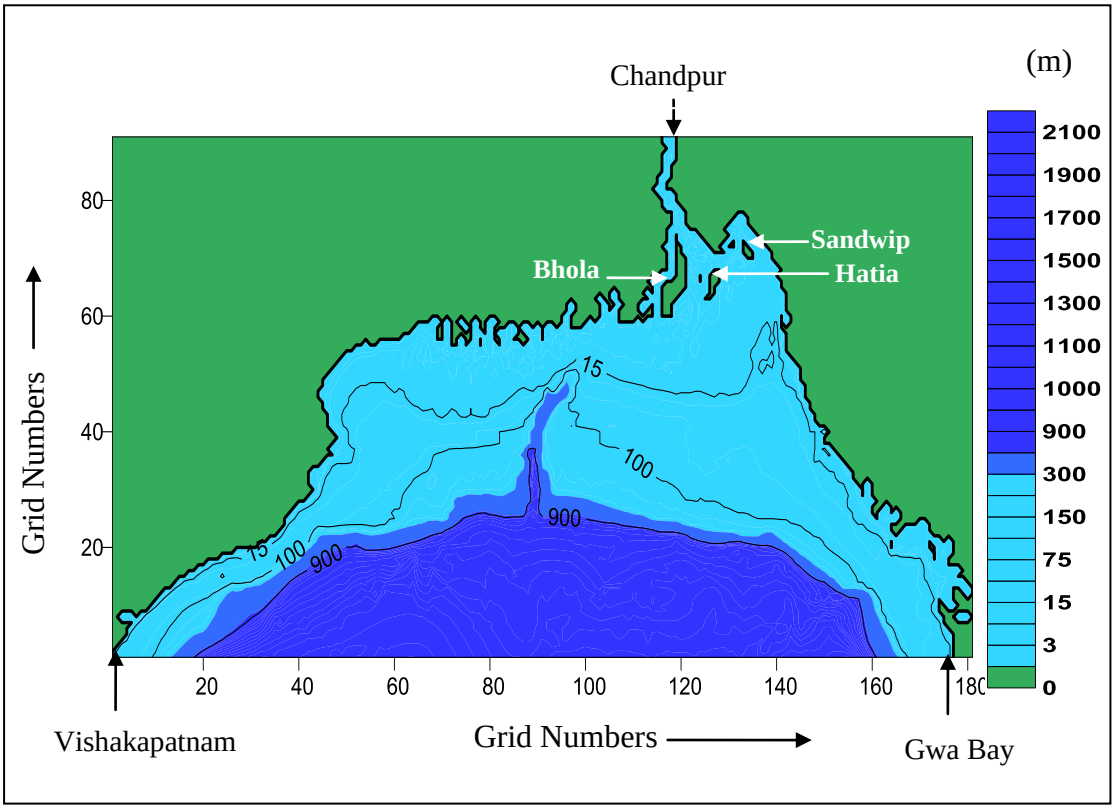

Figure 3.6.1: DIVAST Model Generated Bathymetry of Bay of Bengal

IWM has developed the two-dimensional hydrodynamic model of Bay of Bengal with MIKE 21 flow module. The storm surge modeling study has been done based on the two-dimensional Bay of Bengal model of second CERP. In the (CERP) study the model has been updated with existing data and upgraded in 200 m grid resolution incorporating Sundarban area and it has been extended to the sea up to 16^{o} latitude. The model is two-way nested and includes four different resolution levels (Coarse, intermediate, fine and 200 m grid) in different areas. The Meghna Estuary is resolved on a 600m grid and that of the area of interest for development interventions is resolved on a 200m grid. In this study DIVAST model uses the total model area of Bay of Bengal has one type resolution based on the coarse grid consists of 5680 m square grid size each. So due to this limitation of DIVAST model some small islands and chars in Bay of Bengal are not clearly defined.

Studies reveal that, with the influence of upper region (northern shallower estuarine areas) and the lower region (southern deep sea areas) of the Bay of Bengal the

hydrodynamic behavior of this area has a great concern. Central part of the coastal zone can be described as the zone of transformation of the Meghna River into a wide, shallow shelf followed by a deeper basin. A number of large deltaic islands: Bhola, Hatia and Sandwip are located around the river mouth. The Meghna River falls into the Bay of Bengal through a number of channels: the Tetulia River, the Shahbazpur channel and the Hatia channel (Azam et al., 2000). The coast line of Bangladesh is characterized by a wide continental shelf, especially off the eastern part of Bangladesh. The triangular shape at the head of the Bay of Bengal helps to funnel the sea water pushed by the wind towards the coast and causes further amplification of the tidal levels.

The width of the continental shelf off the coast of Bangladesh varies considerably. It is less than 100 km off the south coast between Hiron Point and the Swatch of no ground and more than 250 km off the coast of Cox's Bazar. Sediments are fine seaward and westward with the thickest accumulation of mud near the submarine canyon, the Swatch of no Ground. The shallow part (less than 20m) of the continental shelf off the coast of Chittagong and Teknaf is covered by sand and the intertidal areas show well-developed sandy beaches. The shallower part of southern continental shelf off the coast of the Sundarbans, Patuakhali and Noakhali is covered by silt and clay and extensive muddy tidal flats are developed along the shoreline. It is known that Swatch of no Ground, a trough-shaped marine valley or canyon that cross the continental shelf diagonally and situated on the south of the Ganges-Brahmaputra Delta, also known as Ganga Trough. Swatch of no Ground has a comparatively flat floor 5 to 7 km wide and walls of about 12° inclination. At the edge of the shelf, depths in the trough are about 1200 m. It is also known that the Swatch of no Ground has a seaward continuation for almost 2000 km down the Bay of Bengal in the form of fan valleys with levees (Banglapedia).

Studies on the Bengal Deep Sea Fan suggest that the sandbars and ridges near the mouth of the Ganga-Brahmaputra delta pointing toward the Swatch of no Ground is the indication of sediments are tunnelled through this trough into the deeper part of the Bay of Bengal. Most of the sediment of the Bengal Deep Sea Fan has been derived from the confluence of Ganges and Brahmaputra Rivers, which drain the

south and north slopes of the Himalayan, respectively. It is concluded that low-density turbidity currents and sand cascading are perhaps dominating process of sediment transport from the shelf to the deep sea through the Swatch of no Ground under the present condition.

3.6.2 Setting up Model with Boundary Condition

Depth Integrated Velocity and Solute Transport (DIVAST) model has been applied to Bay of Bengal with 2001 bathymetry data. DIVAST Model is based on FORTRAN 77 programming language (Navera, 2004). The DIVAST model system has been developed for complex applications with oceanographic, coastal and estuarine environments. The model simulates the water level variations and flows in response to a variety of forcing functions on flood plains, in lakes, estuaries and coastal areas. The Bay of Bengal model area is two-way nested using a mesh of 181 × 91 grid squares with a constant grid spacing of 5680 m. Two open boundaries such as the northern boundary is in the Lower Meghna river near Chandpur and the southern boundary along the immaginary line extended from Vishakhapatnam of India to Gwa Bay of Myanmar are shown in Figure 3.6.2.below.

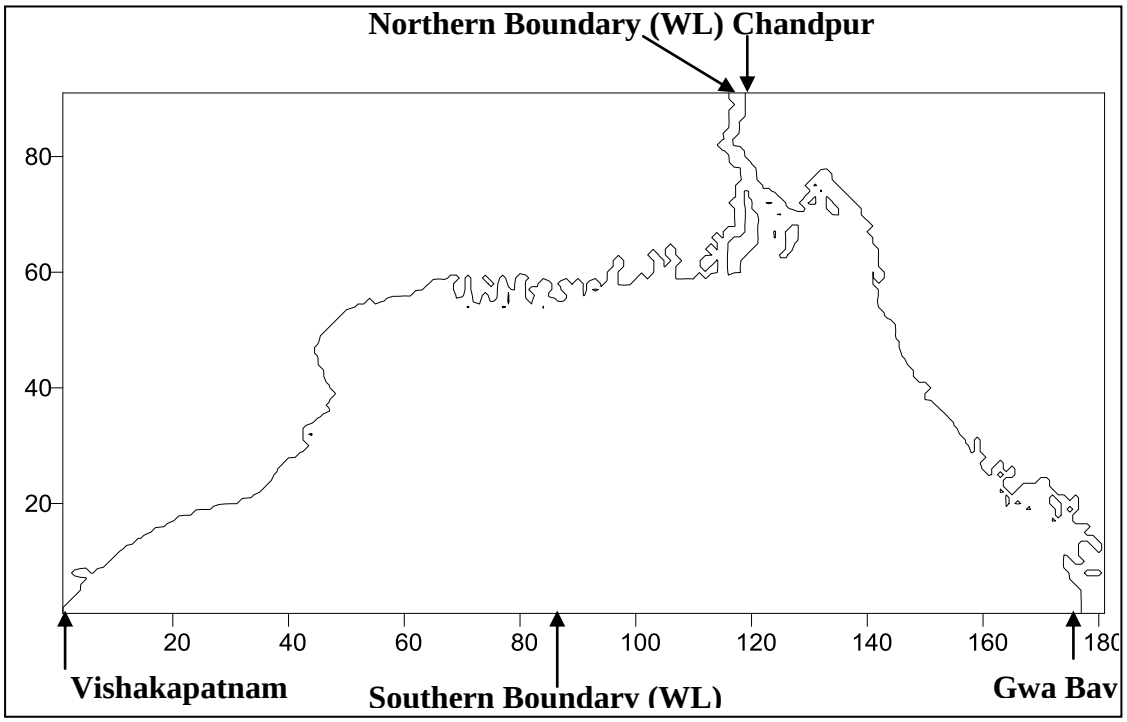

Figure 3.6.2: Northern and Southern Boundary of Bay of Bengal Model

In modeling the hydrodynamic features of Bay of Bengal, it was necessary to introduce the time-varying water level variations at the open seaward southern boundary and also at the northern boundary. For this purpose, the tidal data were obtained for both places, Vishakhapatnam (southern boundary) and Chandpur (northern boundary) to include the initial boundary conditions of the model. The tidal data of both stations named Vishakapatnam and Chandpur were used to set the boundary conditions. The other hydrodynamic input parameters of the model were used after trial and fine tuning, to calibrate and verify the model. The important input parameters used after trial and fine tuning for calibration and verification of model are shown in Table 3.6.1.

Tidal water velocity has been simulated for continuous 62 hours (five tidal cycles) and each tidal cycle is of 12.4 hours. The each simulated tidal level and velocities outputs are after 1.55 hours and there are total 40 tidal level and velocity outputs for five tidal cycles. The time step of 60 seconds is considered to ensure the stability of the numerical scheme. The model has attained stability by maintaining the Courant number ($g^{1/2}h^{1/2}\Delta t/\Delta s$) less than or equal to 1, in which Δt is the computational time step of 60 s and Δs is the grid spacing of 5680 m. As the model area is considerable big and model has the option of selecting only one type scale of grid spacing for simulating tidal velocity, each grid size of Bay of Bengal is considered as 5680 m.

3.6.3 Model Input Data

Reliable data are prerequisite to carry out model study. Water level data has been collected from BWDB. Bathymetry data, velocity data, boundary data, have been collected from IWM. Model input data can be divided into following groups:

- Domain and Time Parameters:
  - Computational square mesh and bathymetry.
  - Simulation length and overall time step.
- Calibration Factors:
  - Bed resistance.
  - Momentum correction factors.

- Wind friction factors.
- Eddy viscosity coefficient.

- Initial Conditions:
  - Water surface level.
  - Velocity components.
- Boundary conditions:
  - Water level.
  - Discharge.
- Other driving forces:
  - Wind speed and direction.
  - Tidal cycle and tidal period.
  - Time phase lag.

The following parameters have been selected after several trials. These parameters are needed for calibration of the model to simulate the tidal velocities:

Table 3.6.1: Input Parameters used for calibration of Model

Model Input	**Meaning of Parameters**	**Value**
TIMESM	Time of simulation in hrs	62
HDT	Half time step in seconds	30
RUFFMM	Value of roughness length k (mm)	40
VISCMM	Kinematic viscosity of fluid (mm^2/sec)	1.31
REMIN	Minimum Reynolds number	1000
BETA	Momentum correction factor for non-uniform velocity distribution	1.016
COED	Eddy viscosity coefficient for non-uniform velocity distribution	0.15
GAMMA	Longitudinal dispersion coefficient	13

DELTA	Lateral turbulent diffusion coefficient	1.20
ADDIS	Additional dispersion-diffusion term	5.0
WINDIS	Wind induced dispersion coefficient	0.0
WINDSPD	Absolute wind speed (m/s)	15.0
DENAIR	Density of air	1.25
DENWAT	Density of water	1026.00
CFSURF	Air-water interfacial friction coefficient	0.0026
GAMSUS	Gamma for suspended sediments	4.07
SPECWT	Specific weight of suspended sediments	2.65
DIAM50	Mean grain diameter in meters	0.0004

The model has option to change the eddy viscosity (ε) each after 12 minutes and Chezy's C with the changes of depth of the bed level. Due to the changes of the Chezy's C, the bed shear stress or resistance also changes due to the variation of the depth of the bed level.

3.6.4 Solution Technique by Finite Difference Schemes

To solve the governing differential equations for the hydrodynamic processes, the partial differential equations are replaced by finite difference equations on the computational mesh based upon Taylor's series approximation. There are three different ways to express the partial differential equation into finite difference representations such as forward, backward or centrally in space time-marching explicit solutions, where the unknown value can be calculated directly from known values without solving a matrix; and implicit solutions, where the unknown value is represented in terms of other neighbouring unknowns.

There must be consistency between finite difference equation and the partial differential equation so that both equations describe the same physical phenomena. The finite difference scheme must be stable so that the cumulative effects of all round-off errors of a computer at any stage of computation are negligible and that the computed solutions only differ insignificantly from the exact solutions of the differential equation. The convergence condition relates the computed solution of the finite difference equation to the exact solution of the partial differential equation. The accuracy criterion defines the permissible magnitudes of the truncation error for a finite difference scheme.

Alternating Direction Implicit method a special type of finite difference scheme has been used in this model. This technique involves the sub-division of each time step into two half time steps. Thus a two-dimensional implicit scheme can be applied but considering only one dimension implicitly for each half time step without the solution of a full two-dimensional matrix. On the first half time step, the water elevation η, the U velocity component (or the unit width discharge) and the solute concentration are solved implicitly in the x-direction, whilst the other variables are represented explicitly. Similarly, for the second half time step, the water elevation η, the V velocity component (or the unit width of discharge) and the solute concentration are solved for implicitly in the y-direction, with other variables being represented explicitly. With the boundary conditions included, the resulting finite difference equations for each half time step are solved using the method of Gauss elimination and back substitution. (Geraid and Wheatly, 1994)

A space staggered grid system is used, with the variables η (elevation) and S (concentration) being located at the grid centre and with U and V at the centre of the grid sides as shown in the figure (3.6.2). The use of a staggered grid system prevents the appearance of oscillatory solutions which tend to occur in a non-staggered grid for space centered differences (Fletcher, 1991). The depths are specified directly at the centre of the grid sides so that twice as much bathymetry detail can be included as in the traditional way which gives depths at the corners.

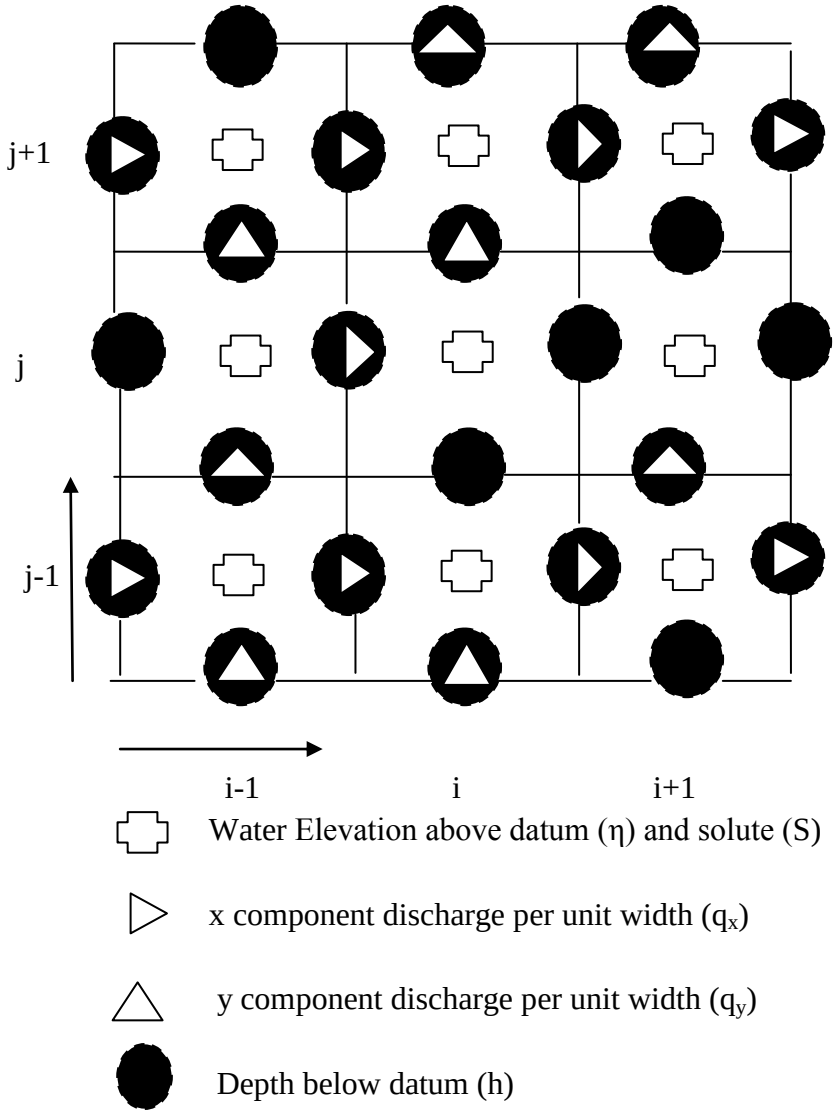

Figure 3.6.3: Computational space staggered grid system.

After disctretization of the governing equations in time and space, a system of finite difference equations are obtained which have to be solved. However, when a three-point finite difference formula is used, the set of equations generate a tridiagonal structure for the coefficient matrix and there is a special algorithm, known as the Thomas algorithm or double sweep algorithm, or Gauss elimination method for efficiently solving the set of equations which takes the advantage of the banded nature of the matrix.

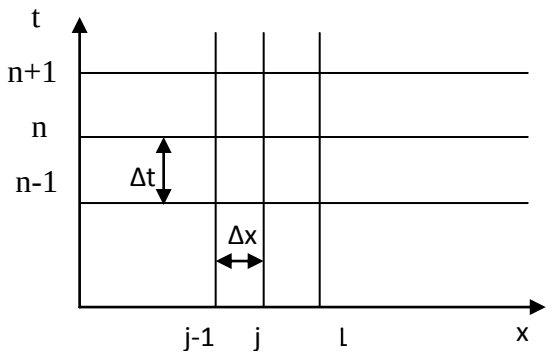

Fig.3.6.4: Finite difference computational grid in (x,t) plane

For an example, considering the diffusion equation $\frac{\partial f}{\partial x} = D\frac{\partial^2 y}{\partial x^2}$ and using a three-point implicit scheme to solve it. Then one will get the system of finite difference equations

$$a_j f_{j-1}^{n+1} + b_j f_j^{n+1} + c_j f_{j+1}^{n+1} = d_j \ldots\ldots\ldots\ldots\ldots\ldots\ldots\ldots\ldots\ldots\ldots\ldots\ldots\ldots (3.6.1)$$

Where a_j, b_j, c_j and d_j $(j = 2, 3, \ldots\ldots\ldots\ldots, J-1)$ are known and f_1^{n+1} and f_j^{n+1} are given as boundary conditions. For J computational points, there is a system of (J-2) equations. With the two given boundary conditions, the system of equations may be solved for any time step Δt. Equation (3.6.1), when repeated for every node, gives the matrix below

$$\begin{vmatrix} b_2 & c_2 & & & & \\ a_3 & b_3 & c_3 & & & \\ & a_4 & b_4 & c_4 & & \\ & & a_5 & b_5 & c_5 & \\ & & & : & : & \\ & & & : & : & \\ & & & a_{J-2} & b_{J-2} & c_{J-2} \\ & & & & a_{J-1} & b_{J-1} \end{vmatrix} \begin{vmatrix} f_2^{n+1} \\ f_3^{n+1} \\ f_4^{n+1} \\ f_5^{n+1} \\ : \\ : \\ f_{J-2}^{n+1} \\ f_{J-1}^{n+1} \end{vmatrix} = \begin{vmatrix} d_2 - a_2 f_1^{n+1} \\ d_3 \\ d_4 \\ \\ : \\ \\ \\ d_{J-1} - c_{J-1} f_J^{n+1} \end{vmatrix} \ldots\ldots (3.6.2)$$

Dropping the superscripts of the unknown quantities f, Eq. (3.6.1) may be written as

$$a_j f_{j-1} + b_j f_j + c_j f_{j+1} = d_j \ldots\ldots\ldots\ldots\ldots\ldots\ldots\ldots\ldots\ldots\ldots\ldots\ldots\ldots\ldots\ldots\ldots\ldots (3.6.3)$$

For j=2, Eq.(3.6.1) becomes,

$$a_2 f_1 + b_2 f_2 + c_2 f_3 = d_2 \ldots\ldots\ldots\ldots\ldots\ldots\ldots\ldots\ldots\ldots\ldots\ldots\ldots\ldots\ldots\ldots\ldots\ldots (3.6.4)$$

Which can be expressed as, $f_2 = \alpha_2 f_3 + \beta_2 \ldots\ldots\ldots\ldots\ldots\ldots\ldots\ldots\ldots\ldots\ldots\ldots\ldots\ldots (3.6.5)$

Where $\alpha_2 = -\frac{c_2}{b_2}$ ……. (3.6.6a) and $\beta_2 = \frac{d_2 - a_2 f_1}{b_2}$ ……. (3.6.6b)

For j=3 Eq.(3.6.1) becomes,

$$a_3 f_2 + b_3 f_3 + c_3 f_4 = d_3 \text{ ……} \quad (3.6.7)$$

Eliminating f_2 it can be expressed as, $f_3 = \alpha_3 f_4 + \beta_3$ …… (3.6.8)

Where $\alpha_3 = -\frac{c_3}{b_3 + a_3 \alpha_2}$ …… (3.6.10a)and $\beta_3 = \frac{d_3 - a_3 \beta_2}{b_3 + a_3 \alpha_2}$ …… (3.6.10b)

Writing similar equations for grids j= 4, 5, ….., J-1, we can have a general equation

$$f_j = \alpha_j f_{j+1} + \beta_j \text{ ……} \quad (3.6.11)$$

Where the recurrence relationships are defined by

$$\alpha_j = -\frac{c_j}{b_j + a_j \alpha_{j-1}} \text{ ……} \quad (3.6.12a) \text{ and } \beta_j = \frac{d_j - a_j \beta_{j-1}}{b_j + a_j \alpha_{j-1}} \text{ ……} \quad (3.6.12b)$$

Since f_j is known from the given boundary condition, Eq. (3.6.11) may be used successively for j = J-1, J-2, …, …, 4, 3, 2 to compute the values of f at the grid points. Thus, the double sweep or tridiagonal matrix algorithm for solving Eq.(3.6.1) consists of two steps. In the first step, called the forward sweep, the coefficients α_j and β_j $(j = 2, 3, 4, \ldots\ldots, J-2, J-1)$ are calculated using Eqs.(3.6.6) and (3.6.12). In the second step, called the return or backward sweep, the values of f_j $(j = J-1, J-2, \ldots\ldots\ldots, 4, 3, 2)$ at the advance time level (n+1) are calculated using (3.6.11) starting from f_j^{n+1} by back substitution.

3.6.5 Model Output

Computed output results of the model at each mesh element and for each time step consist of:

- Basic Variables:
  - Water depth and surface elevation.
  - Flux densities in main directions.
  - Velocities in main directions.
  - Wet and Dry cells in domains.
- Additional Variables:
  - Current speed and directions.
  - Sediment fluxes.

3.6.6 Model Development Stages

The mathematical model is a long, tedious and iterative procedure. The important steps of different modeling activities could be grouped are schematically shown in figure below. Although the steps in the figure are shown in a sequentially, in practice a number those steps may have to be conducted simultaneously. Following are the main stages:

1. Conceptualization
2. Data collection
3. Calibration
4. Validation

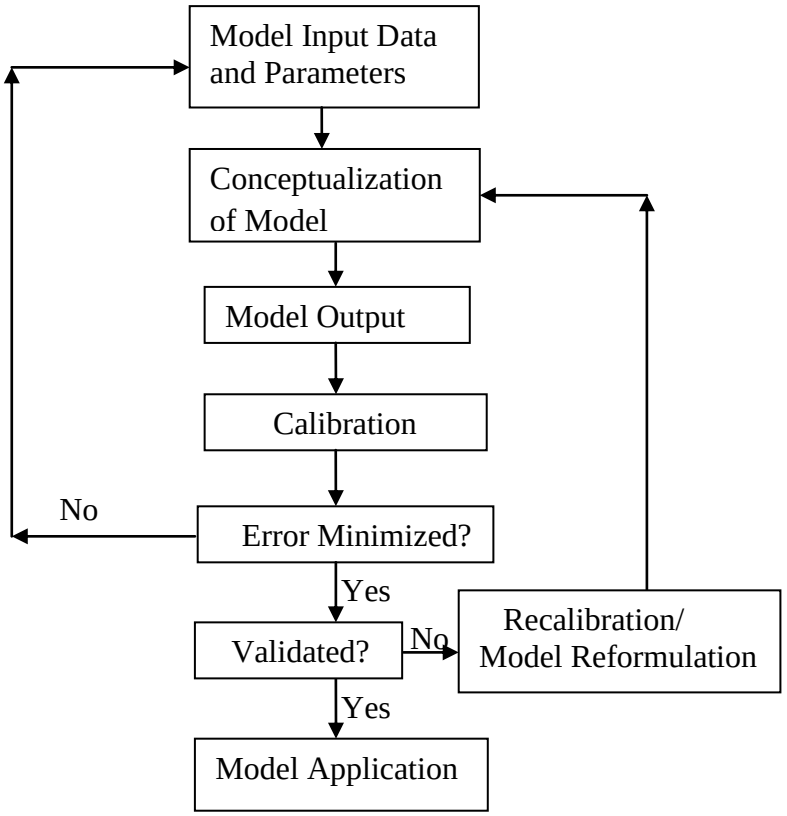

Figure 3.6.5: Schematic diagram of Model development stages.

3.7 Summary

The tidal theories and related hydrodynamic equations required for tidal level and velocity simulation have been described in this chapter. A short description of DIVAST model including the solution technique by finite difference scheme forming tridiagonal coefficient matrix and solution by double sweep method have also been described for the study. The bathymetry of Bay of Bengal of square grid size (5680 m) has been generated. The model input and output including the development stages of model are also outlined for the study.

CHAPTER 4

RESULTS AND DISCUSSIONS

4.1 General

Since the astronomical tide is a continuous process in the sea, the tidal oscillation is the initial state of the sea for tide simulation. But the difficulty in generating the tidal oscillation in a model lies with its variability in amplitude and phase. Since different constituents of tide interact among themselves, the interaction is characterized by diurnal inequalities as to the high and low water; non-periodicity of the tidal oscillation, the variation of tidal amplitude and circulation of residual current due to back-and-forth movement of tidal flow and river discharge in the spring-neap cycle . The complexity of the tidal phenomena is a great constraint in generating actual tidal oscillation in the model simulation process. A mathematical model of Bay of Bengal has been set up and applied to simulate the tidal flow velocity at sevaral locations in the Bay of Bengal in order to verify the simulated velocity with the measured velocity and compared with the other study. In view of that, six locations in the Bay of Bengal have been chosen such as Noakhali-Urirchar Channel, Sandwip-Zahajerchar Channel, Hatia-Noakhali Channel, Sandwip-Sitakundu Channel, Sandwip-Urirchar Channel, and Shahbazpur- Monpura Channel. The set of data of these locations has been split into two parts and each part contains three of them. The one part is used for calibration and other part is used for verification of the model. The detail of the data analysis and results of the model is discussed in the following sections.

It is important to mention here that, there is no velocity measuring gauge installed to record hourly velocity data continuously throughout the years together like water level data measuring gauges in the coastal region. Therefore, time series data for velocity is not available in any location. Measured velocity data are available in the selected locations on different dates and duration but not in all the locations in the same date and duration. As a result the model is calibrated and validated with the velocity data of different locations in different dates and duration based on the availability of the measured velocity data.

4.2 Study Area and its Tidal Behaviour

The coastal areas of Bangladesh are different from rest of the country because of its unique geo-physical characteristics and vulnerability to several natural disasters like cyclones, storm surges, erosion and accretion etc. Natural hazards are increasing with high frequency and intensity along the coast of Bangladesh with the changes of global climate. These extreme natural events are termed as disasters when they adversely affect the whole environment including human beings, their shelters or the resources essential for their livelihoods. Meghna estuary is one of the largest estuaries on the earth in terms of sediment-water discharge and is located at the central part of the coastal zone of Bangladesh.

Tides in Bangladesh coast originate in the Indian Ocean. It enters the Bay of Bengal through the two submarine canyons, the 'Swatch of No Ground' and the 'Burma Trench' and thus arrives very near to the 10 fathom contour line at Hiron Point and Cox's Bazar respectively at about the same time (As-Salek and Yasuda, 2001). Extensive shallowness of the north-eastern bay gives rise to partial reflections thereby increasing the tidal range and the friction distortions concurrently. Large seasonal effects of meteorological origin coupled with the complexity of the non-linear shallow water interaction give rise to considerable number of higher harmonics. All such higher harmonic terms are needed in predicting tide to make it as nearly representative as possible. Besides numerous inlets, there are six entrances of major importance through which tidal waves penetrate into the waterways system in Bangladesh and these are: (1) The Pussur Entrance; (2) Harin Ghata Entrance; (3) The Tentullia Entrance; (4) The Shahbazpur Entrance; (5) The Hatia river Entrance and (6) The Shandwip Channel Entrance. Strong tide in the north of Sandwip is caused by the shallowness and funnel effect in the Hatia river. The spring range here is more than 4 m at upstream of Sandwip (Alam, 2003).

There are many islands and chars in the Bay of Bengal. Notable ones are the Bhola, Hatia, Sandwip, Kutubdia, Gazaria, Char Pirbaksh, Urirchar, Zahajerchar, Monpura, Char Faizuddin, Char Nurul Islam and Nijhum Dwip. The fluvial and the fluvio-tidal sub-units act as a tidal river with very high river discharges in the monsoon where as

the tidal unit behaves as a tidal estuary without significant fresh water discharge from the river. The interaction between the tidal river and the tidal estuary is induced by the open sea connection with Bay of Bengal south of Sandwip island and by two channels between the north of Sandwip channels and the Noakhali mainland. The flow in this two channels induced by the tide level and phase difference between tidal river and the tidal estuary as mentioned above. Brief description of the selected locations of Bay of Bengal is mentioned below to calibrate and verify the velocities of the respective locations

4.2.1 Noakhali-Urirchar Channel

This channel separates Urirchar from mainland of Noakhali. Its location is at Lat: 22˚05'N and Long: and 90˚49'E (Banglapedia). It is under the influence of residual flow of Sandwip channel so it experiences the effects of tidal flow of Bay of Bengal. The nearest mainland areas are Noakhali Sadar on the north and Feni river mouth on the east. This channel carries residual flow from upper part of Sandwip channel towards west then to upper part of Hatia channel. This channel gets some influence of fresh water flow of Feni river mouth but it is very insignificance in comparison with the tidal flow of Sandwip channel which is the part of the counter clockwise residual flow around Sandwip Island.

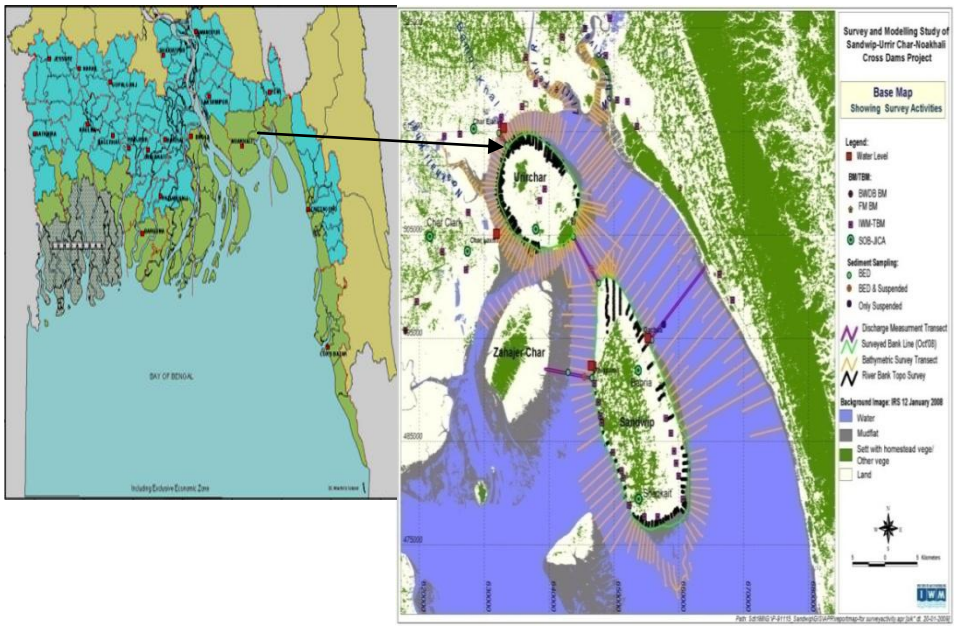

Figure: 4.2.1: Location of Noakhali-Urirchar Channel (Source: IWM)

4.2.2 Sandwip- Zahajerchar Channel

Zahajerchar is a island located at west of Sandwip, and south west of Urir Char. It is the upstresm part of east Hatia channel. This channel separates Zahajerchar from Sandwip island. It is under the influence of tidal effects of the estuary. The form of the estuary also influences the waves. The Sandwip channel is funnel shape, which causes a significant amplification of the tidal wave towards the upper end of the channel. This channel (north-west side of Sandwip) carries the residual flow from Sandwip channel to Hatia east through Urirchar channel. So its flow condition hydrodynamically is more or less similar to the Urirchar channel. This is basically what happens in the amplification of tidal levels in this narrow and shallow area of Sandwip-Zahajerchar channel (CERP, 2000). The tides which have zero amplitude in the deep water quickly builds up to several meters amplitude on the shallow and narrow funnel shape area of the sandwip-Zahajerchar channel.

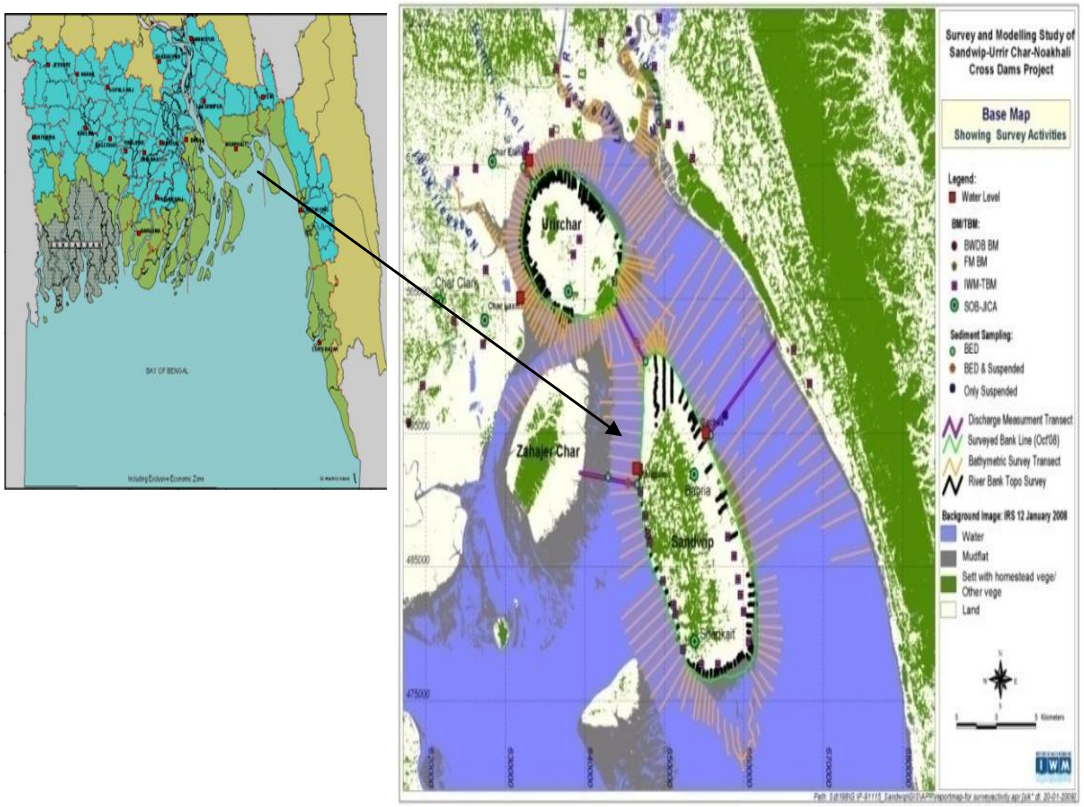

Figure: 4.2.2: Location of Sandwip-Zahajerchar Channel (Source: IWM)

4.2.3 Hatia -Noakhali Channel

Hatia island is an upazila under Noakhali district with an area of 1508.23 sq km and the total population is 2,95,501 which is bounded by Bay of Bengal. The nearest mainland areas are Noakhali Sadar and Ramgati upazillas on the north and Manpura upazilla on the west. This upazilla consists of many big and small offshore islands. Hatia-Noakhali Channel separates Hatia island from mainland of Noakhali. Its location is at Lat: 22˚30'N and Long: 91˚08' E in the Bay of Bengal (Banglapedia). It is located in the downstream side of Lower Meghna River and so it experiences the effects of both river fresh water discharge as well as tidal water of Bay of Bengal (fluvio-tidal area of the estuary). Char Nurul Islam divides the Hatia Channel into east and west Hatia channel. Most of the fresh water from the Lower Meghna River is conveyed towards the Bay of Bengal through the western part of the estuary: upper and mid-estuary, Tetulia and the Shahbazpur Channel west of Hatia Island. The eastern part of the estuary is mainly influenced by the tide and much less by the fresh water flow from the river system. So this channel is virtually the confluence of the river outflow and tidal inflow producing a complex tidal hydrodynamic flow condition.

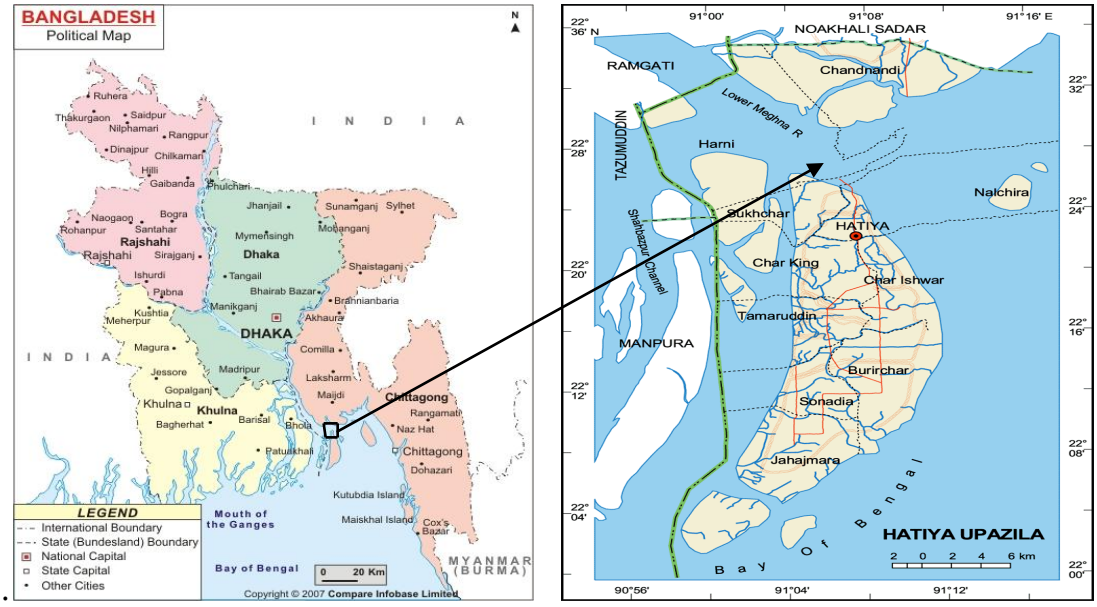

Figure: 4.2.3: Location of Hatia- Noakhali Channel (Source: Banglapedia)

4.2.4 Sandwip-Sitakundu Channel

This is the main part of Sandwip Channel. This huge channel separates Sandwip island from Chittagong main land. This falls under the tidal unit of the three units (fluvial,fluvio-tidal and tidal units) of the estuary due to insignificant fresh water discharge from the river system. The residual tidal flow creates a net transport of water out of the Meghna Estuary mainly through the west Shahbazpur Channel, and an easterly flow outside the estuary. According to MES (2001), a prominent counter-clockwise circulation is found around the Sandwip Island, with a northerly current in the Sandwip channel and southerly current in the southern part of the Hatia channel. The anti-clockwise circulation is mainly forced by tides but is also influenced by river discharge. The circulation traps fresh water from the river in the estuary. This may be the reason for the relatively low salinity in the estuary even during the dry season. The Sandwip-Sitakundu channel carries negligible amount of fresh water flow when compared with the tide induced flow in the channel.

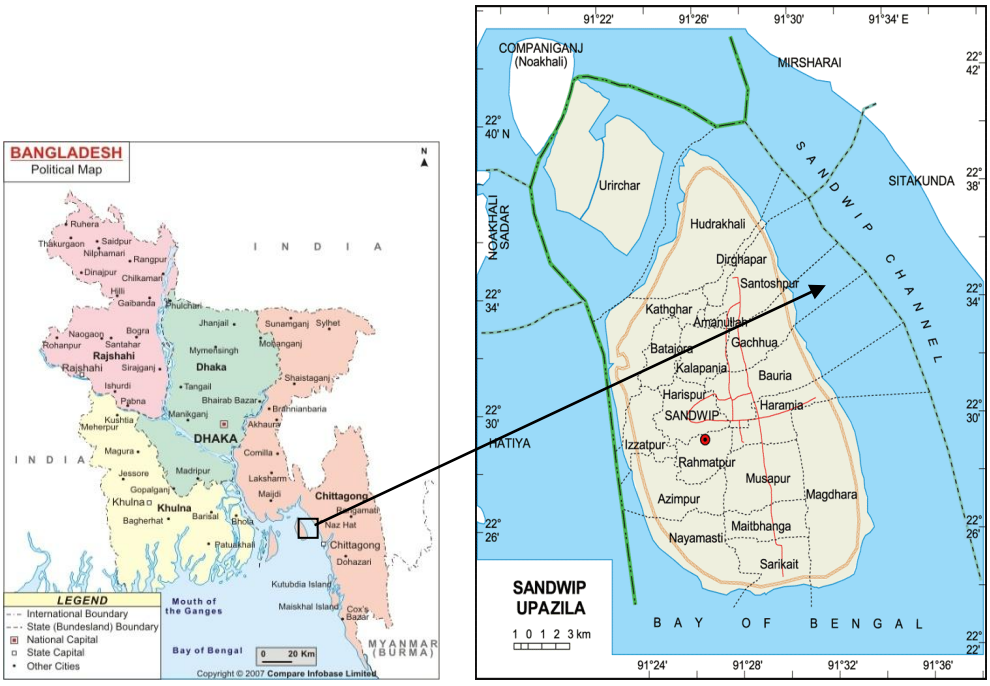

Figure: 4.2.4: Location of Sandwip-Sitakundu Channel (Source: Banglapedia)

4.2.5 Sandwip- Urirchar Channel

It separates Urir Char from Sandwip Island and connects Hatia east channel (through Zahajerchar channel) with Sandwip channel at the upper part. Its location is at north west of Sandwip island at Lat:22˚36'N and Long:91˚24'E (Banglapedia). As it is a tidal channel, tidal flow dominates over fresh water flow from river discharge. It carries the residual circulation from Sandwip channel to Hatia east. The tidal water enters the estuary from the south. At the eastern side, the tidal wave travels faster in the deep Sandwip Channel than over the shallows west of Sandwip Island. Both waves meet in the north-west of Urir Char. The Sandwip Channel has a funnel shape, which causes a significant amplification of the tidal wave towards the upper end of the channel which actually meets at Urirchar then Sandwip-Urirchar channel originates and moves southwest to meet with east Hatia channel. Tidal bores are frequently observed near south of Urir Char because of tidal waves travelling upstream of the estuary undergo deformation due to the bed resistance and difference in the propagation speed at different water depths. The most extreme form of this deformation is a so-called tidal bore, where due to the difference in the propagation speed between the top and the trough of the tidal wave, the top travels so much faster than it actually overtakes the trough. The result is a breaking tidal wave, a nearly vertical front of water moving upstream with a roaring sound. They present extreme danger to fishing boats in the Urirchar area (Banglapedia).

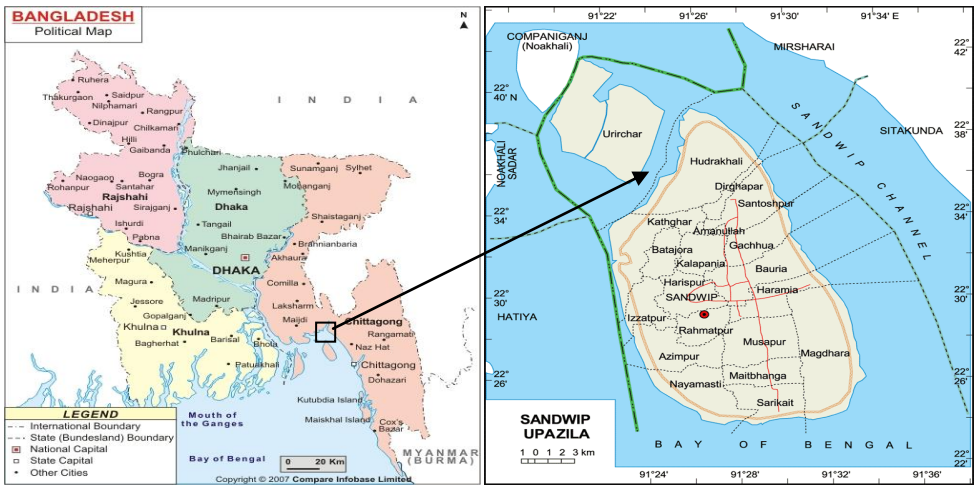

Figure: 4.2.5: Location of Sandwip-Urirchar Channel (Source: Banglapedia)

4.2.6 Shahbazpur-Monpura Channel

Monpura and char Faizuddin divide shahbazpur channel into two i.e east and west shahbazpur channel. The river empties itself into the Bay of Bengal through both the Shahbazpur and the Hatia Channel. Fresh water enters the Lower Meghna River and is distributed through the Tetulia and Shabazpur channels into the Bay of Bengal. The tide enters the lower Meghna River through the east and west Shahbazpur channel, and through the Hatia channel. Shahbazpur- Monpura channel is actually west Shahbazpur channel which is fluvial channel as river outflow dominates over the tidal inflow. During monsoon, the south-westerly monsoon wind is steady and the river discharge is high. Furthermore, the mean water level is higher than that of the dry season due to the low atmospheric pressure systems in the Bay of Bengal. The Lower Meghna River pours several tens of thousands of discharges into the bay through the Tetulia, Shahbazpur-Monpura channel and Hatia channel. These huge volumes of fresh water modify the dry season water circulation mainly induced by tides.

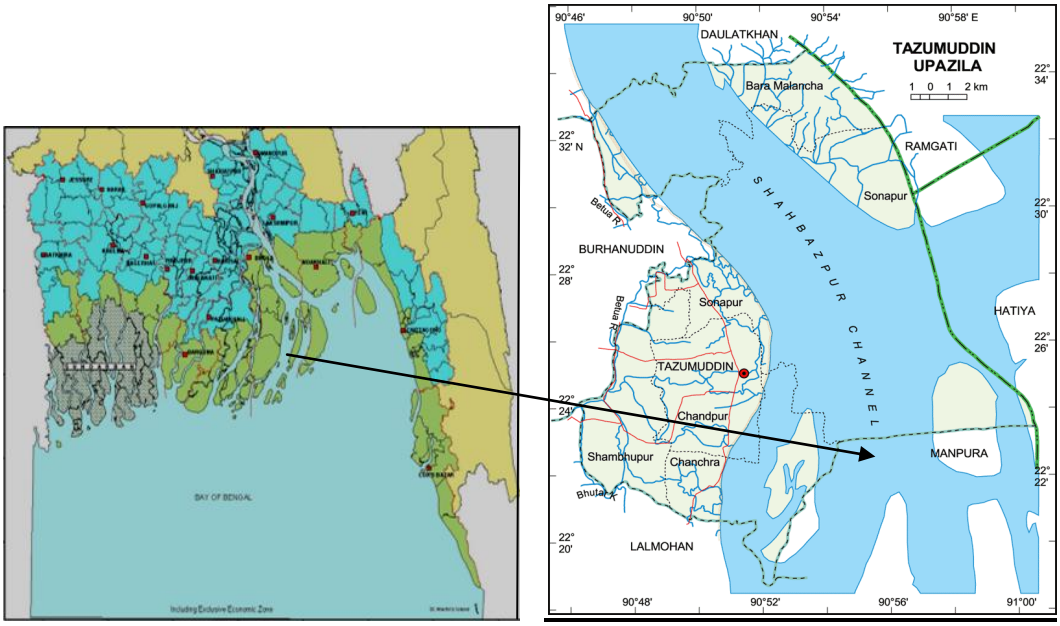

Figure: 4.2.6: Location of Shahbazpur-Monpura Channel (Source: Banglapedia)

4.3 Model Calibration

Model parameters require adjustment due to a number of reasons. Due to insufficient data and in reality it may not be possible to directly measure the data (e.g. the bed roughness of a two dimensional estuary model). Therefore the models contain parameters whose values could only be estimated through the calibration process. However, practically, all models require some degree of calibration to fine tune the predictive ability of the model. In a hydrodynamic model, errors may creep in from three potential sources: (a) Error in input data, (b) Error due to incorrect parameter values, (c) Error due to incomplete or incorrect model formulation.

Errors from source (b) are minimized during calibration process whereas the disagreement between the simulated and observed outputs is due to all the three sources. Errors related to (a) serves as the 'background noise' and determine the minimum level of mismatch between the observed and simulated outputs. Therefore, the objective of model calibration is to minimize the errors from source (b) until they become insignificant compared to the errors from sources (a). As far as the third source is concerned, every effort has to be made to ascertain that the state equation, initial condition and boundary condition have been specified correctly (Halim and Faisal, 1995). If a high level of calibration can be achieved and verified, then it may be possible to extend the application of the model beyond the limits of the data used in the calibration and verification processes.

4.3.1 Calibration data

The model calibration has been accomplished against hourly measured velocity data for certain period at three different locations of Bay of Bengal. The locations are Noakhali-Urirchar Channel, Sandwip-Zahajerchar Channel and Hatia-Noakhali Channel. The calibration periods are selected considering the available measured velocity data. These depth averaged velocity data has been collected from IWM. All the available velocity data for different locations, date, time and duration are summarized below:

Table 4.3.1: Location, Date and Time for Tidal Velocity Calibration

River/Channel	Date	Max. Velocity (m/s)		Time		Duration (Hours)
		Flood Tide	Ebb Tide	Start	End	
Noakhali-Urirchar Channel	15/09/08-16/09/08	1.947	2.745	1200 (pm)	0600 (am)	18
Sandwip-Zahajer Char Channel	08/09/08-09/09/08	0.645	0.732	0600 (am)	0500 (am)	23
Hatia-Noakhali Channel	23/02/07-24/02/07	1.331	1.521	0500 (am)	0500 (am)	24

The model is capable to generate the tidal velocity for continuous five tidal cycles where each tidal cycle consists of 12.4 tide hours. So, the time of simulation of the model is set for 62 hours for all the locations. The time step of 60 seconds is considered to ensure the stability of the numerical scheme. The model has attained stability by maintaining the Courant number ($g^{1/2}h^{1/2}\Delta t/\Delta s$) less than or equal to 1, in which Δt is the computational time step (=60 s) and Δs is the grid spacing of 5680 m. Hydrodynamic model calibration has been done by fine tuning the important variable input parameters of higher sensitivity like: Minimum Reynolds number (=1000), value of roughness coefficient k (=40 mm), Absolute wind speed (=15 m/s) through the calibration process after trial.

As the model area is considerably big and model has the option of selecting only one type grid size for simulating tidal velocity so that the each grid size of Bay of Bengal is considered as 5680 m based on coarse grid size of bathymetry data from IWM. Again the problems in taking small grid size over the whole area are (i) the number of grid points increases tremendously and thus increases the computer overhead and

(ii) smaller grid size requires smaller time step to ensure the Courant-Friedrichs-Lewy (CFL) stability criterion.

4.3.2 Calibration Results

Hydrodynamic model calibration has been accomplished against water velocity at Noakhali-Urirchar Channel, Sandwip-Zahajerchar Channel and Hatia-Noakhali Channel considering 62 hours (five tidal cycles) for each location but date and time are different according to the availability of measured velocity data. The simulated velocity for five continuous tidal cycles of the model are compared with the measured tidal water velocity at above mentioned three different locations and are shown in figure 4.3.1, 4.3.2 and 4.3.3 below. It is important to mention here that in reality measured velocity data is not available for continuous five tidal cycles (62 hours) in any location. So, available measured velocity is compared with simulated tidal velocity and in all the locations simulated velocity shows good agreement with the measured velocity.

4.3.3 Calibration Results at Noakhali-Urirchar Channel

Noakhali-Urirchar channel carries tidal flow from upper part of Sandwip channel towards west then to upper part of Hatia channel. This channel gets some influence of fresh water flow of Feni River but it is very insignificant in comparison with the tidal flow of Sandwip channel.

The simulation time periods of calibration at Noakhali-Urirchar Channel have been considered for continuous five tidal cycles of 62 hours duration from 0000 hr of 15/09/08 to 1400 hrs of 17/09/08. The comparison plot of measured and simulated tidal velocity at Noakhali-Urirchar Channel is shown in Figure 4.3.1. Measured velocity data is not available for continuous five tidal cycles (62 hours) in this location. So, available measured velocity of 18 hours has been compared with the corresponding simulated tidal velocity and simulated velocity shows good agreement with the measured velocity in this location.

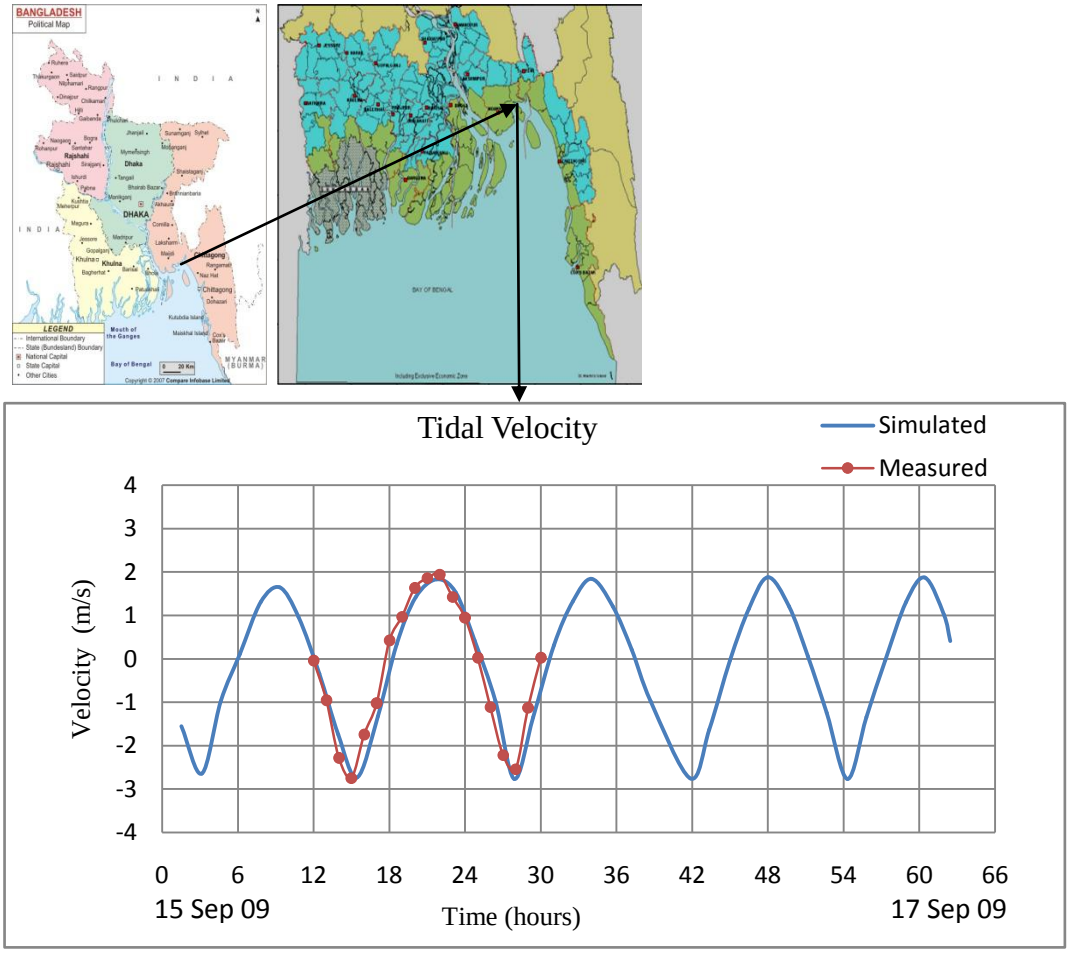

Figure 4.3.1: Tidal Velocity Calibration at Noakhali-Urirchar Channel

From Table 4.3.1 and Figure 4.3.1 it is found that velocity measurement starts at 1200 hours of 15/09/08 and ends at 0600 hours of 16/09/08. Both the measured and simulated tidal velocities of this time period at Noakhali-Urirchar channel are very close and similar in tidal patterns with each other and have insignificant percentage of deviation. Analyzing the above mentioned tidal cycle it is found that, the simulated ebb tide maximum velocity is 2.742 m/s at 15.45 hours and flood tide maximum velocity is 1.867 m/s at 21.75 hours and corresponding measured ebb tide maximum velocity is 2.745 m/s at 15 hours and flood tide velocity is 1.947 m/s at 22 hours and which is very similar and close. Hence during this time period simulated flood and ebb tides have very close and similar result with the measured tidal velocities. The graphical representation of both simulated and measured tidal velocity at Figure 4.3.1 shows excellent result. Moreover the tidal patterns of both the

measured and simulated tidal velocities also show the semi-diurnal tidal environment at Noakhali-Urirchar Channel.

4.3.4 Calibration Results at Sandwip-Zahajerchar Channel

Sandwip-Zahajerchar channel is under the influence of tidal effects of the estuary. The Sandwip channel is funnel shape, which causes a significant amplification of the tidal wave towards the upper end of the channel. This channel (west side of Sandwip) receives tidal flow from Sandwip channel to Hatia east through Urirchar channel. So its flow condition hydrodynamically is more or less similar to the Urirchar channel. Zahazerchar divides the south-west end of Sandwip-Urirchar Channel into two: one flows near the Noakhali mainland and meets Hatia west channel and other is the Sandwip-Zahajerchar channel flows near the Sandwip island and meets Hatia east channel. This channel is under the influence of tidal effects as well as prominent anti-clockwise tidal circulation around Sandwip channel (MES, 2001)

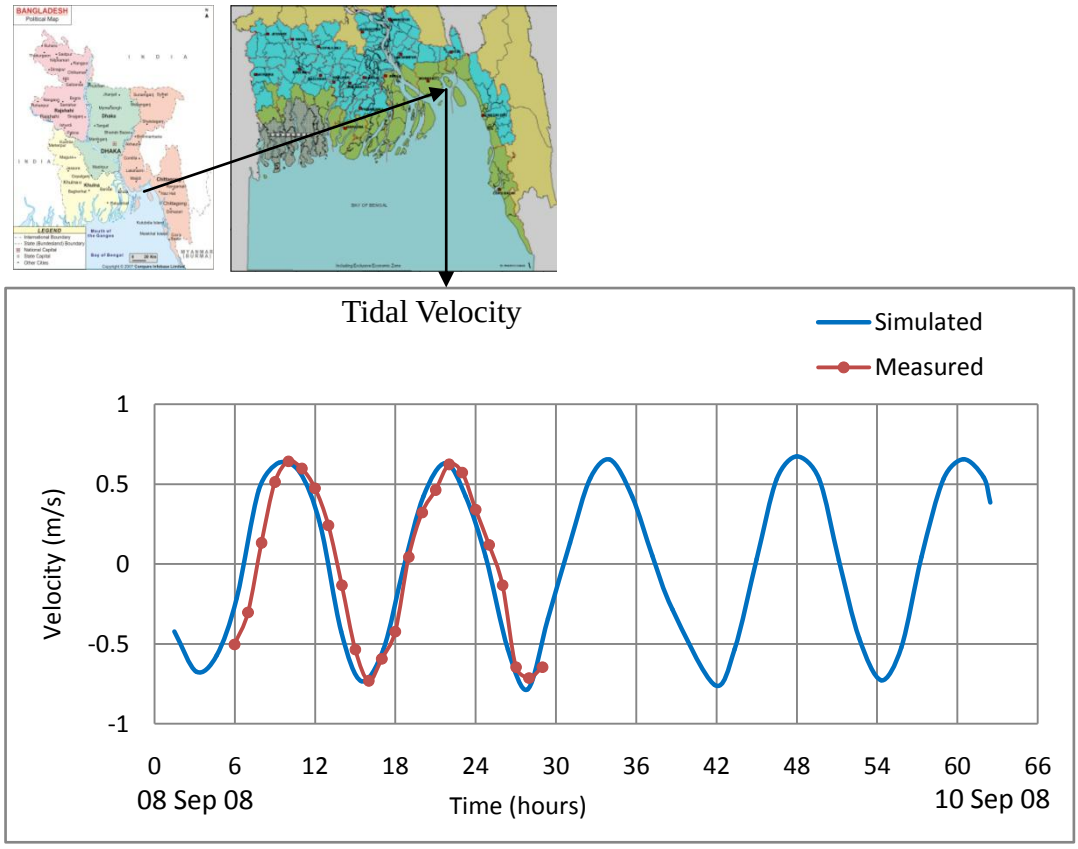

Figure 4.3.2: Tidal Velocity Calibration at Sandwip-Zahajerchar Channel

The simulation time periods of calibration at Sandwip-Zahajerchar Channel have been considered for continuous five tidal cycles of 62 hours duration from 0000 hr of 08/09/08 to 1400 hrs of 10/09/08. The comparison plot of measured and simulated tidal velocity at Sandwip-Zahajerchar Channel is shown in Figure 4.3.2. Measured velocity data is not available for continuous five tidal cycles (62 hours) in any location. So, available measured velocity of 23 hours has been compared with the corresponding simulated tidal velocity and simulated velocity shows good agreement with the measured velocity in this location.

From Table 4.3.1 and Figure 4.3.2 it is found that velocity measurement starts at 0600 hours of 08/09/08 and ends at 0500 hours of 09/09/08. Both the measured and simulated tidal velocities of this time period at Hatia-Noakhali channel are very close and similar in tidal patterns with each other and have insignificant percentage of deviation. Analyzing the above mentioned tidal cycle it is found that, the simulated ebb tide maximum velocity is 0.734 m/s at 9.3 hours and flood tide maximum velocity is 0.635 m/s at 15.75 hours and corresponding measured ebb tide maximum velocity is 0.732 m/s at 9 hours and flood tide velocity is 0.645 m/s at 16 hours and which is very similar and close. Hence during this time period simulated flood and ebb tides have very close and similar result with the measured tidal velocities. The graphical representation of both simulated and measured tidal velocity at Figure 4.3.1 also shows excellent result. The tidal patterns of both the measured and simulated tidal velocities also show the semi-diurnal tidal environment at Sandwip-Zahazerchar Channel.

4.3.5 Calibration Results at Hatia-Noakhali Channel

The dry season is the calm period in the estuary. The wind is weak and the river discharge is much lower than that during the monsoon. Water movement in the estuary is mainly forced by the tide entering from the Bay of Bengal. The influence of fresh water on the water circulation is less pronounced than that of wet season. Fresh water enters the Lower Meghna River and is distributed through the Tetulia and Shabazpur channels. The tide enters the Lower Meghna River through the east and west Shahbazpur channel and through the Hatia Channel (WARPO, 2003). Hatia Channel is the lower end of the Lower Meghna River and it separates Hatia island

from the Noakhali main land. This channel is divided into east and west by char Nurul Islam.

The simulation time periods of calibration at Hatia-Noakhali Channel have been considered for continuous five tidal cycles of 62 hours duration from 0000 hr of 23/02/08 to 1400 hrs of 25/02/08. The comparison plot of measured and simulated tidal velocity at Hatia-Noakhali Channel is shown in Figure 4.3.3. In reality measured velocity data is not available for continuous five tidal cycles (62 hours) in this location. So, available measured velocity of 24 hours has been compared with the corresponding simulated tidal velocity and simulated velocity shows good agreement with the measured velocity in this location.

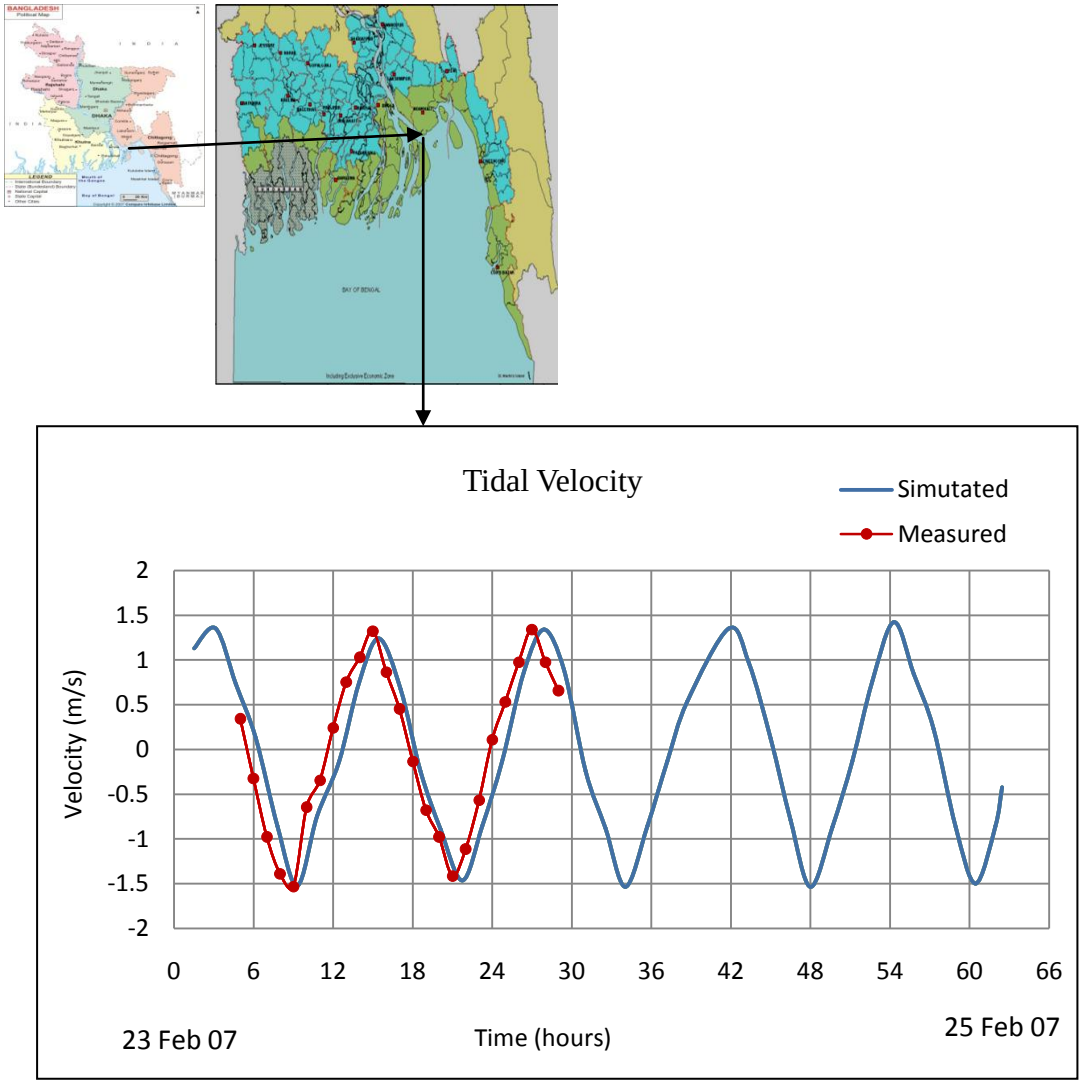

Figure 4.3.3: Tidal Velocity Calibration at Hatia-Nakhali Channel

From Table 4.3.1 and Figure 4.3.3 it is found that velocity measurement starts at 0500 hours of 23/02/07 and ends at 0500 hours of 23/02/07. Both the measured and simulated tidal velocities of this time period at Hatia-Noakhali channel are very close and similar in tidal patterns with each other and have insignificant percentage of deviation. Analyzing the above mentioned tidal cycle it is found that, the simulated ebb tide maximum velocity is 1.531 m/s at 9.3 hours and flood tide maximum velocity is 1.232 m/s at 15.75 hours and corresponding measured ebb tide maximum velocity is 1.521 m/s at 9 hours and flood tide velocity is 1.331 m/s at 16 hours and which is very similar and close. Hence during this time period simulated flood and ebb tides have very close and similar result with the measured tidal velocities. The tidal patterns of both the measured and simulated tidal velocities also show the semi-diurnal tidal environment at Hatia-Noakhali Channel.

The comparative result of both the measured and simulated tidal velocities is very close and similar with each other and with negligible deviations for all the three different locations of our coastal area. The tidal velocities of different locations have dissimilarity for the difference of geographic configuration and variation of depth but represent the semi-diurnal tidal patterns that prevail in coastal areas of Bangladesh.

4.4 Model Verification

In the verification process, a second and independent data set is used to verify that the calibration process established optimum parameter values. The calibration may have been achieved purely by numerical curve fitting without considering whether the parameter values so obtained are physically reasonable. Moreover, it might be possible to achieve multiple calibrations or apparently equally satisfactory calibrations based on different combination of parameter values. It is therefore important to find out if a particular calibration is satisfactory or which of the several calibrations is the best one by testing (verifying) the model with a different set of data not used during calibration.

According to Klemes (1986), a simulation model should be tested to show how well it can perform the task for which it is intended. Performance characteristics derived

from the calibration data set are insufficient as evidence of satisfactory model operation. Thus the verified or validated data must not be the same as those used for calibration but must represent a situation similar to that to which the model will be applied operationally.

The basic model structure could be validated by solving simple test problems for which analytical solutions exists. A common practice during the calibration-validation phase is to conduct 'split sample test'. This means dividing the data into two and using one part to calibrate the model and the other part to validate it. The final model should also be transferable to a great extent to another problem area having similar characteristics. Finally, sensitivity analysis is conducted whenever possible to determine the sensitivity of the simulated results to the changes in model parameters (Halim and Faisal, 1995).

4.4.1 Verification Data

The model verification has been accomplished against hourly measured velocity data for certain period at three different locations such as Sandwip- Sitakundu Channel (two data are found two hourly in this location, Figure 4.4.1), Sandwip-Urirchar Channel and Shahbazpur-Monpura Channel. The verification of tidal velocity has been considered based on location, date, time and duration are shown in table 4.4.1. The depth averaged tidal velocity data has been collected from IWM. All the input variable parameters are fixed same as those of the calibration process shown in Table 3.6.1.

The model has simulated five tidal cycles of 62 hours at date and time mentioned in above table. The model generated output has total 40 points of tidal levels and velocities where each tidal velocity is generated after 1.55 hrs up to total duration of 62 hours. Each simulated tidal cycle consists of 12.4 tide hours and has one high and one low tidal velocity. For the purpose of verification and analysis, the simulated result of the tidal velocity is compared with the measured velocity data of different locations individually and has been discussed with figures in the subsequent paragraphs.

Table 4.4.1: Location, Date and Time for Tidal Velocity Verification.

River/Channel	Date	MaxVelocity (m/s) Flood Tide Ebb Tide	Time Start End	Duration (Hours)
Sandwip-Sitakunda Channel	14/10/08-15/10/08	1.542 1.927	0600 (am) 0500 (am)	23
Sandwip-Urirchar Channel	14/01/08-15/01/08	1.13 1.59	1600 (pm) 2100 (pm)	29
Shahbazpur-Monpura Channel	14/12/07-15/12/07	0.968 1.552	0600 (am) 0600 (am)	24

4.4.2 Verification Results

Hydrodynamic model verification has been accomplished against water velocity at Sandwip-Sitakudu Channel, Sandwip-Urirchar Channel and Shahbazpur-Monpura Channel considering 62 hours (five tidal cycles) for each location but date and time are different according to the availability of measured velocity data. The simulated velocity for five continuous tidal cycles of the model are compared with the measured tidal water velocity at the above mentioned three different locations and are shown in figure 4.4.1, 4.4.2 and 4.4.3 below. It is important to mention here that in reality measured velocity data is not available for continuous five tidal cycles in any location. So, validation is done comparing available measured velocity with simulated tidal velocity and in all the locations simulated velocity shows good agreement with the measured velocity.

4.4.3 Verification Results at Sandwip- Sitakudu Channel

It is observed in MES (2001) study that Shandwip-Sitakunda channel is ‘tidal’ because the inflow of sea dominates over the river discharge. It is also found that most of the fresh water from the Lower Meghna River is conveyed towards the Bay

of Bengal through the western part of the estuary: upper and mid-estuary, Tetulia and the Shahbazpur Channel west of Hatia Island. The eastern part of the estuary is mainly influenced by the tide and much less by the fresh water flow from the river system. The water flow is generally very strong and turbulent. High Current velocities have been observed in the Sandwip Channel during spring tide and in the upper reach of the Lower Meghna during high monsoon.

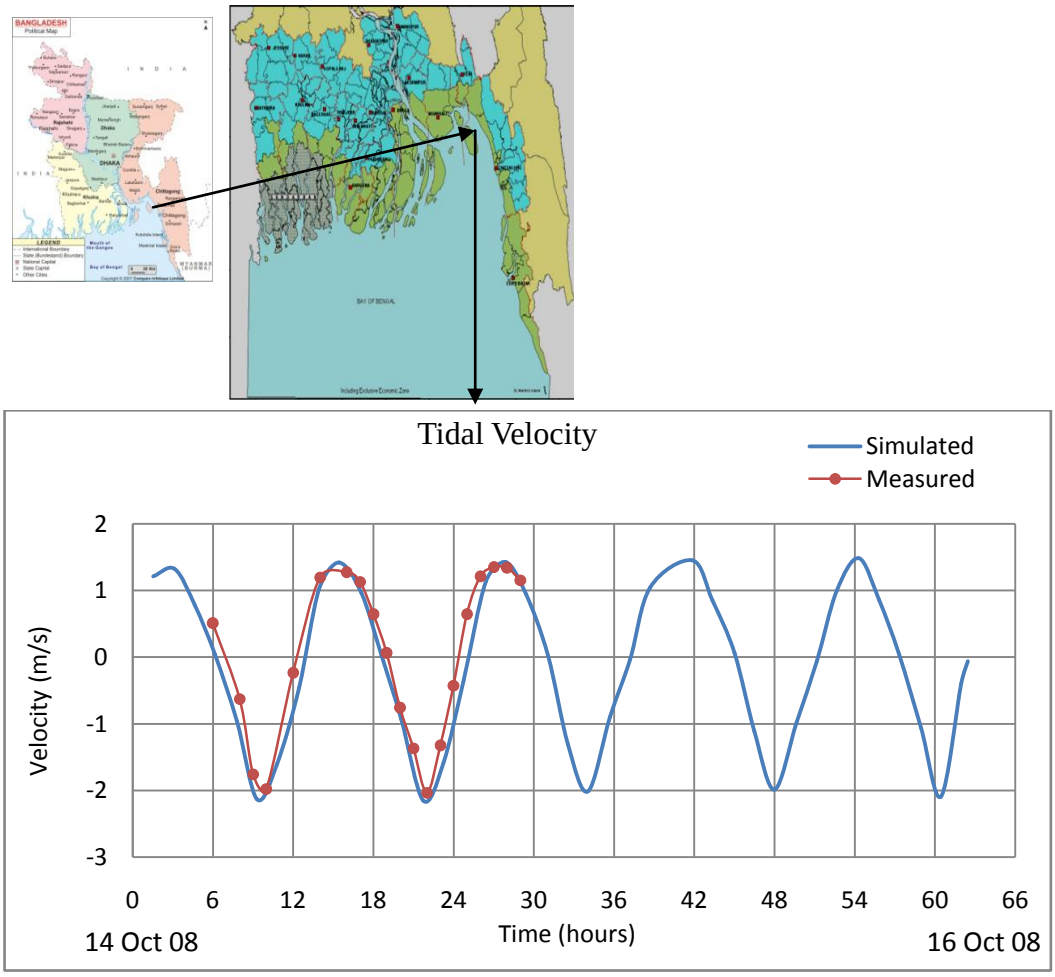

Figure 4.4.1: Tidal Velocity Verification at Sandwip-Sitakundu Channel

The simulated tidal velocity of model from 0000 hours of 14/10/08 to 1400 hours of 16/10/08 (62 hours duration) has been compared with the measured tidal velocity at Sandwip-Sitakundu channel in Figure 4.4.1. Measured velocity data is not available for continuous five tidal cycles (62 hours) in this location. So, available measured

velocity of 23 hours has been compared with the corresponding simulated tidal velocity and simulated velocity shows good agreement with the measured velocity in this location.

From Table 4.4.1 and Figure 4.4.1 it is found that velocity measurement starts at 0600 hours of 14/10/08 and ends at 0500 hours of 15/10/08. Both the measured and simulated tidal velocities of this time period at Sandwip-Sitakunda channel are very close and similar in tidal patterns with each other and have insignificant percentage of deviation. Analyzing the above mentioned tidal cycle it is found that, the simulated ebb tide maximum velocity is 2.132 m/s at 9.3 hours and flood tide maximum velocity is 1.423 m/s at 15.45 hours and corresponding measured ebb tide maximum velocity is 1.927 m/s at 9.0 hours and flood tide velocity is 1.542 m/s at16.0 hours, which are very similar and close. Hence during this time period simulated flood and ebb tides have very close and similar result with the measured tidal velocities. The tidal patterns of both measured and simulated tidal velocities also show the semi-diurnal tidal environment at Sandwip-Sitakundu Channel.

4.4.4 Verification Results at Sandwip-Urirchar Channel

In MES (2001) study it has been found that Shandwip-Urirchar channel is ‘tidal’ because effects of tidal inflow of sea dominates over outflow of river discharge which is insignificant in this area. The simulated tidal velocity of model from 0000 hours of 14/1/08 to 1400 hours of 16/1/08 (62 hours duration) has been compared with the measured tidal velocity at Sandwip-Urirchar channel and shown in Figure 4.4.2. Measured velocity data is not available for continuous five tidal cycles (62 hours) in this location. So, available measured velocity of 29 hours has been compared with the corresponding simulated tidal velocity and simulated velocity shows good agreement with the measured velocity in this location.

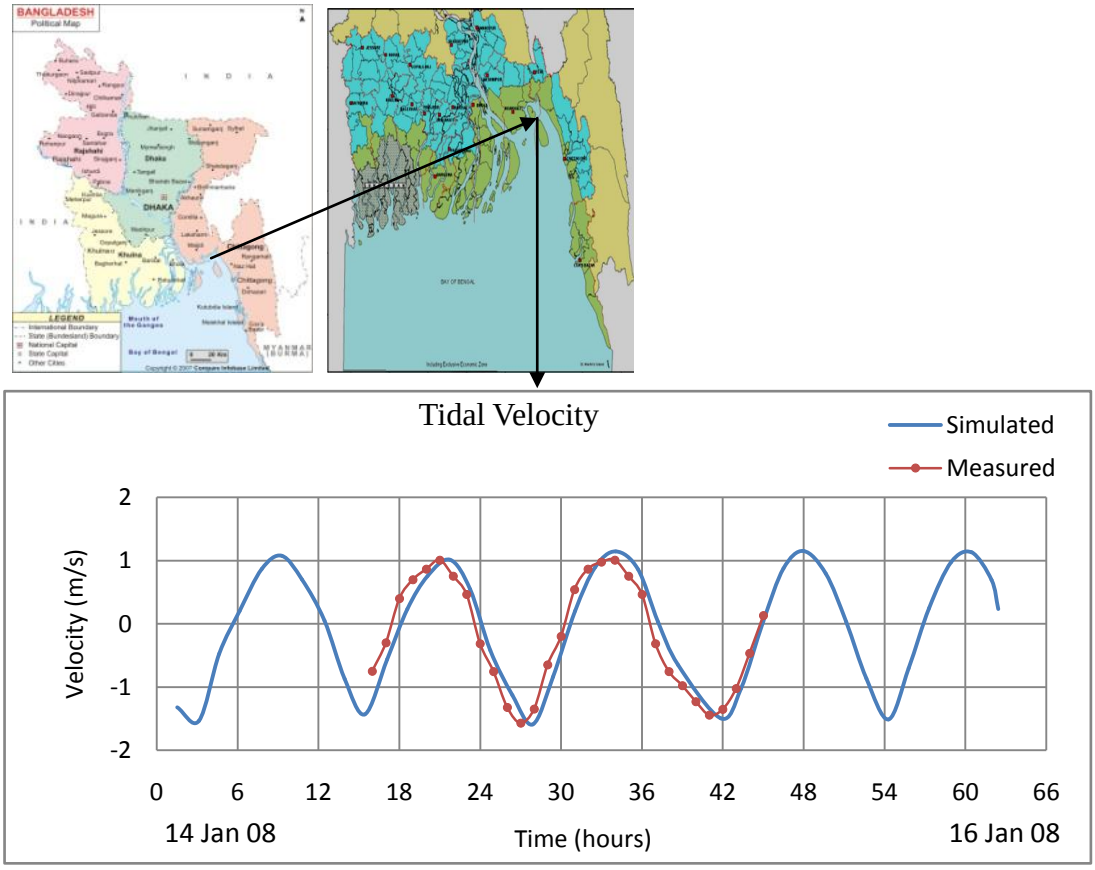

Figure 4.4.2: Tidal Velocity Verification at Sandwip-Urirchar Channel

From Table 4.4.1 and Figure 4.4.2 it is found that velocity measurement starts at 1600 hours of14/01/08 and ends at 2100 hours of 15/01/08. Both the measured and simulated tidal velocities of this time period at Sandwip-Urirchar channel are very close and similar in tidal patterns with each other and have insignificant percentage of deviation. Analyzing the above mentioned tidal cycle it is found that, the simulated flood tide maximum velocity is 1.012 m/s at 21.75 hours and ebb tide maximum velocity is 1.592 m/s at 27.9 hours and corresponding measured flood tide maximum velocity is 1.13 m/s at 22 hours and ebb tide velocity is 1.59 m/s at 28 hours and which is very similar and close. Hence during this time period simulated flood and ebb tides have very close and similar results with the measured tidal velocities. The tidal patterns of both the measured and simulated tidal velocities also show the semi-diurnal tidal environment at Sandwip-Urirchar.

4.4.5 Verification Results at Shahbazpur-Monpura Channel

In MES (2001) study it has been found that west Shahbazpur channel can be termed as 'fluvial' because the Lower Meghna River outflow dominates over the tidal inflow. The simulated tidal velocity of model from 0000 hours of 14/12/07 to 1400 hours of 16/12/07 (62 hours duration) has been compared with the measured tidal velocity at Shahbazpur-Monpura in Figure 4.4.3. In reality measured velocity data is not available for continuous five tidal cycles (62 hours) in this location. So, available measured velocity of 24 hours has been compared with the corresponding simulated tidal velocity and simulated velocity shows good agreement with the measured velocity in this location.

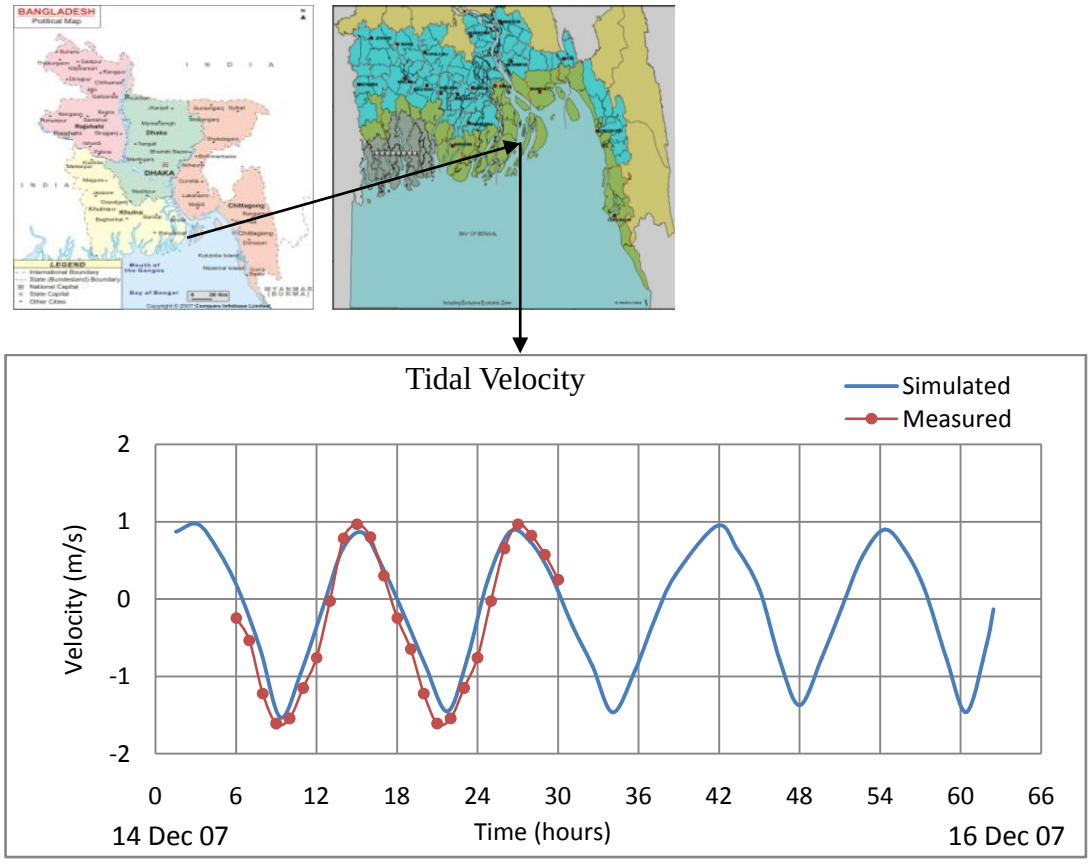

Figure 4.4.3: Tidal Velocity Verification at Shahbazpur-Monpura Channel

From Table 4.4.1 and Figure 4.4.3 it is found that velocity measurement starts at 0600 hours of 14/12/07 and ends at 0600 of 15/12/07. Both the measured and simulated tidal velocities of this time period at Shahbazput-Monpura are very close

and similar in tidal patterns with each other and have insignificant percentage of deviation. Analyzing the above mentioned tidal cycle it is found that, the simulated ebb tide maximum velocity is 1.532 m/s at 9.3 hours and flood tide maximum velocity is 0.856 m/s at 15.45 hours and corresponding measured ebb tide maximum velocity is 1.552 m/s at 9 hours and flood tide velocity is 0.968 m/s at 15.0 hours and which is very similar and close. Hence during this time period simulated flood and ebb tides have very close and similar result with the measured tidal velocities. The tidal patterns of both the measured and simulated tidal velocities also show the semi-diurnal tidal environment at Shahbazpur Channel.

It is observed in MES (2001) study that Lower Meghna Estuary (LME) is highly influenced by tidal interactions and consequential back water effect. As Lower Meghna riverine processes likely to dominate the LME and west Shahbazpur channel so that the tidal velocity is comparatively lower at Shahbazpur channel due to low influence of tide. MES (2001) also studied that mean tidal range from western boundary of Chandpur up to north and west of Bhola is classified as micro-tidal (0 to 2 m). The tidal velocity is weak in Shahbazpur channel because of shallowness of the outlet of LMR at the west Shahbazpur channel.

4.5 DIVAST Model generated Tidal Velocity Profile over the Model Domain

A tidal wave travelling from deep sea through the estuary causes gradients (spatial differences in surface level) in the water surface. As water always flows to the lowest point, these gradients are the cause of tidal flows observed in the estuary. Just like the tidal wave, this flow is periodical and changes from flood when the flow is directed upstream towards land to ebb when the flow is directed back towards the sea. The maximum current velocities in the Meghna Estuary can reach more than 3.5 m/s in the main tidal channels and 0.5 m/s in the shallow areas (MES II, 2001). The neap tide velocities are generally lower than the spring tide velocities. Sediment distribution in the estuary is mainly governed by the magnitude and net flow direction of the tidal flow. Erosion and accretion along the banks and shorelines of the estuary are very much related to the flow velocities dominated by the tidal flow.

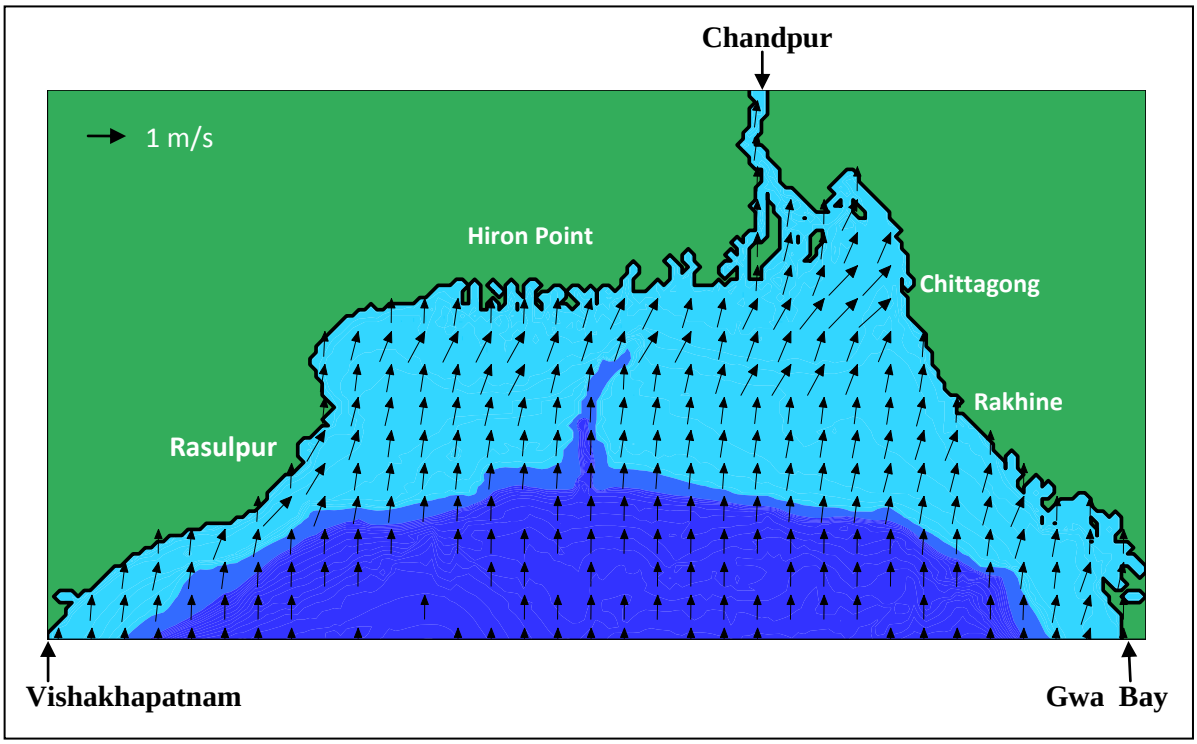

Figure 4.5.1: Tidal Velocity Profile during Flood Tide condition at t= 3.1 Hours

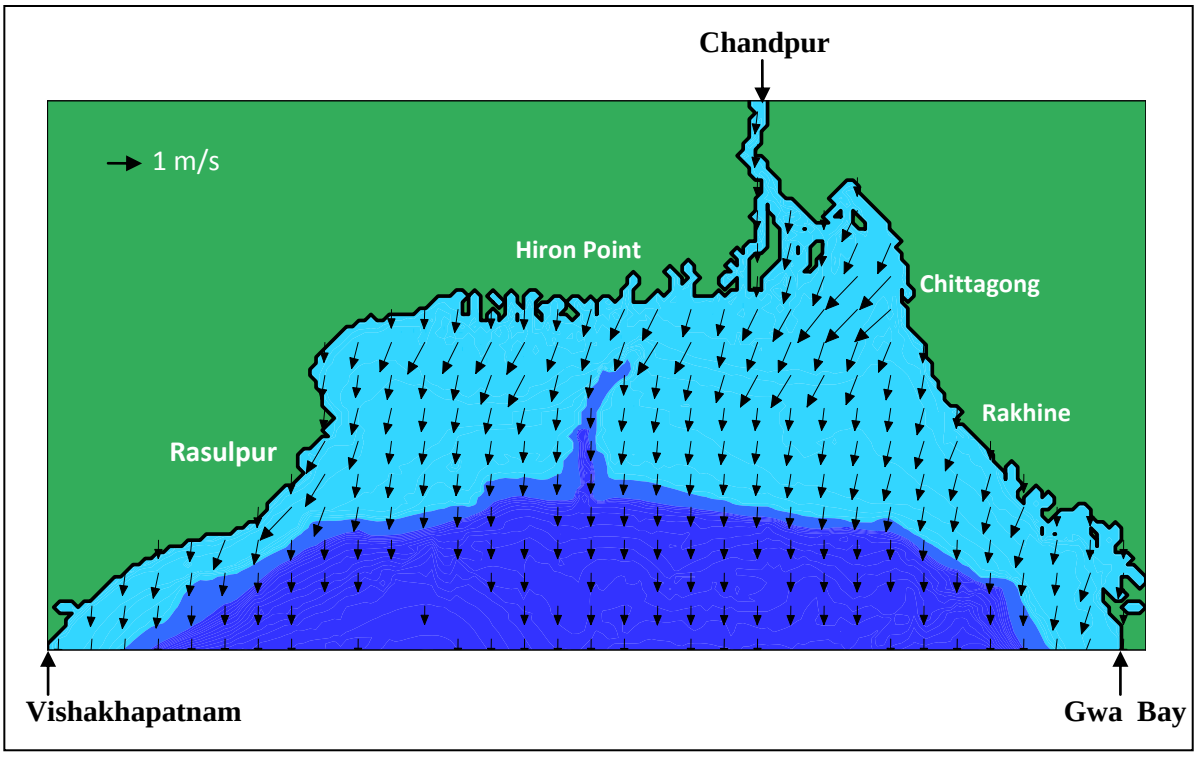

Figure 4.5.2: Tidal Velocity Profile during Ebb Tide condition at t= 9.3 Hours

Tidal velocity profile over the Bay of Bengal model domain for flood and ebb tide conditions generated by DIVAST model are shown in Figure 4.5.1 and 4.5.2 respectively. It is observed from the velocity profile that during flood tide, flow is towards land and higher velocities are seen in the main tidal channel like Sandwip channel than other fluvial channel like Tetulia, Shahbazpur channels. On the other hand during ebb tide, flow is towards sea and velocities are higher in the tidal channel than those in fluvial channels too. It is also found that the tidal velocities in the main channels are around 2 m/s in both flood tide and ebb tide conditions but ebb tide velocities are little higher than flood tide velocities.

4.6 Summary

In this chapter the calibration and verification of model has been done against measured tidal velocities at six different locations of coastal areas in different dates and time periods. In this process measured velocity has been compared with the corresponding model simulated tidal velocity. DIVAST model generated velocity profile over the model domain during flood tide and ebb tide conditions are shown and their features have also been interpreted and discussed in this chapter. Viewing over the simulated results it is found that simulated flood tide and ebb tide conditions have very close and similar results with the measured velocities. On the other hand tidal pattern of both the simulated and the measured data are also similar. Hence, it can be concluded that DIVAST model shows an encouraging and good performance in the Bay of Bengal.

CHAPTER 5

COMPARISON OF TIDAL VELOCITY WITH OTHER STUDY

5.1 General

The coastal region of Bangladesh is marked by morphologically dynamic river network, sandy beaches and estuarine system. The interaction of huge fresh water and sediment load coming from the upstream river system and saline waterfront penetrating inland from the sea are the key factors for a vulnerable coastline. Different modeling studies like: Impact assessment of climate change on the coastal zone of Bangladesh (IWM, 2005); Salinity intrusion, coastal and fluvial flood modeling (Khan et al., 2006); Impacts of climate change and sea-level rise on cyclonic storm surge floods in Bangladesh (Karim and Mimura, 2008); Residual flow in the Meghna Estuary on the coastline of Bangladesh (Jacobsen et al., 2002) etc have been carried out to asses various impact and vulnerability of our coastal region.

5.2 Comparison of Tidal Velocity with other Study

The calibration and verification of model with tidal velocities at six different locations of Bay of Bengal have been discussed in details in chapter 4. Now the comparison of simulated tidal velocities of DIVAST Model at three other different locations will be discussed based on availability of simulated tidal velocities of other study. The hydrodynamic model of Bay of Bengal generated by IWM with MIKE 21 has been utilized in different studies to assess the vulnerability of different natural hazards like climate change, storm surge, salinity intrusion, sediment dynamics, tsunami etc in our coastal areas. In these studies, the hydrodynamic model of Bay of Bengal has been calibrated or validated against either water level or discharge or velocity data in different locations at different time periods. Therefore, DIVAST model simulated tidal velocities are compared with the simulated tidal velocities of MIKE 21 FM of other studies in different locations and discussed in the following sections.

5.3 Tidal Velocity Comparison with 'Climate Change Modeling' of IWM

A study on climate change prediction modeling for 'Impact assessment of climate change causing increased rainfall and sea level rise on monsoon flooding' was carried out by Climate Change Cell (CCC) of Department of Environment (DoE) in collaboration with Ministry of Environment and Forests, Comprehensive Disaster Management Program (CDMP) and Ministry of Food and Disaster Management. The final report has been published in CCC, 2009.

Institute of Water Modelling (IWM) was engaged by Comprehensive Disaster Management Programme (CDMP) to carry out the 'Impact assessment of climate change causing increased rainfall and sea level rise on monsoon flooding' based on the recommendations of the Fourth Assessment Report (AR4) of the Intergovernmental Panel on Climate Change (IPCC). The Fourth IPCC report was approved in 2007 described the current state of understanding of the climate system and provides estimates of its projected future evolution and their uncertainties. Climate change scenario for predicted sea level rise is summarized below:

• About 11% more area (4,107 sq.km) will be inundated due to 88 cm sea level rise in addition to the existing (year 2000) inundation area under the same upstream flow. Sea would enter more landward and at Chandpur water level will rise by 50 cm for 88 cm rise of sea level and 15 cm for 32 cm rise of sea level.

• 5 ppt saline front moves landward remarkably for sea level rise of 88 cm. In the southeast corner of the area (including Sundarbans) 4 ppt isohaline moves further inland by 4 km and 12 km due to sea level rise of 32cm and 88cm respectively. In the middle part of area the landward movement with this isohaline be within the range of 6 to 8 km for the same level of sea level rises. Salinity in Khulna will be increased by 0.5 to 2 ppt for the 32 cm and 88 cm sea level rise.

• About 84% of the Sundarbans area becomes deeply inundated due to 32 cm sea level rise, and for 88 cm sea level rise Sundarbans will be lost.

• A significant number of coastal polders will be facing acute drainage congestion due to sea level rise.

• Due to 32 cm sea level rise, surge height increase in the range of 5 to 15% in the eastern coast. It also observed that 10% increase in wind speed of 1991 cyclone along with 32 cm sea level rise would produce 7.8 to 9.5 m high storm near Kutubdia-Cox's Bazar coast.

However, It is necessary to mention that our aim is to compare the tidal velocities. Therefore, only the hydrodynamic model of the Bay of Bengal of this study developed by IWM is highlighted for making subsequent comparison of tidal velocities of DIVAST model.

Development of the mathematical model of Bay of Bengal is done by using MIKE21 FM module of DHI Water and Environment. The MIKE 21 FM model system is based on an unstructured flexible mesh consisting of linear triangular elements. The numerical hydrodynamic model is founded on a combination of specific regional information and a generic numerical modelling system MIKE 21 FM. A 2D depth integrated numerical model of the Meghna Estuary and Bay of Bengal has been applied in this study. The coverage of the model area starts from Chandpur on Lower Meghna river to 16^{o} latitude in the Bay of Bengal. The model applies PWD datum which is 0.46m higher than MSL. The grid or mesh size decreases (or the resolution increases) towards coastlines and islands.

Two open boundaries are identified in the model, one in the north in the Lower Meghna River at Chandpur and the other in the south in the southern Bay of Bengal. The Bay of Bengal is quite deep and the maximum depth along the southern open boundary is more than 2000 m. The hydrodynamic model of this study was calibrated and validated against the measured water level and discharge data for both dry and monsoon periods. However, three locations such as Feni River Mouth, Charchenga, and Patenga have been selected to compare simulated tidal velocity of DIVAST model with that of MIKE 21 for different time periods. Comparison of velocities for both the models with figures are shown and discussed below.

5.3.1 Tidal Velocity Comparision at Feni River Mouth

Feni River originates from the hill ranges of the Indian state of Tripura at 23°20'N and 91°47'E, flows southwest marking the boundary with the Chittagong Hill Tracts, then flows west, separating Tripura from Chittagong up to Aliganj and then emerges out of the hills and passes through the plains dividing Chittagong from Noakhali before falling into the Bay of Bengal at 22°50'N and 91°27'E (Banglapedia). The simulated tidal velocity of DIVAST model from 0000 hours 31 May 09 to 1400 hours 02 June 09 (62 hours duration) have been compared with the simulated tidal velocity of MIKE 21 FM model for the same period.

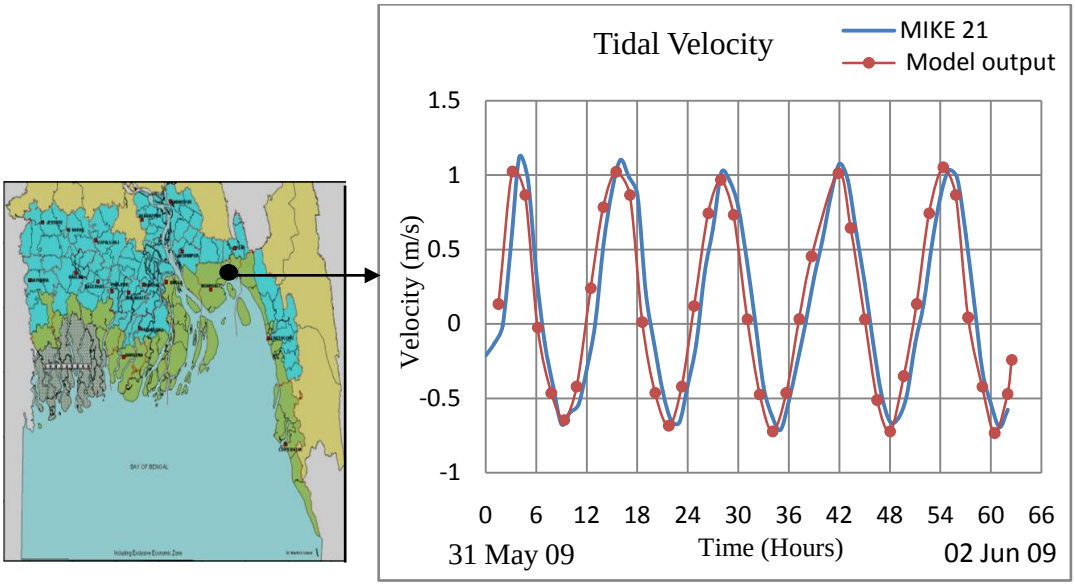

Figure 5.3.1: Tidal velocity Comparison at Feni River Mouth

From Figure 5.3.1 the simulated tidal velocities of both the models at Feni River outlet shows good agreement. It has been noticed that simulated tidal velocity of DIVAST model have negligible variation with the MIKE 21 tidal velocity during the flood tides and ebb tides among all the five tidal cycles. However, the small variation of tidal velocity as mentioned above does not have significant percentage of errors and as a whole agreement of the results are very encouraging.

5.3.2 Tidal Velocity Comparison at Charchenga

Charchenga is located at the central region of Meghna estuary at south-west of Hatia Island. The Hatia channel flows in the western side of Charchenga. As DIVAST model simulated tidal velocities consist of five tidal cycles of 62 hours duration, the time period from 0000 hours 14/02/2006 to 0200 hours 16/02/2006 has been considered for making the comparison of simulated tidal velocities at Charchenga. The comparison plot of MIKE21 and DIVAST model output is shown below in Figure 5.3.2.

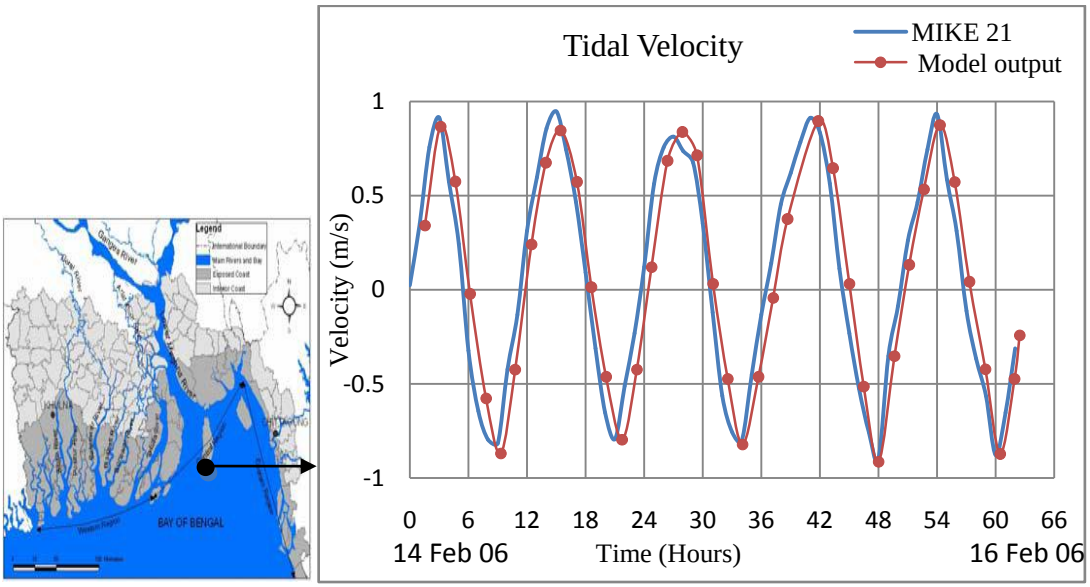

Figure 5.3.2: Tidal velocity Comparison at Charchenga.

From Figure: 5.3.2. semi-diurnal tidal pattern has been observed at Charchenga in the comparison plot of both the MIKE21 and DIVAST model simulated tidal velocities at different time periods. The comparison of simulated tidal velocities at Charchenga shows good result. It is found that simulated tidal velocities have small deviations with the MIKE21 generated tidal velocities during flood tides and ebb tides in all the tidal cycles. The ebb tidal velocities at different time periods are very close to each other but two flood tide peaks at 15.45 hours and 27.9 hours deviates a very small amount. All the deviations of tidal velocity cycles as mentioned above are very insignificant and as a whole the result shows good agreement.

5.3.3 Tidal Velocity Comparison at Patenga

Patenga is located at about 2 km. north of the Karnaphuly River estuary where it meets the Bay of Bengal. The simulated tidal velocity of DIVAST model have been compared with that of MIKE 21 tidal velocities of Patenga from 0000 hours 31 May 08 to 1400 hours 02 June 08 of 62 hours duration and shown in Figure 5.3.1.

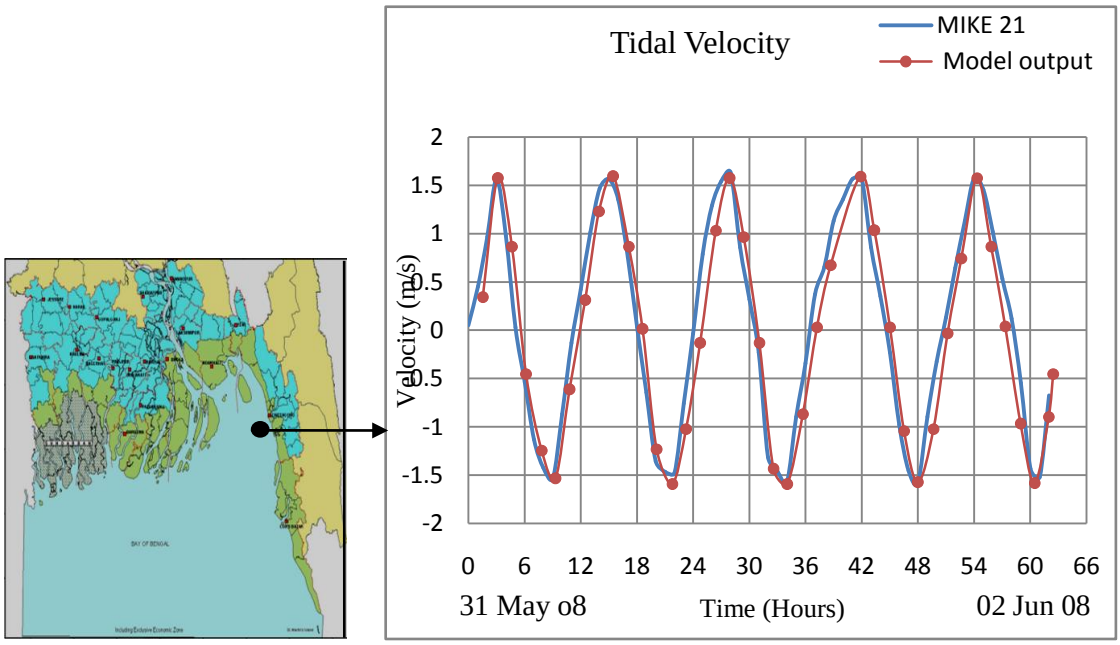

Figure 5.3.3: Tidal velocity Comparison at Patenga

Figure 5.3.3 shows the comparison plot of the simulated tidal velocities of DIVAST Model and MIKE 21 at Patenga for five tidal cycles of 62 hours time periods. It has been noticed that simulated tidal velocities for both the models match with each other in case all five tidal cycles. Although there are small variations in simulated tidal velocities, result shows very close similarity and percentage of variation can be considered as insignificant.

5.4 Analysis of the Results

The hydrodynamic model of Bay of Bengal developed by IWM is two way nested and includes four different resolution levels (Coarse, Intermediate, Fine and 200 m grid). The coastal region of Bangladesh and the Meghna estuary are resolved on a 200 m grid. The software used for the development of the mathematical model of

Bay of Bengal is MIKE21 FM module of DHI Water and Environment. The MIKE 21 FM model system is based on an unstructured flexible mesh consisting of linear triangular elements. In this study, the hydrodynamic model of Bay of Bengal has been developed with DIVAST model based on the FORTRAN program. The total model area of Bay of Bengal has one resolution based on the coarse grid consists of 5680 m square grid size each. Hence, the coastal region of Bangladesh and adjacent areas are not defined in details like MIKE 21 model and some of the small islands and chars are not pictured clearly in DIVAST model area. However, the simulated tidal velocities of both the models in different seasons are very close and nearer with insignificant percentage of deviations at Charchenga, Feni River Mouth, and Patenga. Charchenga is located at the central region of Meghna estuary at south-west of Hatia Island. The Hatia channel flows in the western side of Charchenga. As the simulated tidal velocities are based on the spring tidal conditions at dry period so the tidal velocity range is less than that of monsoon period. The location is tidal force dominated area as Hatia channel is likely to receive less amount of fresh water from the lower Meghna River at the dry period. More tidal velocity range is likely to be seen in this area during monsoon period due to the interaction of huge amount of discharge from lower Meghna River and tidal water from deep sea.

5.5 Summary

In this chapter the simulated tidal velocities of DIVAST Model have been compared with the simulated tidal velocities generated by IWM with MIKE 21 FM software. It has been observed that simulated tidal velocities for both the models match with each other in all five tidal cycles with very small deviations in all the three mentioned locations. In spite of the similarities small variations in simulated tidal velocities were also observed. Nonetheless, the percentage of error is insignificant as the results are very close and satisfactory.

CHAPTER 6
CONCLUSIONS AND RECOMMENDATIONS

6.1 General

The coastal areas of Bangladesh are different from other parts of the country due to its unique geo-physical characteristics and vulnerability to several natural disasters like cyclones, storm surges, erosion and accretion, SLR etc. Meghna estuary is one of the largest estuaries on the earth in terms of sediment-water discharge and is located at the central part of the coastal region. The estuary comprises of a number of deltaic islands and evidenced to be morphologically highly dynamic. The tidal behavior, upland discharges and wind fields vary distinctly from season to season and show noticeable variation of the hydrodynamics in the estuary and adjacent bay region.

Bathymetry of Bay of Bengal has been generated based on data of MES phase I and phase II using DIVAST model. The model area of Bay of Bengal consists of 181 × 91 grid squares with a constant grid spacing of 5680 m. The model has two open boundaries: the northern boundary is in the Lower Meghna River near Chandpur and the southern boundary is in the open sea located along the line extending from Vishakhapatnam of India to Gwa Bay of Myanmar. The coast line of Bangladesh is characterized by a wide continental shelf, especially off the eastern part of Bangladesh. The triangular shape at the head of the Bay of Bengal helps to funnel the sea water pushed by the wind towards the coast and causes amplification of the tidal levels at the exposed low lying coastal areas. This is basically what happens in the amplification of tidal levels on Bangladesh coast. The tides in the coastal and estuarine areas of Bangladesh are semi-diurnal in nature with two successive tidal cycles per lunar day 24 hours 50 minutes duration and each cycle having a period of 12 hours 25 minutes.

In this study a two dimensional hydrodynamic model DIVAST (Depth Integrated Velocity and Solute Transport) has been used considering the different parameters like co-efficient of eddy viscosity, Manning roughness, advective and diffusion co-efficient etc. of Bay of Bengal. The model is set up on a combination of specific information as input of the model area i.e. bathymetry, topography, wind and water

level etc. The model is based on FORTRAN PROGRAMING. The model has been used to simulate the tidal velocity as output along the selected important locations of coastal region of Bangladesh.

6.2 Conclusions

The hydrodynamics of the selected area of Bay of Bengal is simulated by solving two-dimensional depth integrated continuity and momentum equations numerically with finite difference (ADI-Scheme) method. Consequently the water elevation η and the respective velocity components U, V in the x and y directions are calculated across the selected locations of coastal domain for prescribed set of initial and boundary conditions. Simulated velocity has been verified at selected locations of coastal area with the measured field data and compared with the other study carried out in the coastal region. The following conclusions can be made viewing over all discussion and summarizing this research work:

1. The model has been calibrated and verified with the measured data at six locations such as: Noakhali-Urirchar Channel, Sandwip-Zahajerchar Channel, Hatia-Noakhali Channel, Sandwip-Sitakundu Channel, Sandwip-Urirchar Channel and Shahbazpur-Monpura Channel of the Bay of Bengal. Outcome of this work shows a good agreement between the measured and model simulated velocities of nearshore areas of the Bay of Bengal.

2. The model simulated tidal velocity has been compared with another model study by MIKE 21 model for the Bay of Bengal at three locations such as: Charchenga, Feni River Mouth and Patenga. This comparison gives satisfactory results.

3. Close agreement between the simulated results of this study and measured data and simulated results of other study justifies that the DIVAST model works reasonably well for the domain of the Bay of Bengal.

6.3 Recommendations for future study

The following recommendations can be made based on the present study and that may produce better results for future study.

1. This model study has been carried out for simulated tidal flow velocity. Further studies may be carried out such as a comparison of two models in terms of data requirements, CPU time, simulation of salinity concentration, sediment concentration, environmental impact assessment etc.

2. Further study may be done with comparatively smaller area and smaller grid size to define clearly all islands and chars in the Bay of Bengal to get improved simulated results

3. Bathymetry data of 2001 has been used in this research work. Inclusion of more recent and up to date bathymetry will improve the reliability of the model results of the research work.

References:

Ahmed, S.,1998, Residual tidal and sediment volume, their circulation patterns and Land cover changes in the Meghna Estuary, Journal of Civil Engineering, The Institute of Engineers, Bangladesh, Vol. CE 26, No. 1, 1998.

Alam, M., 2003. Bangladesh Country Case Study, National Adaptation Programme of Action (NAPA) Workshop, 9–11 September 2003, Bhutan.

Ali, A., Mynett, A.E. and Azam, M.H., "Sediment Dynamics in the Meghna Estuary, Bangladesh: A Model Study", Journal of Waterway, Port, Coast and Ocean Engineering. Vol-133, pp 255-264, 2007.

Ali, A., Rahman, H., Sazzad, S., Choudhary, S. S. H. and Begum, Q. N., 1997, Back water effect of tides and storm surges on fresh water discharge through the Meghna estuary. Journal of Remote Sensing & Environment, Vol-1, pp 85-95.

Ali, A., Rahman, H., Sazzad, S. and Choudhary, S. S. H., 1998, River discharge, storm surges and tidal interaction in the Meghna river mouth in Bangladesh. Mausan. 48, pp 531-540.

Allison, M. A., 1998, Historical changes in the Ganges- Brahmaputra delta front. Journal of Coastal Research, Vol-14, pp 1269-1275.

Allison, M. A., Khan, S. R., Goodbred, J. S. L. and Kuehl, S. A., 2003, Stratigraphic evolutions of the late Holocene Ganges–Brahmaputra lower delta plain. Sedimentary Geology, Vol-155, pp 317–342.

As-Salek, J. A., 1997, Negative surges in the Meghna estuary in Bangladesh. Monthly Weather Review.,Vol- 125, pp 1638–1648.

As-Salek, J. A., 1998, Coastal trapping and funneling effect on storm surges in the Meghna estuary in relation with the cyclones hitting Noakhali– Cox's Bazar coast of Bangladesh. Journal of Physical Oceanography, Vol-28, pp 227–249.

As-Salek, J. A. and Yasuda, T., 2001, Tide–Surge Interaction in the Meghna Estuary: Most Severe Conditions. Journal of Physical Oceanography, Vol- 31, pp 3059–3072.

Azam, M. H., Jakobsen, F., Kabir, M. and Hye, J. M. A., 2000, Sensitivity of the tidal signal around the Meghna Estuary to the changes in river discharge: A model study. The 12th International APD-IAHR Conference, Bangkok.

BBS, 2001, Bangladesh Bureau of Statistics, Population Census 2001.

Black, K.P., Gorman, R.M and Symonds, G., 1995 "Sediment transport near the break point associated with cross-shore gradients in vertical eddy diffusivity", Victoiarn Institute of Marine Sciences, Melbourne, Australia Geography and Oceanography Department Australian Defence Force Academy Canberra, 1995.

Bretana, G., 1987, Admiralty Manual of Navigation, Volume 1, Chapter 11, p. 227

Brommer, M. B. and Bochev, V. L. B., 2009, Sustainable coastal zone management: A concept for forecasting long-term and large-scale coastal evolution. Journal of Coastal Research, Vol-25, Issue-1, pp 181 – 188.

CZPo, 2005., Coastal Zone Policy, Ministry of Water Resources, Government of the People's Republic of Bangladesh, Dhaka.

CERP, 2000., 2nd Coastal Embankment Rehabilitation Project. Hydraulic modeling study, prepared by IWM/DHI.

CSPS, 1996., Cyclone Shelter Preparatory Study. Stage 1: Feasibility Phase, Final Report, Prepared for European Commission, Directorate General External Economic Relations and Technical Unit for Asia, ALA-91-16 Bangladesh, May.

Dabrowski, T., Hartnett, M. and Berry, A., 2003, Modelling hydrodynamics of Irish Sea. National University of Ireland, Galway, Civil Engineering Department, University Road, Galway, Ireland.

David E. Cartwright, 1999, Tide: An Scientific History, Cambrige, UK: Cambridge University Press.

Ebersole et al., 1986, Study of wave shoaling, refraction and diffraction within a study area, U.S. Army Corps of Engineers,

Falconer, R. A., and Alstead, 1990, Flow and water quality modeling in coastal and inland water. Journal of Hydraulic Research, Volume 30, Issue 4, page 437-452.

Falconer, R. A., George, D. G. and Hall, P., 1991, Three-dimensional numerical modeling of wind driven circulation in a shallow homogeneous lake. Journal of Hydrology, Vol-124, pp 59-79.

Falconer, R. A., 1992, Flow and water quality modeling in coastal and inland waters. Journal of Hydrology, IAHR, Vol-30, pp 183-185.

Falconer, R. A. and Chen, Y., 1996, Modelling sediment transport and water quality processes on tidal floodplains. In Floodplain Processes (Anderson, M. G., Walling, D. and Bates, P. D. (eds)). Wiley, Chichester, 1996, pp 361–398.

Flather, R. A., 1994, A Storm Surge Prediction Model for the Northern Bay of Bengal with Application to the Cyclone Disaster in April 1991. Journal of Physical Oceanography, Vol- 24, pp 172–190.

Fletcher, C. A., 1991, Computational Techniques for Fluid Dynamics, Vol-II, Specific techniques for different flow catagories, 2nd edition, Springer-Verlag, Berlin.

Flierl, G. R., and Robinson, A. R., 1992, Deadly surges in the Bay of Bengal: Dynamics and storm tide tables. Nature, 239, pp 213-215.

Geraid, C. and Wheatly, P. O., 1994, Applied numerical analysis. Addison-Wesley Publishing Company Inc, USA.

Goldstein, S., 1938, Modern Developments in Fluid Dynamics, Vol-1. Oxford University Press, Oxford.

Gulizar, O., and Ayşen, E., 2010, Improving coastal vulnerability assessments to sea-level rise: A new indicator-based methodology for decision makers. Journal of Coastal Research, Vol-26, Issue-2, pp 265 – 273.

Halim, M.A., and Faisal, I.M., "Mathematical Modeling", Department of Water Resources Engineering, BUET, Dhaka, 1995.

Hossain, M. S., 2001, Biological aspects of the coastal and marine environment of Bangladesh, Journal of Ocean Coast Management, Vol-44, pp 261-282.

Huang, W., Liu, Y. and Chen, X., 2008, Numerical modeling of hydrodynamics and salinity transport in little Manatee River. Journal of Coastal Research, Special Issue-52, pp 13 – 24.

Iftekhar, M. S. and Islam, M. R., 2004, Managing mangroves in Bangladesh: A strategy analysis. Journal of Coastal Conservation, Vol-10, pp 139-146.

Islam, M.S., 2001, Sea-level changes in Bangladesh: The Last Ten Thousand Years. Asiatic Society of Bangladesh, Dhaka.

Islam, M. S., 2003, Perspectives of the coastal and marine fisheries of the Bay of Bengal. Bangladesh Ocean & Coastal Management, Vol-46, pp 763-796.

Islam, M. R. (ed.), 2004. Where Land Meets the Sea: A Profile of the Coastal Zone of Bangladesh. The University Press Limited, Dhaka.

IWM and CEGIS, 2007, Investigating the impact of relative sea level rise on coastal communities and their livelihoods in Bangladesh, submitted to UK Department for Environment Food and Rural Affairs.

IWM, 2005, Impact assessment of climate change on the coastal zone of Bangladesh.

IWM, "Climate Change Prediction Modeling: Impact assessment of climate change of sea level rise on momsoon flooding", 2008.

Jain, I., Rao, A. D., Jitendra, V. and Dube, S. K., 2010, Computation of expected total water levels along the east coast of India. Journal of Coastal Research, Vol-26, Issue-4, pp 681 – 687.

Jakobsen, F., Azam, M. H. and Kabir, M. M., 2002, Residual flow in the Meghna Estuary on the coastline of Bangladesh. Estuarine, Coastal and Shelf Science, Vol-55, Issue-4, pp 587-597.

Jena, G. K., Sinha, P. C. and Rao, A. D., 2008, A breadth-averaged model for tidal circulation and sediment transport in the gulf of Khambhat, west coast of India. Journal of Coastal Research, Issue-2, supplement: pp 197 – 202.

Kabir, M.M., Azam, M.H. and Hye, J.M.A., "Application of the two dimensional computer model for impact assessment of the interventions for the purpose of land reclamation in the Meghna Estuary", 2000.

Kabir, M. M., Hye, J. M. A., Azam, M. H, 1999, application of the two dimensional computer model for impact assessments of the proposed interventions for the purpose of land reclamation in the meghna estuary, Surface Water Modeling Centre, Bangladesh, muk@swmcbd.org

Kashefipour, S.M., and R.A. Falconer, 1999, "Numerical Modelling of Suspendend Sediment Fluxes in Open Channel Flows" ,XXVII IAHR Congress, Graz, Austria.

Kamal, A. H. M. and Khan, M. A. A., 2009, Coastal and estuarine resources of Bangladesh: management and conservation issues. Maejo International Journal of Science and Technology, Vol-3, Issue-2, pp 313-342.

Karim, M. F. and Mimura, N., 2008, Impacts of climate change and sea-level rise on cyclonic storm surge floods in Bangladesh, Global Environmental Change, Vol-18, Issue-3, pp 490-500.

Kevin, A. and Daniel, M., 2004, Process based modeling of total long shore sediment transport. Journal of Coastal Research, Vol-20, Issue-3, pp 853 – 861.

Khan, Z. H., Mohal, N. and Khan, A. S., 2006, Salinity intrusion, coastal and fluvial flood modeling, Workshop on climate change prediction modeling, Dhaka, Bangladesh.

Klemes, V., 1986, Operational testing of hydrological simulation models, Hydrologic Science Journal, Vol- 31(1), pp 13-24.

Leont'yev, I.O., "Modeling of morphological changes due to coastal structures", Russian Academy of Sciences, P.P. ShirshoÍ Institute of Oceanology, NakhimoÍ Prospect, 36, 117851 Moscow, Russia, 1999.

Lin, B. and Simon, N., 1996, A depth-integrated 2D coastal and estuarine model with conformal boundary-fitted mesh generation. International journal for methods in fluids, Vol- 23, pp 819-846.

MES II, 2001, Hydro-morphological dynamics of the Meghna estuary. Submitted to Ministry of Water Resources, Bangladesh Water Development Board by DHV Consultants and associates.

Moller, George L., 1999, Introduction to Physical Oceanography. Springer. p. 169.

Morton, R. A., 2008, Historical changes in the Mississippi-Alabama barrier island chain and the roles of extreme storms, sea level, and human activities. Journal of Coastal Research, Vol-24, Issue-6, pp 1587 – 1600.

Navera, U. K., 2004, Development of a Model for Predicting Wave-Current Interactions and Sediment Transport Processes in Nearshore Coastal Waters, Ph.D Thesis, University of Wales, Cardiff, Wales, United Kingdom.

NOAA, "Types and causes of tidal cycle" National Ocean and Atmospheric Administration, National Ocean Service, U.S Govt.

Patullo, J., Munk, W. H., Revelle, R. and Strong, E., 1989, The seasonal oscillation in sea level. Journal of Marine Research, Vol-14,pp 88-156.

Radjawane, I.M and Riandini, F., 2009, Numerical Simulation of Cohesive Sediment Transport in Jakarta Bay, International Journal of Remote Sensing and earth sciences, Vol. 6: 65-76.

Rahman, S. M. N., Gafoor, A. and Hossain, T. I. M. T., 2001, Coastal zone monitoring using remote sensing techniques. Bangladesh Space Research and Remote Sensing Organization (SPARRSO), Dhaka.

Sankarnarayan, S. and Deborah, F. M., 2003, Three-Dimensional Modeling of Tidal Circulation in Bay of Fundy . Journal of Waterway, Port, Coastal and Ocean Engineering, Vol-129, pp 314-328.

Sarwar, M. G. M, 2005, Impacts of Sea Level Rise on the Coastal Zone of Bangladesh, Masrers Thesis, Lund University International Masters Programme in Environmental Science, Lund University, Sweden.

Swerdlow, Noel M., Neugebauer, Otto, 1984, Mathematical Astronomy in Copernocus's Derevolutionibus, Volume 1, Springer-verlag. p.76.

Thurman, H.V., (1994) Introductory Oceanography (7 ed.), New York, NY. Macmillan, pp. 252-276

Tanaka, H. and To, D.V., “Initial motion of sediment under wave and wave-current combined motions”, Dept. of Civil Eng., Tohoku Univ. Aoba, Sendai 980-77, Japan. Dept. of Geophysics, University of Ho Chi Miah City, Ho Chi Miah City, Viet Nam, 1995.

Valk, C.F., “Estimation of 3-D current fields near the Rhine outflow from HF radar surface current data”, ARGOSS, PO Box 61, 8325 ZH VollenhoÍe, Netherlands Coastal Engineering, Vol-37, pp 487-511, 1999.

WARPO, 2003, Integrated Coastal Zone Management Plan Project, Knowledge Portal on Estuary Development (KPED).

William, B. M., Chung, C. F. and Hancock, K., 2005, Predictions of relative sea-level change and shoreline erosion over the 21st century on Tangier island, Virginia. Journal of Coastal Research, Vol-21, Issue-2, pp e36 – e51.

Wolf, J. and Prandle, D., “Some observations of wave current interaction”, CCMS, Proudman Oceanographic Laboratory, Bidston Observatory, Birkenhead, Merseyside, L43 7RA, UK Coastal Engineering, Vol-37, pp 471-485, 1999.

Wood, Fergus J., 2001, Tidal Dynamics Volume I: Theory and Analysis of Tidal Forces; Volume II Extreme Tidal Peaks and Coastal Flooding. 3rd Ed. West Palm Beach, Fl: The Coastal Education and Research Foundation [CERF] ISBN: 0-938415-08-03

Yan, D. and Wang, S. Y., 2008, Development and application of a coastal and estuarine morphological process modeling system. Journal of Coastal Research, Special Issue-52, pp 127 – 140.